2018 NANOPORTUGAL International Conference

February 07-09, Lisboa (Portugal)

www.nanopt.org

Abstracts Book

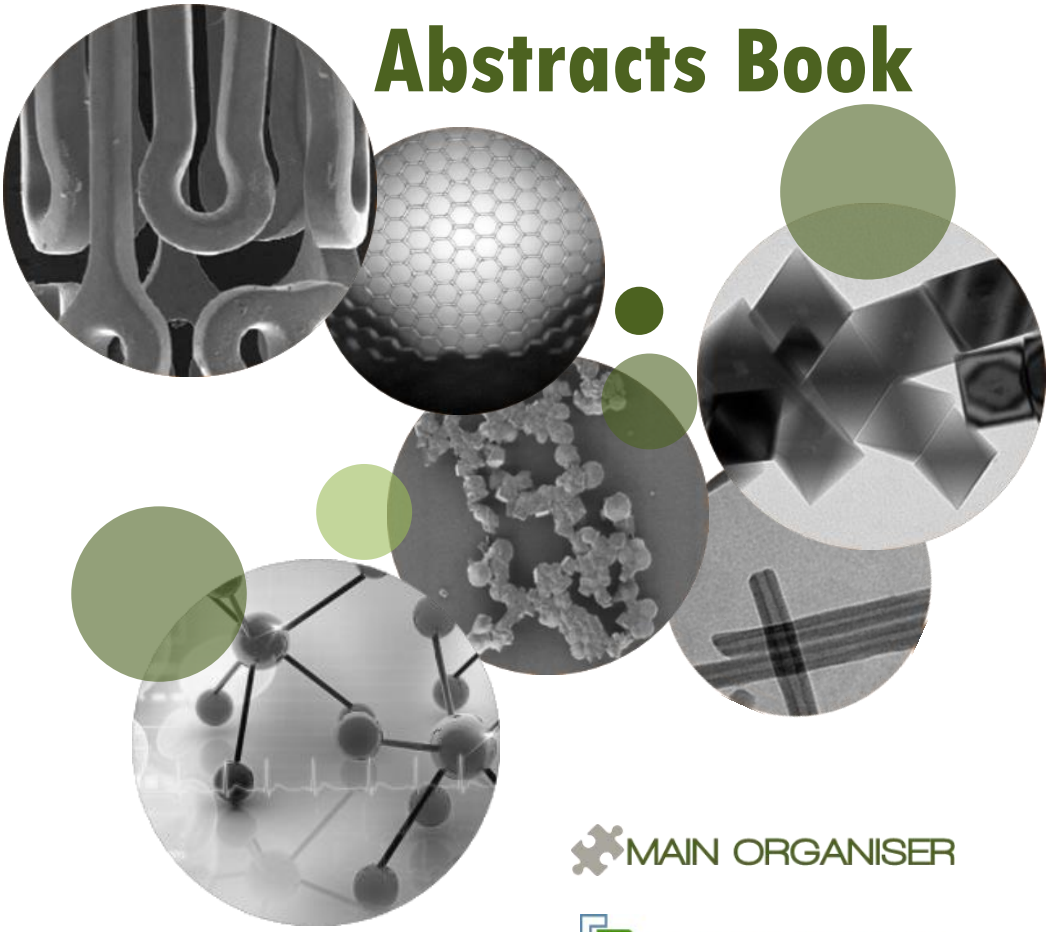

MAIN ORGANISER

PHANTOMS foundation

Index

Foreword

On behalf of the Steering, Programme and Technical Committees we take great pleasure in welcoming you to Lisboa (Portugal) for the 6th edition of the nanoPT International Conference (nanoPT2018).

The aim of nanoPT is to bring together again the Portuguese and International Community (students, researchers, engineers and stakeholders from academia, national laboratories, industry and other organisations) to discuss the latest developments and innovations in the fields of Nanoscience and Nanotechnology.

We are indebted to ThermoFisher Scientific and Lusofona University for their financial support. We would also like to thank the following companies for their participation as exhibitor: ScienTec Ibérica, Paralab, Tecnasa, ThermoFisher Scientific and Specs.

In addition, thanks must be given to the staff of all the organising institutions whose hard work has helped planning this conference.

We would like to thank all participants, speakers, sponsors and exhibitors that joined us this year. Hope to see you again in the next edition of nanoPT (2019).

2018 nanoPORTUGAL International Conference

February 07-09, Lisboa (Portugal)

Organisers

PHANTOMS foundation

UNIVERSIDADE LUSÓFONA

Universidade do Minho

Sponsors

ThermoFisher SCIENTIFIC

UNIVERSIDADE LUSÓFONA

Committees

Steering Committee

Antonio Correia (Phantoms Foundation, Spain)

Pedro Fonte (Universidade Lusófona, Portugal)

Vasco Teixeira (University of Minho, Portugal)

Programme Committee

Elvira Fortunato (CENIMAT-I3N, Portugal)

Rogério Gaspar (Faculty of Pharmacy of the University of Lisbon, Portugal)

Nuno Miguel Machado Reis Peres (University of Minho, Portugal)

Jose Rivas (Santiago de Compostela University, Spain)

Stephan Roche (ICREA/ICN2, Spain)

Technical Committee

Conchi Narros Phantoms Foundation (Spain)

Jose Luis Roldán Phantoms Foundation (Spain)

Malvern and PANalytical are pleased to announce that effective 1 January 2017 they will be merging their activities.

Both companies are owned by parent company Spectris plc and are operating companies within the Materials Analysis segment of Spectris. Both companies are world leading suppliers of analytical instrumentation, PANalytical for X-ray instrumentation and software for the purpose of materials analysis and Malvern Instruments for materials and biophysical characterization technology. The combined entity is a strong player in the materials characterization market and will be able to leverage the strengths of the individual companies in their end markets ranging from building materials to pharmaceuticals and from metals and mining to nanomaterials.

The merger is based on the belief that there are clear benefits through this more collaborative relationship, leveraging the very strong brands and highly-skilled employees of the two companies, in order to deliver a more complete range of products, solutions and services to a broader set of markets and customers.

The companies will be working together to ensure a smooth and effective integration guaranteeing our usual high level of support to all our customers. The combined group will continue to develop and invest in the Malvern and PANalytical technologies and the highly-talented workforce.

Eoghan O'Lionaird, Business Group Director responsible for the Materials Analysis segment within Spectris, says: "This is an exciting time for Malvern and PANalytical. Joining the two companies will enable us to leverage new resources to further grow our service offering and add even more value to our clients and customers. We are committed to ensuring a smooth integration process and will be actively engaging with our customers on how the combined entity can better serve their needs."

www.malvernpanalytical.com
luis.vital@panalytical.com

ScienTec Ibérica

Scientec Ibérica specializes in surface analysis at the micro-nano scale in the fields of nanotechnology, Scientific Research, R&D&I and Industrial Metrology and microfabrication.
Scientec provides innovative products for topographycal metrology and chemical characterization.
By high resolution topographic characterization we mean: AFM microscopes, optical and mechanical profilers, interferometers, digital holography, nanoindentation, filmetrics thin film and special 3D confocal for high aspect ratio geometries and reverse engineering (CAD).
By Chemical characterization we mean, high resolution microRaman, IR nanoespectroscopy, TERS, nanocalorimetry and ultrahigh vacuum spectroscopy systems ESCA, XPS, ARPES.

www.scientec.es
Info@scientec.es

LOT QuantumDesign

LOT-QuantumDesign group is a leading European distributor of high-quality scientific instruments and components supplying academic and industrial scientific research customers. The group offers components and systems used in material sciences, imaging, spectroscopy, photonics, nanotechnology and life science research. The group was founded almost 45 years ago and now employs more than highly-qualified 140 staff across Europe. The headquarters are in Darmstadt, Germany, further offices are located in Paris, London, Rom und Lausanne. Together with the parent company Quantum Design International Inc. and sister companies in North America, Asia and South America LOT-QuantumDesign offers the only global distribution network for high-tech instruments.

www.lot-qd.com

Grupo I.L.C.

Founded in 1977, the group I.L.C. - Laboratory and Scientific Instruments, Lda, commercializes all kinds of analytical solutions for scientific research and quality control. Present in all Portuguese territory and Portuguese Autonomous Regions, we cover activity sectors and areas as diverse as environment, life sciences…

www.ilc.pt

Index alphabetical order

Speakers

K: Keynote Speakers
I: Invited Speakers
O: Orals
P: Poster Session

Abstracts Keynote & Invited

P. Alpuim[1,2], R. Campos[1], E. Fernandes[1], P.D. Cabral[1,2], F. Cerqueira[1,2], J. Borme[1]

[1]INL - International Iberian Nanotechnology Laboratory, Braga, Portugal
[2] Center of Physics, University of Minho, Braga, Portugal

pedro.alpuim.us@inl.int

Highly target-specific graphene devices for biomedical applications

The importance of biosensors in biomedical research is increasing fast, as they are routinely used in a wider range of applications, from prognosis and diagnosis to personalized medicine. Graphene low-dimensionality, high carrier mobility and chemical stability, allow to fabricate relatively simple and highly sensitive biosensors with transducing capability, based on different types of devices. Ion-sensitive field-effect transistors (ISFETs), where the graphene channel is directly exposed to the analyte, have exceedingly high sensitivity, whereas electrochemical microelectrode arrays (EMAs) have all the advantages of single microelectrodes (higher current density, faster mass transport and lower detection limits), while providing amplification of the signal by the array. In this work we fabricate both ISFET and EMA devices. Using EMAs for direct detection of DNA hybridization based on cyclic voltammetry and electrochemical impedance spectroscopy, we achieved detection of a 25 nucleotide long target DNA in the range 5 pM to 50 nM, with single nucleotide polymorphism (SNP) sensitivity.

Graphene immuno-ISFETs with a receded, integrated gate architecture, are fabricated at the 200 mm wafer scale, for detection of a panel of biomarkers of the hemorrhagic transformation of ischemic stroke. Specific target biorecognition requires surface functionalization and so we immobilize probe molecules on graphene, using a pyrenic linker (PBSE) that binds to graphene through π-π interactions, and reacts with a primary amine from the antibody protein at the other end of the molecule. The device is able to detect MMP-9 in concentrations down to 0.01 ng/mL, in a range up to 10 ng/mL. Compared to existing MMP-9 immunoassays, it has a shorter time to diagnostic since it is based on a simpler label-free protocol.

For use of the ISFET as genosensor we functionalized graphene with the same 25 nucleotide DNA sequence used before, with a C7-amino modification on the 3'-end that binds to the ester group of the PBSE linker. Fully complementary target DNA is detected in a linear range between 1 aM and 100 fM, with SNP sensitivity down to 10 aM. The results are normalized for different initial probe surface densities, estimated by fitting the transistor transfer curves to an electrostatic model relating the observed shift in the charge neutrality point to local gating induced by the negatively charged DNA. The results of this work pave the way for a wide range of application of graphene devices in analyte detection for the health and food industries.

References

[1] N. C. S. Vieira et al., J. Phys.: Condens. Matter, 28 (2016) 085302
[2] A. Bonanni, M. Pumera, ACS Nano, 5 (2011) 2356
[3] Y. Ohno, K. Maehashi, K. Matsumoto, J. Am. Chem. Soc., 132 (2010) 18012

Figures

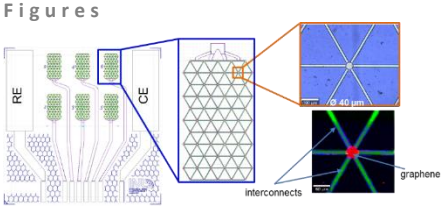

Figure 1: Layout of the EMA and Raman map (bottom right) of one microelectrode.

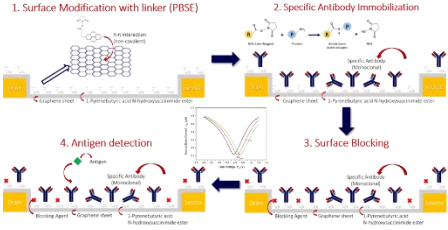

Figure 2: Graphene ISFET channel functionalization steps for biorecognition.

Maria Cristina Bonferoni

Dep Drug Sciences, University of Pavia,
Vle Taramelli 12, Pavia, Italy

cbonferoni@unipv.it

Nanoparticle systems based on hydrophobically modified chitosan

Electrostatic interactions between the amino groups of chitosan and the carboxylic groups of fatty acids, such as oleic acid, result in hydrophobically modified polymers (HMC) that in aqueous medium undergo self-assembling in polymeric micelles. These nanostructures are characterized by the presence of hydrophobic domains in which poorly soluble drugs can be loaded to improve their colloidal dispersion in aqueous environment [1,2].

The amphiphilic properties of the HMC can be exploited to stabilize o/w nanoemulsions. In these cases the hydrophobic moieties of the polymer arrange at the interface between aqueous continuous phase and oil droplet surface while the hydrophilic chains form a shell around them. Positive charge and steric effect of the polysaccharide contribute to further emulsion stabilization. The peculiar stabilization efficiency is probably due to the high number of anchoring points of the HMC at the o/w interface [3]. It has been seen that the chitosan shell maintains the peculiar bioactive properties of chitosan, such as for example mucoadhesion, antibacterial effect, wound healing promotion. This has been verified by encapsulating essential oils, such as lemongrass, whose antimicrobial activity was not only maintained but even improved after encapsulation in chitosan oleate. This result can be attributed not only to improved distribution of the oil in water, but also to antimicrobial properties of chitosan and oleic acid. It was moreover observed that encapsulation of the antioxidant alpha tocopherol improves its activity in promoting wound healing [4,5].

The amphiphilic properties of HMC can be also exploited to prepare nanoparticles by methods involving an emulsification step. This is the case of polymeric nanoparticles based on hydrophobic biodegradable polymers, such as PLGA, or of lipid based systems, such as solid lipid nanoparticles (SLN) or nanostructured lipid carriers (NLC). In both cases the use of HMC to stabilize nanoemulsions during the preparation process results in chitosan coated nanoparticles, as it was confirmed by positive zeta potential values.
All these systems are especially suitable for topical administration, for example in ocular pathologies, mucosal lesions or inflammatory conditions and skin wounds. They represent quite versatile carriers that can be loaded with poorly soluble anti-infectives, antioxidant and anti-inflammatory drugs.

References

[1] Bonferoni MC et al, Eur J Pharm Biopharm. 87, 101 (2014)
[2] Dellera E et al. Eur J Pharm Biopharm. 88, 643 (2014).
[3] Tadros T., Adv. Colloid Interface Sci. 147–148 (2009) 281–299
[4] Bonferoni MC et al, Oil in water nanoemulsions. WO2016/063119 A1.
[5] Bonferoni MC et al, Colloids and Surfaces B: Biointerfaces 152, 385 (2017)

Figures

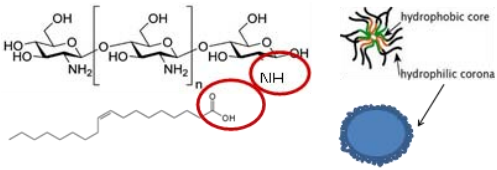

Figure 1: Interaction occurring between chitosan and oleic acid and a scheme of polymeric micelles or nanoparticles based on it.

Fèlix Casanova

CIC nanoGUNE, 20018 San Sebastian, Basque Country (Spain)
f.casanova@nanogune.eu

Graphene-based heterostructures as spintronic devices

The integration of the spin degree of freedom in charge-based electronic devices has revolutionized both sensing and memory capability in microelectronics. Further development in spintronic devices requires electrical manipulation of spin current for logic operations. In this presentation we will show two examples of graphene-based devices that work along this direction.

The mainstream approach followed so far, inspired by the seminal proposal of the Datta and Das spin modulator [1], has relied on the spin-orbit field as a medium for electrical control of the spin state [2-4]. However, the still standing challenge is to find a material whose spin-orbit coupling (SOC) is weak enough to transport spins over long distances, while also being strong enough to allow their electrical manipulation. In our recent work [5], we demonstrate a radically different approach by engineering a van der Waals heterostructure from atomically thin crystals [6], and which combines the superior spin transport properties of graphene with the strong SOC of MoS_2, a transition metal dichalcogenide with semiconducting properties (Fig. 1). The spin transport in the graphene channel is modulated between ON and OFF states by tuning the spin absorption into the MoS_2 layer with a gate electrode [5]. Our demonstration of a spin field-effect switch using two-dimensional materials identifies a new route towards spin logic operations for beyond CMOS technology. Furthermore, the van der Waals heterostructure at the core of our experiments opens the path for fundamental research of exotic transport properties predicted for transition metal dichalcogenides [7], in which electrical spin injection has so far been elusive.

An alternative way to exploit spin currents for logic operations is the recent proposal of a spin-orbit logic [8] which takes advantage of the discovery of new spin-to-charge conversion effects (spin Hall effect, Rashba-Edelstein effect, spin-momentum locking). Finding routes to maximize the conversion efficiency is thus crucial. We show how to achieve a very large spin-to-charge voltage output at room temperature by combining Pt with a graphene channel [9], opening up exciting opportunities towards the implementation of these spin-orbit-based logic circuits.

Figures

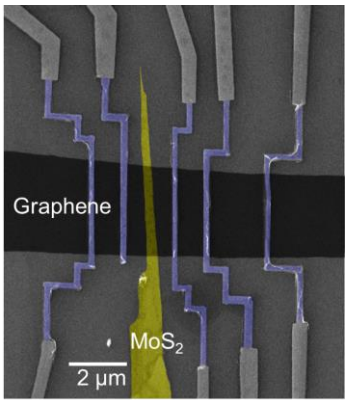

Figure 1: False-coloured SEM image of the 2D van der Waals heterostructure to be used for switching the spin transport. Purple nanostructures are Co electrodes used for spin current injection and detection in the graphene channel. The spin current flowing through the graphene can be switched ON and OFF by modulating the conductivity of MoS_2 with a backgate voltage.

References

[1] S. Datta and B. Das, Appl. Phys. Lett. 56, 665 (1990)
[2] H.C. Koo et al., Science 325, 1515 (2009)
[3] J. Wunderlich et al., Science 330, 1801 (2010)
[4] P. Chuang et al., Nat. Nanotechnol. 10, 35 (2015)
[5] W. Yan et al., Nat. Commun. 7, 13372 (2016)
[6] A. K. Geim and I. V. Grigorieva, Nature 449, 419 (2013)
[7] Y. Song and H. Dery, Phys. Rev. Lett. 111, 026601 (2013)
[8] S. Manipatruni et al., arXiv:1512.05428 (2017)
[9] W. Yan et al., Nat. Commun. 8, 661 (2017)

Antonio Correia

Phantoms Foundation, Calle Alfonso Gomez 17, 28037 Madrid (Spain)
antonio@phantomsnet.net

"Graphene and 2D Materials" EUREKA Cluster: Fostering European Competitiveness

The "Graphene & 2D Materials" EUREKA cluster is defined as a complementary enabling and accelerator instrument in the European scene, fully piloted by industries to further take graphene from the mature research developed at academic laboratories into the European society in the space of 5 years, boosting economic growth, jobs creation and international leadership and investment attractiveness. This cluster will help Europe having a more dominant position in graphene patenting, will deploy the proper winning industrial strategies to gain worldwide competitiveness, and will ensure that for all promising industrial sectors of technology innovation, a fully integrated EU-value chain is established, integrating into consortia the relevant actors from low to high Technology Readiness Levels (TRL).

The cluster will clarify the differentiating potential in all sectors where EU-industries is strong and could further gain in competitiveness and will develop proper incentives towards the achievement of EU-leadership in the fields of graphene commercialization and graphene-driven technology improvement. The cluster will elaborate and foster industrially-driven innovation strategies, that will take advantage of the existing excellent science and transnational platforms in Europe (national networks, Graphene-Flagship, etc.), and will focus on solving current challenges which are limiting the time to market and business growth of graphene-related EU companies.

Graphene has a huge potential to impact established industrial sectors, building new emerging industries and niche segments and creating economic value. The "Graphene and 2D Materials" Strategic Research Agenda currently targets 7 interlinked priority R&D areas for Europe. These areas are (1) Standardization, (2) Production and Scalability, (3) Composites, (4) Energy, (5) Biosensors and Health, (6) Optoelectronics and Electronic Devices; (7) Functional coatings. Currently, 243 Institutions from 27 countries (among them 154 companies) expressed interest in joining the Cluster...

Crecente-Campo, J.; Cordeiro, A.S.; Alonso, M.J.

Center for Research in Molecular Medicine and Chronic Diseases (CIMUS), Campus Vida, Universidade de Santiago de Compostela, Santiago de Compostela 15782, Spain

jose.crecente@usc.es

Modulating the immune system through nanotechnology

Based mainly on the molecular principles that govern the interaction between pathogens and immune cells, nanotechnology has created a tunable way of communication with the immune system. Both, the composition and the physicochemical characteristics of nanocarriers, can influence their interaction with immune cells. [1].

During my presentation I would like to focus on the work that our team has been doing in the vaccination field. We started working with toxoid antigens, later with whole purified proteins and, currently, we are focused on the use of peptides and mRNA as purer and safer antigens. At the same time, we have used different nanotechnologies, such as nanoparticles and nanocapsules. The evolution of our work has moved from nanosystems that functioned as monolithic compartments, where the carrier worked as a simple antigen container, to a nanosystems designed at a molecular level. We are capable of modifying the physicochemical properties of the nanosystems to drain more favourably to the lymph nodes and to be uptaken more efficiently by the immune cells. Besides we can include different immunoregulators in the nanosystems to potentiate the immunostimulation, in the case of infectious diseases or, on the contrary, to generate tolerance in the case of autoimmune diseases.

With the modification of their physicochemical properties and the incorporation of different immunoregulators, NCs constitute highly tuneable nanosystems that offers a whole language in the communication with the immune system.

References

[1] S. Cordeiro, M.J. Alonso, M. de la Fuente, Nanoengineering of vaccines using natural polysaccharides, Biotechnol. Adv. 33 (2015) 1279–1293.

[2] S. Vicente, M. Peleteiro, B. Díaz-Freitas, A. Sanchez, Á. González-Fernández, and M. J. Alonso, "Co-delivery of viral proteins and a TLR7 agonist from polysaccharide nanocapsules: A needle-free vaccination strategy," *J. Control. Release*, vol. 172, no. 3, pp. 773–781, 2013.

Figures

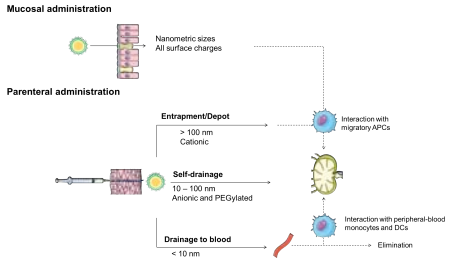

Figure 1: Summary of the influence of the physicochemical properties of nanocarriers (particle size and surface charge) in the fate of the nanosystems after administration: both particle size and surface charge play an important role in the outcome of nanosystems once administered, either by mucosal or parenteral routes.

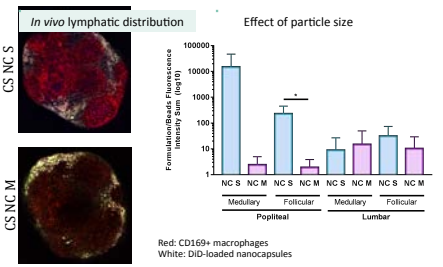

Figure 2: lymphatic distribution of small size (NC S, < 100 nm) and medium size (NC M, > 200 nm) nanocapsules after subcutaneous administration in the paw of mice.

Aires Ferreira

Department of Physics, University of York,
YO10 5DD, York, U.K.

aires.ferreira@york.ac.uk

Charge-spin conversion in atomically-thin van der Waals heterostructures

Abstract

In the past decade, graphene has emerged as a strong contender for next-generation spintronic devices due to its long spin diffusion lengths and gate tunable spin transport at room temperature [1]. However, the lack of a band gap and its weak spin–orbit coupling (SOC) pose major limitations for injection and control of spin currents. The recent capability to assemble layered crystals into vertical heterostructures offers a realistic prospect of overcoming graphene's weaknesses [2]. When graphene is paired with group-VI (semiconducting) dichalcogenide monolayers [MX_2 (M = Mo, W; X = S, Se)], its band structure develops rich spin-orbital textures via proximity effect [3], providing a clear and exciting path towards realising all-spin logic devices from ultra-thin and gate-tuneable van der Waals (vdW) heterostructures.

In this talk, I will present an overview of our latest results on graphene with interface-induced SOC [4-5]. I will show that graphene-MX_2 heterostructures generally support current-driven spin polarization; a relativistic transport phenomenon known as the inverse spin galvanic effect (ISGE). Owing to the characteristic spin winding of interfacial states in graphene on a MX_2 monolayer, the predicted ISGE possesses striking similarities to charge-to-spin conversion generated by ideal topologically protected surfaces. The ISGE conversion efficiency is found to be little sensitive to impurity scattering, with the proper figure of merit attaining values as great as 30% at room temperature [4]. The giant charge-to-spin conversion in a graphene system with proximity spin-orbital effects promises unique advantages for low-power applications, including the tuning of spin polarization by a gate voltage (see Figure). The implications of our general microscopic theory of charge-spin dynamics to 2D Dirac interfaces of current experimental relevance will be briefly discussed [5].

Figures

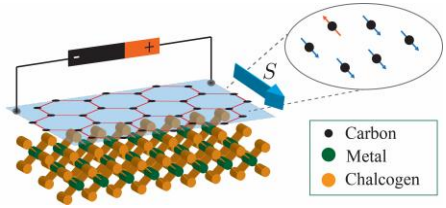

Figure 1. Graphene is placed on top of an ultra-thin semiconducting base with two types of atoms forming an atomically-thin "sandwich". The proximity to the semiconducting layer re-orients the spin of conduction electrons in graphene, allowing all-electrical generation of 'spin signals' (i.e., a net spin polarization) by application of a small gate voltage. (Credit: A. Ferreira)

References

[1] N. Tombros *et al.* Nature 448 (2007) 571; M. Kamalakar *et al.* Nat. Comm. 6 (2015) 6766

[2] A.K. Geim and I.V. Grigorieva. Nature 499 (2013) 419; A. Soumyanarayanan, *et al.* Nature 539 (2016) 509

[3] A. Avsar *et al.* Nat. Comm. 5 (2014) 4875; Z. Wang, *et al.* PRX 6 (2016) 041020; B. Wang, *et al.* PRB 96 (2017) 041409(R); T.S. Ghiasi, J. I.-Aynés, A. Kaverzin and B. J. van Wees, Nano Lett. 17 (2017) 7528; L. Benitez, *et al.* Nat. Phys. (2017) on-line

[4] M. Offidani, M. Milletari, R. Raimondi, A. Ferreira. Phys. Rev. Lett. 119 (2017) 196801

[5] M. Milletari, M. Offidani, A. Ferreira, R. Raimondi. Phys. Rev. Lett. 119 (2017) 246801

P. J. Ferreira[1,2], Charles Amos[1,2], John Goodenough[2], Manuel Roldan[2]

[1]INL - International Iberian Nanotechnology Laboratory, Av. Mestre José Veiga s/n, 4715-330 Braga, Portugal

[2]Materials Science and Engineering Program, The University of Texas at Austin, Austin, Texas 78712, USA.

paulo.ferreira@inl.int

Understanding the Surface Structure of $Li_{1-x}[Mn_2]O_4$ by Aberration-Corrected STEM and EELS

Abstract

$Li[Mn_2]O_4$ (LMO) is a well-known cathode material for Li-ion batteries, but it is plagued with cyclability problems associated with the surface disproportionation of Mn ($2Mn^{3+} \rightarrow Mn^{2+} + Mn^{4+}$) and consequent loss of Mn^{2+} to the organic liquid electrolyte during electrochemical cycling.

In this paper, we use a combination of high-angle annular dark-field (HAADF) aberration-corrected scanning transmission electron microscopy (STEM) and electron energy loss spectroscopy (EELS) to identify the atomic surface structure and composition of LMO. We confirm the underlying spinel structure and for the first time we find, in as-processed LMO, a surface structure composed of Mn_3O_4 and a lithium-rich $Li_{1+x}Mn_2O_4$ subsurface layer which occurs as a result of the surface reconstruction.

In addition, we have applied an aqueous acid treatment, a non-aqueous chemical delithiation, and an oxygen plasma treatment to LMO in order to understand how this surface reconstruction is affected by chemical treatments. We find that Mn_3O_4 is a robust surface phase in the $Li_{1-x}[Mn_2]O_4$ system regardless of the chemical treatment and level of lithiation. The surface Mn_3O_4 phase is cubic whereas bulk Mn_3O_4 undergoes a cooperative Jahn-Teller distortion to tetragonal symmetry. Thicker Mn_3O_4 surface layers are tetragonal.

References

[1] J. Song et al., Chem. Mater. 24 (2012), 3101.

[2] C. Amos, M. Roldan, M. Varela, J. Goodenough, P. Ferreira, "Revealing the Reconstructed Surface of $Li[Mn_2]O_4$", Nanoletters, 16, (2016), 2899.

Figures

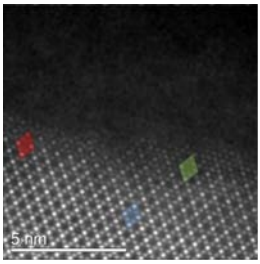

Figure 1. HAADF STEM image of $LiNi_{0.45}Mn_{1.55}O_4$ along the [110] zone axis. Shown in the figure are the normal spinel phase (blue), the rock-salt phase (green) and the ring phase (red).

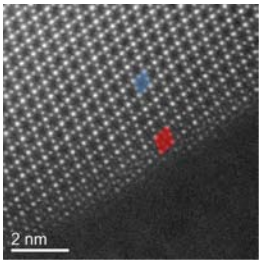

Figure 2. HAADF STEM image of $LiNi_{0.45}Mn_{1.55}O_4$ along the [110] zone axis. Observed are the normal spinel phase in the bulk (blue) and the ring phase at the surface (red). No rock-salt phase is observed in this image.

Cristina Freire

REQUIMTE/LAQV, Departamento de Química e Bioquímica, FCUP, Rua Campo Alegre, 4169-007 Porto, Portugal

acfreire@fc.up.pt

Graphene nanocomposites in chemical, energy related electrocatalysis and sensing

Graphene materials, including pristine graphene, oxidized graphene and heteroatom doped graphene, are revolutionizing the way high performance devices are designed and fabricated, particularly in the areas of sustainable energy and environmental technologies.[1,2] From environmental remediation and sensing to energy conversions and storage, there are numerous effective cases of graphene-based materials applications.[3] Graphene materials are typically coupled with other active materials as a nanocomposite. With their outstanding properties (high surface to-bulk ratio, efficient heat transfers and electron conduction), the interface with graphene benefits the bare materials by actually emphasizing their properties.

To achieve this, the strategy of surface functionalization of graphene with inorganic materials (e.g., metal nanoparticles, oxides, semiconductors), holds the key to enabling the fabrication of high performance nanocomposites. The resultant nanoarchitectures should yield the highest achievable properties and should be unique to the specific applications.

This talk provides a bottom-up approach encompassing the design of graphene-based nanocomposites and their selected applications in high performance systems relevant to chemical catalysyis, energy related electrochemical reactions and electro-sensing.

Heteroatom-doped graphene was studied in the selective reduction of nitro- into amine-arenes, with high catalytic activity and stability/reusability. Furthermore, several graphene nanocomposites with metals oxides: mixed valence cobalt/manganese oxide, phosphomolybdates and phosphotungstates have been successfully applied in energy-related electrochemical reactions involving hydrogen and oxygen evolution reactions (HER and OER, respectively), as well as oxygen reduction. The same type of graphene nanocomposites was used as electrochemical nanosensors for biologically relevant molecules such as ascorbic acid, dopamine and uric acid.

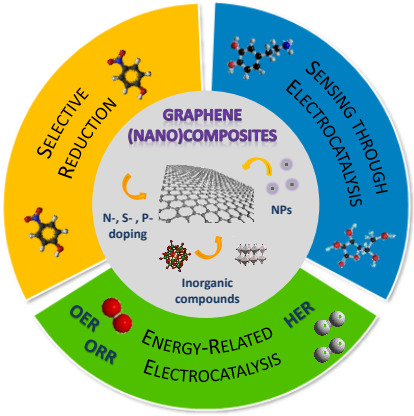

Figure 1: Graphene-based (nano)composites and their applications in selective chemical catalysis, electro-sensing and energy-related reactions.

References

[1] V. Singh, D. Joung, L. Zhai, S. Das, S. I. Khondaker, S. Seal, Progress in Materials Science 56 (2011) 1178.

[2] Y. Sun, Q. Wu, G. Shi, Energy Environ. Sci. 4 (2011) 1113.

[3] A. Ambrosi, C. K. Chua, A. Bonanni, M. Pumera, Chem. Rev. 114 (2014) 7150.

Acknowledgements

The work was funded by Fundação para a Ciência e a Tecnologia (FCT)/MEC under FEDER under Program PT2020, projects UID/QUI/50006/2013-POCI/01/0145/FEDER/007265, UniRCell", POCI-01-0145-FEDER-016422 and Program FCT – UT Austin, project ref UTAP-ICDT/CTM-NAN/0025/2014).

Jose H. Garcia[a], Aron W. Cummings[a], Stephan Roche[a,b].

[a] Catalan Institute of Nanoscience and Nanotechnology (ICN2), CSIC and BIST, Campus UAB, Bellaterra, 08193 Barcelona, Spain.
[b] Institució Catalana de Recerca i Estudis Avançats (ICREA), 08010 Barcelona, Spain.

josehugo.garcia@icn2.cat

Tailoring Spin Dynamics through Proximity Effects in Graphene/Transition Metal Dichalcogenide Heterostructures

Since its discovery, graphene has been a promising material for spintronics: its low spin-orbit coupling, negligible hyperfine interaction, and high electron mobility are obvious advantages for transporting spin information over long distances. However, such outstanding transport properties also limit the capability to engineer active spintronics, where strong spin-orbit coupling is crucial for creating and manipulating spin currents. To this end, transition metal dichalcogenides, which present larger spin-orbit coupling and good interface matching with graphene, appear to be highly complementary materials for enhancing the spin-dependent features of graphene while maintaining its superior charge transport properties. In this work, we present a recently developed theoretical framework used to understand the current experimental measurements. Specifically, we will concentrate on the effect of valley-Zeeman and inter-valley scattering in weak anti-localization, spin lifetime anisotropy and spin Hall Effect, providing a comprehensive theoretical description of the interconnection between these phenomena. We will also discuss on the possibilities of Graphene/TMDCs heterostructures as a spin-orbit torque platform.

References

[1] Jose H. Garcia , Aron W. Cummings and Stephan Roche. Nano Lett., 8(2017) 5078.
[2] Aron W. Cummings, Jose H. Garcia, Jaroslav Fabian, and Stephan Roche. Phys. Rev. Lett., 119(2017) 206601.
[3] Talieh S. Ghiasi, Josep Ingla-Aynés, Alexey A. Kaverzin, Bart J. van Wees. arXiv:1708.04067 (2017).
[4] L. A. Benítez, J. F. Sierra, W. Savero Torres, A. Arrighi, F. Bonell, M. V. Costache, S. O. Valenzuela. arXiv:1710.11568 (2017)

Figures

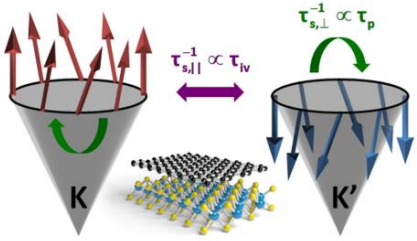

Figure 1: Schematic of spin relaxation in graphene-TMDC heterostructures. The tall arrows depict the effective spin-orbit field within the Dirac cones at K and K0 valleys. Intervalley scattering dominates the in-plane spin dynamics, while overall momentum scattering controls the out-of-plane behavior.

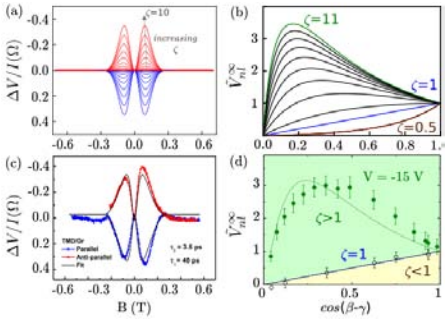

Figure 2: (a) Theoretical non-local resistance for in-plane magnetic field for different values of anisotropy ranging for 1 to 10. (b) Normalize asymptotic non-local voltage as a function of an oblique magnetic field, for different values of anisotropies. (c) Experimental values of the non-local resistance modulated by an in-plane magnetic field obtained from ref. [3]. Normalized asymptotic non-local voltage as a function of the oblique angle for pristine graphene and Gr/WS$_2$ obtained from ref. [4].

Rogério Gaspar

Faculdade de Farmácia & Institute for Bioengineering and Biosciences, University of Lisbon, Lisbon, Portugal

rgaspar@ff.ulisboa.pt

Integrative healthcare challenges and the emergence of convergence in Nanomedicine: from health sciences to health care

Abstract (Calibri 8)

Nanomedicine is bringing converging sciences to healthcare through an adequate platform of technologies allowing new horizons for better health care. It also enables innovation both in the design of clinical research and the clinical use to face unmet clinical needs.

Advances brought by nanomedicines in oncology and infectious diseases are now expanding both within these clinical areas and also looking at their use to previously unmet clinical needs. The advances in the last five decades of basic research and the last 30 years of clinical practice with nanomedicines, will certainly allow for significant improvements in the next phase. This will be sustained by both solid basic research and an increased amount of clinical data compiled across different technologies and therapeutic areas.

New developments are allowing the introduction of both personalized medicine and combination therapy as drivers for innovation in clinical practice with nanomedicines. Meanwhile, current developments in the research landscape of nanomedicines brought the attention to the fact that, as an already well established area of clinical practice, nanomedicines now face also some relevant questions previously also addressed by new chemical entities and biologicals.

The innovation in materials science has to meet the challenges of clinical standards already established for already approved medicinal products. Dozens of nanomedicines went through the challenge of regulatory approval for both clinical experiences (under clinical trials) but also for marketing authorization and routine clinical use having to face the need to demonstrate both safety and efficacy but also compliance and effectiveness in routine clinical use.

New challenges arising from current debate within Regulatory Science will have to be met by better integration between advances in materials science and translational issues like validation of adequate models (i.e. preclinical human cells and tissues in appropriate setting to foster clinical translation and better outcomes within clinical phase). Targeting adequate disease stage and disease evolution conditions are at forefront of priorities trying to address appropriate personalized medicine issues.

Regulatory framework in Europe and elsewhere is currently adjusting to new realities and incorporating the best scientific standards, in anticipation of the regulatory needs both to follow-on products, combination products and integrative platforms bringing together therapy and diagnostics.

References

[1] Duncan R, Gaspar R. “Nanomedicine(s) under the microscope”. Molecular Pharmaceutics 2011;8(6): 2101-2141.

[2] Gaspar R, Duncan R. “Polymeric carriers: Preclinical safety and the regulatory implications for design and development of polymer therapeutics”. Adv. Drug Deliver. Rev. 2009; 61: 1220-1231.

[3] Gaspar R, Florindo H, Silva LC, Videira M, Corvo L, Lima BS. “Regulatory aspects of oncologicals: nanosystems main challenges”. In Nano-Oncologicals, Springer International Publishing, 2014, pp. 425-452.

[4] Schellekens H, Stegemann S, Weinstein V, de Vlieger JSB, Fluehmann B, Muhlebach S, Gaspar R et al. “How to Regulate Nonbiological Complex Drugs (NBCD) and Their Follow-on Versions: Points to Consider”. AAPS J. 2014; 16 (1): 15-21.

Ana Grenha

CCMar, CBMR - University of Algarve, Campus de Gambelas, 8005-139, Faro, Portugal

amgrenha@ualg.pt

Polysaccharide nanoparticles: Unveiling applications in mucosal drug delivery

Nanomedicines as a whole have been gathering tremendous attention. Many of the proposed formulations are based on natural polymers and, among these, polysaccharides have been a privileged category. They are particularly suited for nanoparticle preparation, offering advantages like high flexibility and propensity to comply with requisites of biocompatibility and biodegradability. Nevertheless, while some polysaccharides have been exhaustively explored, such as chitosan and hyaluronic acid, many others remain quite unknown [1]. The reduced dimensions of nanoparticles provide increased surface-to-volume ratio and maximal epithelial contact, permitting the concomitant protection of the encapsulated therapeutic agents from pH and enzymes. Nanoparticles have been frequently proposed as vehicles of drugs to the lungs, taking benefit of the characteristics provided by the lung route for either systemic or local delivery. Importantly in this regard, nanoparticles have demonstrated the ability to delay or avoid uptake by alveolar macrophages an effect that is more efficient for sizes below 500 nm [2]. Naturally, considering the small size of nanoparticles, inhalation requires a strategy to provide suitable aerodynamic properties. The microencapsulation of nanoparticles has been proposed for this end [3]. Applications of nanoparticles in other routes are also proposed often, particularly in oral delivery.

Considering the need to explore the potential of less explored polysaccharides, we have developed several nanoparticle formulations (Figure 1) based on polysaccharides such as pullulan, locust bean gum, chondroitin sulfate and fucoidan. All nanoparticles were produced using the method of polyelectrolyte complexation, which requires the presence of charged groups in the polymers. Therefore, some of the polysaccharides (pullulan, locust bean gum) had to undergo chemical modification to provide the necessary charges.

The physicochemical characteristics of the developed nanocarriers were easily modulated according to their composition, resulting in suitable characteristics for mucosal administration. Sizes around 180 – 300 nm were obtained for the various formulations and zeta potential shifted from strongly negative (-35 mV) to highly positive (+60 mV), depending on particle composition. Insulin and bovine serum albumin were associated with efficiencies up to 60% to several carriers proposed for lung delivery of biopharmaceuticals. Additionally, ovalbumin and an extract of *Salmonella* Enteritidis were used as model antigens in locust bean gum nanoparticles proposed for oral mucosal vaccination (association efficiencies up to 30%). *In vitro* biocompatibility assays in oral and pulmonary epithelial cells generally evidenced absence of toxicological effect of nanoparticles.

Funding from the Portuguese Foundation for Science and Technology (PTDC/SAU-FCF/100291/2008, PTDC/DTP-FTO/0094/2012, UID/Multi/04326/2013 and UID/BIM/04773/2013 is acknowledged.

References

[1] MA dos Santos, A Grenha, Advances in Protein Chemistry and Structural Biology, 98 (2015) 223

[2] K Makino et al., Colloids and Surfaces B: Biointerfaces, 27 (2003) 33

[3] A Grenha, B Seijo and C Remuñán-López, European Journal of Pharmaceutical Sciences, 25 (2005) 427

Figures

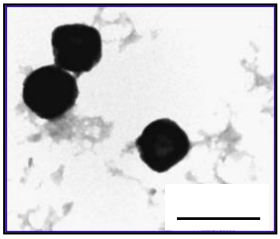

Figure 1: TEM microphotograph of representative polysaccharide-based nanoparticles produced by polyelectrolyte complexation.

Lifeng Liu,* Junyuan Xu

International Iberian Nanotechnology Laboratory , Av. Mestre Jose Veiga, 4715-330 Braga, Portugal

lifeng.liu@inl.int

Development of Earth-Abundant Electrocatalysts for Efficient and Durable Water Splitting

Abstract

Water splitting has been proposed to be a promising approach to renewable energy storage through converting the off-peak solar or wind energy to hydrogen fuels. Presently, one of major challenges facing widespread deployment of water splitting devices is their high cost, which primarily results from the use of precious and scare noble metal catalysts. Following our previous success in fabricating self-supported transition metal phosphide (TMP) electrodes to catalyze the hydrogen and oxygen evolution reactions (HER & OER) [1-4], we recently found that the catalytic performance of TMP nanoparticles (NPs) for the HER or OER can be improved by fine-tuning the NP's shape and composition as well as by synergy with other catalytic materials.

In this presention, I will showcase three examples: 1) Hollow CoP octahedron (OCH) nanostructures with well-defined exposed crystal facets [5]. The hollow CoP OCH NPs were prepared by solution phase synthesis of CoO OCH precursors, followed by a post-phosphorization treatment and subsequent chemical etching process. They show excellent electrocatalytic performance for the OER, substantially outperforming CoP nanospheres without any preferentially exposed facets. 2) Trends in the OER activity of TMP catalysts [6]. We have investigated the alkaline OER electrolysis of a series of TMP catalysts and observed a notable trend in OER activity which follows the order of FeP < NiP < CoP < FeNiP < FeCoP < CoNiP < FeCoNiP. Our results show that the introduction of a secondary metal(s) to a mono-metallic TMP can remarkably boost the OER performance. This promotional effect can be ascribed to the enhanced oxidizing power of bi- and tri-metallic TMPs that can facilitate the formation MOH and chemical adsorption of OH^- groups, which are rate-limiting steps for these catalysts according to our Tafel analysis. 3) RuCoP nanoclusters showing superior HER performance in alkaline solution [7]. The RuCoP clusters were prepared by wet chemical reduction of metal cations followed by a low-temperature phosphorization treatment. When used to catalyze the HER, they show exceptional activity with a very low overpotential (η) of 23 mV to reach -10 mA cm^{-2} and a high turnover frequency (TOF) value of 3.85 s^{-1} at η = 100 mV. The superior HER performance can be attributed to the partial electron transfer from CoP to Ru, which substantially improves the HER kinetics on active Ru sites.

References

[1] X.G. Wang, Y.V. Kolen'ko, X.Q. Bao, K. Kovnir, L.F. Liu, Angew. Chem. Int. Ed., 54 (2015) 8188.

[2] X.G. Wang, W. Li, D.H. Xiong, D.Y. Petrovykh, L.F. Liu, Adv. Funct. Mater., 26 (2016) 4067.

[3] W. Li, X.F. Gao, X.G. Wang, D.H. Xiong, P.P. Huang, W.G. Song, X.Q. Bao, L.F. Liu, J. Power Sources, 330 (2016) 156.

[4] W. Li, X.F. Gao, D.H. Xiong, F. Xia, J. Liu, W.G. Song, J.Y. Xu, S.M. Thalluri, M.F. Cerqueira, X.L. Fu, L.F. Liu, Chem. Sci. 8 (2017) 2952.

[5] J.Y. Xu, J.J. Li, L.F. Liu, under preparation

[6] J.Y. Xu, J.J. Li, D.H. Xiong, B.S. Zhang, Y.F. Liu, K.H. Wu, I. Amorim, W. Li, S.M. Thalluri, L.F. Liu, submitted to Nano Lett.

[7] J.Y. Xu, J.J. Li, T.F. Liu, K. Yu, Y.F. Liu, D.H. Xiong, K.H. Wu, I. Amorim, S.M. Thalluri, W. Li, P.J. Ferreira, L.F. Liu, under preparation

Figures

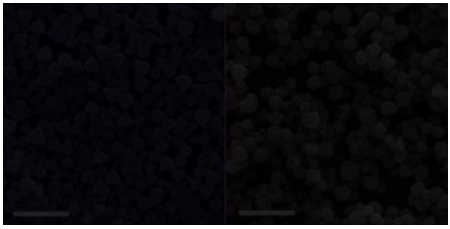

Figure 1: (left) CoP octahedron nanoparticles. (d) porous CoP nanospheres.

Artur M. Pinto [1,2,3], Friedrich H. [1]

[1] Laboratory of Materials and Interface Chemistry, Eindhoven University of Technology, The Netherlands
[2] INEB-i3S | [3] FEUP - Portugal

a.d.moreira.pinto@tue.nl

Graphene-based materials and their polymer composites for flexible electronics and biomedical applications

Graphene-based materials biocompatibility

Studies frequently show that mammalian cell viability decreases slightly after exposure to graphene-based materials (GBMs). These materials were shown to induce oxidative stress and apoptosis. The most hydrophilic forms of GBMs were found to penetrate the cellular membrane. Even so, these materials were found to be generally less toxic than hydrophobic forms, which accumulate on cell membrane surfaces.

The *in vivo* effect of GBMs depends on their physical–chemical properties, concentration, time of exposure, and administration route, and also on the characteristics of the animals used. Most studies report no occurrence of adult animal death. However, there are some reports of GBMs accumulation and histological findings associated with inflammation, and, more rarely, fibrosis. Encapsulation of GBMs in a matrix reduces potential toxicity. In addition, incorporation of hydrophilic forms improves cell adhesion at the biomaterials surface. Some reports of antibacterial properties and improved hemocompatibility in GBM-based composites offer interesting perspectives for future research and developments. [1]

Graphene-based materials and their polymer composites for biomedical applications

Production and characterization of polymer/graphene composites, exploring and improving available methods was performed, in parallel with the characterization of graphene-based materials biological properties when dispersed in liquid media, and the effect of their morphology, degree of oxidation, and surface modification with polymers. These materials have potential uses in biomedical implants for orthopedics and cardiology, amongst others. [2]

Graphene-based materials for flexible electronics

Low-cost high-throughput printing of solution processed electronics is a rapidly expanding field that already encompasses many large-scale applications such as roll-to-roll printed solar cells, including current collecting grids, displays, and radio frequency identification (RFID) devices. Here, solution-processed graphene holds considerable promise for printed electronics as it is widely available, inexpensive, flexible, and most importantly, highly conductive. For flexible electronic devices, *e.g.*, organic photovoltaics, a sheet resistance < 10 Ω/□ mil is required, while for printed RFID antennas, one needs a few Ω/□ mil. Following printing of the conductor pattern, typically post-treatments such as drying, annealing, or top-coating can be employed to maximize conductivities. The conditions of post-treatment define the substrate that can be used for printing. Materials with suitable properties for above mentioned applications were obtained and new strategies are under development. [3]

References

[1] Pinto *et al.*, Colloids Surf B 111 (2013) 188.
[2] Pinto *et al.*, Carbon 99 (2016) 318.
[3] Kirill et al., Adv. Funct. Mater 26 (2016) 586.

Figures

Figure 1:

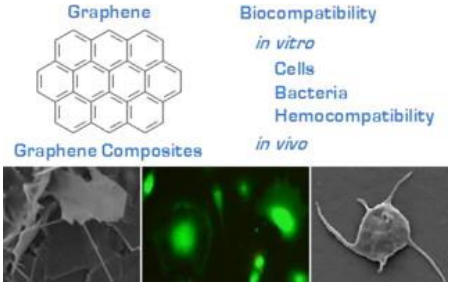

Figure 2: (Calibri 6)

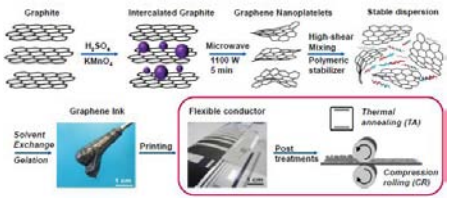

Lluis F. Marsal, Josep Ferré-Borrull, Elisabet Xifré-Pérez

Departament d'Enginyeria Electrònica, Elèctrica i Automàtica, Universitat rovira i Virgili.
Av. Països Catalans 26, 43007 Tarragona, Spain.
Lluis.marsal@urv.cat

Recent advances in nanoporous anodic alumina for sensing and drug delivery applications

Nanoporous anodic alumina (NAA) is a nanostructured material that under specific conditions, their structure presents a self-ordering defined by a close-packed hexagonal array of parallel cylindrical nanopores [1]. By controlling anodization conditions, its porous geometry can be modified, for example the diameter of the nanopores can be tuned from 10 nm up to 400 nm. NAA presents an outstanding set of properties (good mechanical and chemically stability, photoluminescence, large effective surface area-hundreds of m^2/cm^3) and is obtained by a cost-effective fabrication processes [2]. In addition, its chemical surface functionalization makes of NAA an excellent candidate for biosensing platforms and drug delivery systems [3-4].

In this context, we will present some recent advances in the design and fabrication of NAA structures and introduce different electrochemical approaches to modify the pore geometry during or after the fabrication processes. Some examples of optical NAA structures (microcavities, Bragg reflectors, graded refractive index) [5] and surface functionalization are presented (figure 1) and analyzed as examples of sensitive biosensing. Finally, 2D and 3D pore geometries of nanoporous anodic alumina are presented for efficient sustained drug release platforms [6]. Moreover, examples of surface functionalization for a controlled and stimuli-responsive drug release (figure 2) is presented and discussed.

References

[1] A Santos, P Formentín, J Ferré-Borrull, et al., Materials Letters 67 (2012), 296.
[2] A Santos, P Formentín, et al., Journal of electroanalytical chemistry 655 (2011), 73.
[3] T Kumeria, A Santos, MM Rahman, J Ferré-Borrull, et al., ACS Photonics 1 (2014), 1298.
[4] T Kumeria, MM Rahman, A Santos, et al., ACS applied materials & interfaces 6 (2014), 12971.
[5] MM Rahman, LF Marsal, et al., ACS applied materials & interfaces 5 (2013), 13375.
[6] M Porta-i-Batalla, C Eckstein, E Xifré-Pérez, et al. Nanoscale research letters 11 (2016), 372.

Acknowledgements

This work was supported by the Spanish Ministry of Economy and Competitiveness TEC2015-71324-R (MINECO/FEDER), the Catalan authority AGAUR 2017SGR1527, and ICREA under the ICREA Academia Award.

Figures

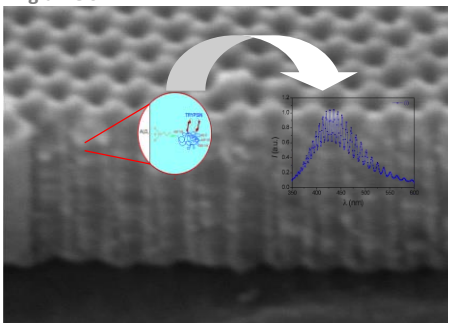

Figure 1: Cross-section SEM image of NAA. Inset: schematic illustration of the chemical functionalization of the pore surface and reflectometric interference spectroscopy spectrum of NAA. Pore diameter ≈ 45 nm.

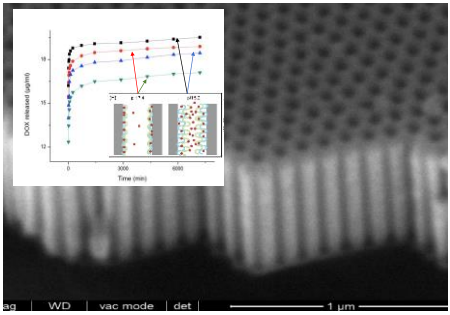

Figure 2: SEM image of NAA. Inset: DOX release at pH 5.2 and 7.4 for NAA (black and red symbols) and NAA coated with a PH stimuli-response polyelectrolyte (blue and green symbols).

Hanne Mørck Nielsen[1,*], Mie Kristensen[2], Ditlev Birch[1], Sofie Fogh Hedegaard[1], Henrik Franzyk[3]

[*]Presenting author
[1]Center for Biopharmaceuticals and Biobarriers in Drug Delivery
[2]CNS Drug Delivery & Barrier Modelling, [3]Natural Products and Peptides
All: University of Copenhagen, Copenhagen, Denmark

hanne.morck@sund.ku.dk

Conjugation to cell-penetrating peptides influences their membrane interaction and safety

Therapeutic peptide and protein drug entities are of high therapeutic relevance due to their potency and specific mode of action. A major obstacle for the successful delivery of peptide/protein drugs to their target site is their poor transport across biological membranes. This renders that administration is to a large extent done by injection, which is often experienced as inconvenient for the patients. Oral administration may, however, be pursued for some peptide molecules if pharmacologically relevant. Sufficient delivery of peptide drugs via the gastrointestinal tract is, however, limited both by their poor enzymatic stability and their large molecular size, the latter hindering non-aided permeation across the intestinal epithelium.

A class of membrane-interacting peptides, cell-penetrating peptides (CPPs), has demonstrated promising potential as carriers for delivery of therapeutic cargoes across biological membranes. To enhance the transmembrane delivery of a cargo peptide like the parathyroid hormone fragment 1-34 by using CPPs, conjugates of the therapeutic cargo with the CPP molecule has been pursued. The mechanism by which CPPs interact with biological membranes and act as carriers for transmembrane delivery of a conjugated cargo is heavily debated but known to depend on the molecular properties of the CPP. Numerous studies seek to elucidate the mechanism of membrane interaction of the CPPs by applying a range of techniques involving conjugation of fluorophores to the CPP.

Conjugation of a therapeutic molecule or a fluorophore to CPPs inevitably will change the physicochemical properties of the CPP. This fact likely influences the degree and mechanism of membrane interaction, affect delivery efficiency, and potentially lead to undesired cellular effects [1]. We here report on the importance of molecular properties of CPP conjugates in relation to their effect on biological membranes employing studies on lipid bilayers as well as cell culture models.

Figures

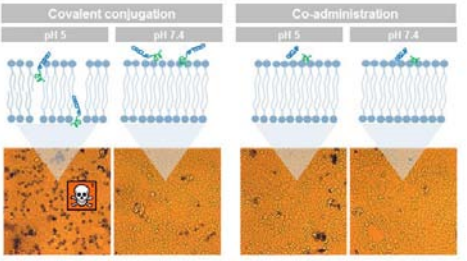

Figure 1: Conjugation of a cell-penetrating peptide, penetratin, to parathyroid hormone 1-34 alters the mode and degree of interaction with epithelial cells compromising safety [2].

References

[1] Birch, D, Christensen, MV, Staerk, D, Franzyk, H, Nielsen, HM. BBA-Biomembranes, 1859 (2017) 2483-2494.

[2] Kristensen, M, Nielsen, LH, Zór, K, Boisen, A, Christensen, MV, Berthelsen, J, Nielsen, HM, Bioconjugate Chem. (2018) *in press*.

Bruno Sarmento

University of Porto, Portugal

bruno.sarmento@ineb.up.pt

Functional nanomedicines for modulation the interaction with mucosal barriers

In drug delivery field, bioavailability and specificity are key challenges in the establishment of advanced products. Nanoparticles have been proposed by our group as valid approaches to provide successful systems to deliver drugs to their site of action, particularly to explore no-invasive, mucosal administration. Besides the proper control of nanoparticle matrix to provide a suitable release of drug payload, the surface of nanoparticles has a major impact on the interaction with biological barriers.

We have studied thoroughly the interaction of nanoparticles with cells and mucus regarding their adhesive properties that modulates their mucoadhesive behaviour, ultimately related with passive targeting to mucosae. Understanding how nanosystems interact with individual mucin chains and the 3D structure of mucus is paramount, as a passive functionalization of nanoparticles may concerns, exploring different biomaterials as mucus-modulators. Our active targeting approach for nanoparticles has been focused on ligand molecules attached to the surface of nanoparticles to increase the probability of binding to unregulated cell membrane receptors in key local effector sites. New and less-explored receptors are being targeted in engineered nanosystems, providing enhanced local and intracellular levels of drugs, without compromise the safety of the systems.

In this talk, application of nanosystems for mucosal delivery of drugs with physiological and social impact, developed in our research group, will be presented.

References

Araujo, Sarmento, ++, Chemical modification of drug molecules as strategy to reduce interactions with mucus, Advanced Drug Delivery Reviews, in press

Gomes, Sarmento, ++, Delivery of siRNA silencing P-gp in peptide-functionalized nanoparticles causes efflux modulation at blood-brain barrier, Nanomedicine, 12, 1385-1399, 2017

Araujo, Sarmento, ++, Functionalized materials for multistage platforms in the oral delivery of biopharmaceuticals, Progress in Material Sciences, 306-344, 89, 2017

Andrade, Sarmento, ++, Pharmacological and toxicological assessment of polymeric micelles as powders for insulin pulmonary delivery, Nanomedicine, 11, 2305-2317, 2016

Machado, Sarmento,++, Development and in vivo safety assessment of tenofovir-loaded nanoparticles-in-film as a novel vaginal microbicide delivery system, Acta Biomaterialia, 44, 332-340, 2016

Araujo, Sarmento, ++, In vivo dual-delivery of glucagon like peptide -1 (GLP-1) and dipeptidyl peptidase-4 (DPP4) inhibitor through composites prepared by microfluidics for diabetes therapy, Nanoscale, 8, 10706 – 10713, 2016

Catarina Oliveira Silva

CBIOS - ULHT, Campo Grande, 376, 1749-024 Lisboa, Portugal; Faculty of Pharmacy, University of Alcalá, Ctra. Universidad Complutense, 28871 Alcalá de Henares, Spain.

catarina.m.oliveira.silva@gmail.com

Advances and current approaches of photoactivated functionalized nanoparticles in cancer targeting treatment

Cancer is one of the leading causes of mortality worldwide, and is foreseen that its incidence will continue to rise, as a result of the population aging and increasing risk factors [1]. Over the last decades, scientific research and medical care are focused on finding more effective and safer solutions to reduce the burden of cancer and improve patients' survival and quality of life. In this context, precision medicine has evolve, improving the access to innovative technologies, which offer early diagnosis and better treatment options. While contributing greatly to this recent progress, the Nanotechnology field provide multiple functionalities and a promising role in targeted tumor therapy. For instance, hybrid nanoparticles, made of polymers, metallic or bioactive compounds, have been developed to mitigate limitations associated with tumor targeting, safety issues and multiple resistance to conventional treatments. Amongst all the available nanostructures, gold nanoparticles have been widely studied for light-based applications, due to high absorption coefficient, potential versatility and functionalization [2]. Photothermal therapy, using targeted gold nanoparticles and laser irradiation with near-infrared light (NIR, 700-1200 nm), is a technique that enhance tumor cell death, penetrating deeper into the tumor tissue and preventing its growth. Currently, some of these nanosystems moved forward in clinical trials, combining both diagnostic and therapeutic approaches and photothermal chemotherapy. Hence, we have developed multifunctional nanoparticles with the potential to destroy melanoma cells at their initial stage [3, 4]. Briefly, two strategies were appraised: 1) polymeric nanoparticles with a core-shell structure, loaded with Parvifloron D (cytotoxic drug); 2) gold nanoparticles functionalized with the ligand Epidermal Growth Factor (EGF) and photoactivated by NIR laser irradiation. Overall, nanoparticles with a size of 100 nm and spherical morphology were successfully coated with hyaluronic and oleic acids, maintaining their long-term stability (Figure 1). Functionalization was achieved with multiple targeting moieties, by electrostatic interactions. Both nanosystems were able to internalize the cells overexpressing specific cancer receptors, decrease melanoma cells viability and showed a safe *in vitro* cytotoxic profile over normal-like cells. In preliminary *in vivo* studies, these therapeutic approaches promoted extensive necrosis of human cutaneous melanoma A375 cells and reduced tumor growth (up to 80%), without damage of the surrounding tissue.

Acknowledgments

Financial support was provided by the Portuguese Foundation for Science and Technology (PTDC/BBB-BMC/0611/2012) and Universidad de Alcalá and CBIOS/ULHT under the EHEA Doctorate Programme in Health Sciences.

References

[1] Ferlay J., et al., Int J Cancer, 5 (2016) E359-86.
[2] Abdeer N.S., Murphy C.J., J Phys Chem C 120 (2016), 4691–4716.
[3] Silva C.O., et al., Ther Deliv, 7 (2016), 521-44.
[4] Silva C.O., et al., PLoS ONE 11 (2016), e0165419.

Figures

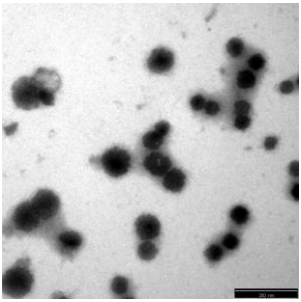

Figure 1: TEM image of EGF conjugated hybrid gold nanoparticles for photothermal therapy (at scale bar of 250 nm).

Mário G. Silveirinha

University of Lisbon-Instituto Superior Técnico and Instituto de Telecomunicações, Portugal

mario.silveirinha@co.it.pt

Topological Photonic Systems

The discovery of topological light states unveiled a myriad of physical platforms wherein the wave propagation is impervious to perturbations of the propagation path and immune to back-reflections [1, 2].

In this talk, I will present an overview of our work on topological photonic systems [1-7]. In particular, I will highlight that there is a wide class of three-dimensional photonic systems – in some cases formed only by time-reversal invariant materials – wherein the transport of light is protected against back-scattering [4]. Specifically, an optical system invariant under the action of the composition of the parity, time-reversal, and duality operators (*PTD*) may enable bidirectional waveguiding immune to arbitrary deformations of the propagation path (see Fig. 1). Furthermore, I will discuss the consequences of the intriguing properties of topologically protected unidirectional edge states in the context of fluctuational electrodynamics. It will be shown that topological edge states may induce a circulation (with no net sinks or sources) of thermal (or zero-point) energy in closed orbits, such that the angular momentum of the electromagnetic field is nonzero [5]. Furthermore, the topological edge states may also induce a spontaneous lateral recoil force when an excited atom is placed in the vicinity of a topological material [6-7].

References

[1] M. G. Silveirinha, "Chern Invariants for Continuous Media", Phys. Rev. B, 92, 125153, 2015.

[2] M. G. Silveirinha, "Bulk-edge correspondence for topological photonic continua", Phys. Rev. B, 94, 205105, 2016.

[3] M. G. Silveirinha, "Z2 Topological Index for Continuous Photonic Materials", Phys. Rev. B, 93, 075110, 2016.

[4] M. G. Silveirinha, "PTD Symmetry Protected Scattering Anomaly in Optics", Phys. Rev. B, 95, 035153, 2017.

[5] M. G. Silveirinha, "Topological Angular Momentum and Radiative Heat Transport in Closed Orbits", Phys. Rev. B, 95, 115103, 2017.

[6] M. G. Silveirinha, S. A. H. Gangaraj, G. W. Hanson, M. Antezza, "Fluctuation-induced forces on an atom near a photonic topological material", arXiv:1711.04941

[7] S. A. H. Gangaraj, G. W. Hanson, M. Antezza, M. G. Silveirinha, "Spontaneous lateral atomic recoil force close to a photonic topological material", arXiv:1711.04939

Figures

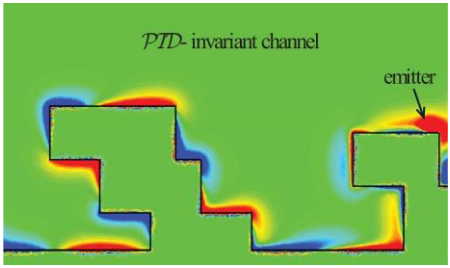

Figure 1: Waveguiding in a bi-directional PTD-invariant channel that supports edge waves protected against back-scattering.

Raquel Verdejo, Marianella Hernández, Miguel A. Lopez-Manchado

Instituto de Ciencia y Tecnología de Polímeros, ICTP-CSIC, C/Juan de la Cierva, 3, Madrid, Spain
www.nanocomp.ictp.csic.es

r.verdejo@csic.es

Polymer nanocomposites: from thermosets to elastomeric matrices

The addition of carbon nanotubes (CNT) to polymer matrices has already been shown to improve their mechanical, electrical and thermal properties. Although significant advances have been made in recent years, these tend to be modest compared to the theoretical performance due to unresolved processing issues. Hence, graphene sheets provide an alternative option to produce functional nanocomposites due to their excellent properties and the natural abundance of its precursor, graphite [1].

The purpose of the studies reported here was to investigate the inclusion of thermally exfoliated graphene (TRG) sheets in a range of polymer systems, both thermoset and elastomers, and to understand their effects on the curing, morphology and properties [2-10].

The graphene sheets used in these studies were synthesised in our laboratories from the thermal exfoliation and reduction of graphite oxide (GO). GO was produced using natural graphite powder (universal grade, 200-mesh, 99.9995%) according to the Brödie method. This method presents a lower disruption of the Csp2 graphitic structure than the Hummers method due to a lower oxidation degree, the oxygen contents by elemental analysis are 28% and 48%, respectively. The exfoliation was carried out at 1000 °C under inert atmosphere and did not completely remove the oxygen-containing groups [12].

Both elastomeric [2-5] and thermosets [6-11] matrices showed improved mechanical and functional properties when compared to the CNT systems without adversely affecting processing. The different systems are especially interesting because of the widespread industrial application.

References

[1] R. Verdejo, M. M. Bernal, L. J. Romasanta and M. A. Lopez-Manchado, J. Mater. Chem., 21, (2011), 3301.
[2] R. Verdejo, F. Barroso-Bujans, M. A. Rodriguez-Perez, J. A. de Saja and M. A. Lopez-Manchado, J. Mater. Chem., 18, (2008), 2221.
[3] R. Verdejo, C. Saiz-Arroyo, J. Carretero-Gonzalez, F. Barroso-Bujans, M. A. Rodriguez-Perez and M. A. Lopez-Manchado, Eur. Polym. J., 44, (2008), 2790.
[4] L. J. Romasanta, M. Hernandez, M. A. Lopez-Manchado and R. Verdejo, Nanoscale Res. Lett., 6, (2011), 508.
[5] M. Hernandez, M. D. Bernal, R. Verdejo, T. A. Ezquerra and M. A. Lopez-Manchado, Compos. Sci. Technol., 73, (2012), 40.
[6] M. Martin-Gallego, R. Verdejo, M. Khayet, J. M. O. d. Zarate, M. Essalhi and M. A. Lopez-Manchado, Nanoscale Res. Lett., 6, (2011), 610
[7] M. Martin-Gallego, R. Verdejo, M. A. Lopez-Manchado and M. Sangermano, Polymer, 52, (2011), 4664.
[8] M. Martin-Gallego, M. Hernandez, V. Lorenzo, R. Verdejo, M. A. Lopez-Manchado and M. Sangermano, Polymer, 53, (2012), 1831.
[9] J.M. Vázquez-Moreno, V. Yuste-Sánchez, R. Sánchez-Hidalgo, R. Verdejo, M.A. Lopez-Manchado, L. Fernández-García, C. Blanco, R. Menéndez, Eur. Polym. J., 93, (2017), 1.
[10] M. M. Bernal, M. Martin-Gallego, L. J. Romasanta, A. C. Mortamet, M. A. Lopez-Manchado, A. J. Ryan and R. Verdejo, Polymer, 53, (2012), 4025.
[11] M. M. Bernal, I. Molenberg, S. Estravis, M. A. Rodriguez-Perez, I. Huynen, M. A. Lopez-Manchado and R. Verdejo, J. Mater. Sci., 47, (2012), 5673.
[12] C. Botas, P. Álvarez, P. Blanco, M. Granda, C. Blanco, R. Santamaría, L.J. Romasanta, R. Verdejo, M.A. López-Manchado, R. Menéndez, Carbon, 65, (2013), 156.

Guilherme Vilhena, Ruben Perez
Departamento de Física Teórica de la Materia Condensada, Universidad Autónoma de Madrid, E-28049 Madrid, Spain
guilhermevilhena@gmail.com

Atomistic understanding of the mechanical properties of bio-molecules

In the past decades, single molecule (SM) experiments have allow us to unravel many different complex mechanisms at a molecular level. Interestingly, its achievements may be found in very disparate research fields, e.g.: unraveling the origins of superlubric (lack of) friction between some solid surfaces, controlling chemical reactions with atomic resolution, understanding the operation of molecular motors present in living cells, and most recently they have also shown the ability to track relevant metabolic information of living cells (volume, size, mass) with an unprecedented time and spacial resolution. The ubiquity of these findings reminds us of the general interest in controlling processes at a molecular scale while extracting relevant observables when doing so.

Despite their undisputed merit, associating mechanical response of a given molecule with conformational changes at an atomic level it is still an utmost challenging task. In this talk, we will give a birds eye view of how atomically detailed molecular dynamics (MD) simulations allow us to not only qualitatively reproduce the results obtained in these experiments but also it allow us to overcome this SM limitation particularly by providing insights on how deformations/motions occurring at the atomic scale relate to their physical properties. In particular, we shall show how these simulations allow us to understand: how a single atom may drastically alter mechanical properties of a molecule (DNA/RNA)[1]; how internal molecular degrees of freedom allows us to tune friction and adhesion at a molecular level in vacuum conditions [2,3,4]; how the complex force/indentation curve obtained in Atomic-Force-Microscopy experiments of complex biomolecules conducted in liquids may be deconvoluted into simpler atomistic mechanisms, namely local molecular elasticity and (hydrophobic) adhesive effects[].

References

[1] A. Marin-Gonzalez, J. G. Vilhena, et al. **Proc. Natl. Acad. Sci.** 114 (27), 7049 (2017)
[2] J. G. Vilhena, et al. **ACS Nano** 10(4), 4288 (2016)
[3] J. J. Mazo, et al **Phys. Rev. Lett.** 118 (24), 246101 (2017)
[4] J. G. Vilhena, et al. **J. Phys. Chem. B** (2017)
[5] Marta P. Ruiz, et al. **J. Am. Chem. Soc** 139 (43), 15337 (2017)
[6] P. Rubio-Pereda, J. G. Vilhena, et al. **J. Chem. Phys.** 146(21), 214704 (2017)
[7] Guillermo López-Polín, et al. **Carbon** 116, 670 (2017)
[8] J. G. Vilhena, et al. **Langmuir** 32 (7), 1742 (2016)
[9] J. G. Vilhena, et al. **Nanoscale** 8 (27), 13463 (2016)

Figures

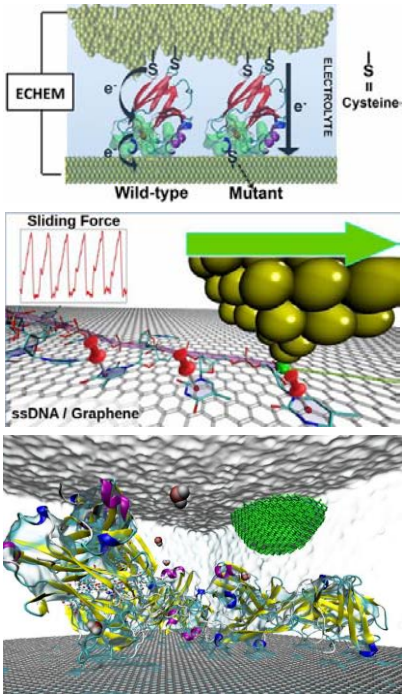

Figure 1: Atomistic representation of: (top) how single point mutation in a protein drastically affect its electronic properties [5]; (middle) sliding a single-stranded DNA molecule over a graphene surface in vacuum while measuring the corresponding friction force [4]; (bottom) virtual atomic force microscope – atomistic simulation of the indentation of an antibody (IgG) deposited over a graphene surface with the system fully embedded in water.

Abstracts Orals

Bruno Amorim

CeFEMA, Instituto Superior Técnico, Universidade de Lisboa, Av. Rovisco Pais, 1049-001, Lisboa, Portugal

bruno.a.c.amorim@tecnico.ulisboa.pt

General theoretical description of photoemission spectroscopy of van der Waals heterostructures

Abstract

Angle resolved photoemission spectroscopy (ARPES) is an extensively used tool to characterize the electronic properties of materials, generally interpreted as a direct probe to their electronic band structure. This view is not strictly true as the signal measured in ARPES is actually weighted by matrix elements, which describe the photo-induced electronic transition from a crystal bound state to a nearly free photoemitted electron state. These matrix elements can have a strong momentum dependence, which affect the visibility of different bands in ARPES. ARPES matrix elements are known to play an important role in cases where different bands are strongly coupled, such as in graphene and graphite [1], and in systems where there is a competition between different periodicities [2]. Both these effects are important in van der Waals (vdW) heterostructures - which are formed by stacked layers of different two-dimensional materials, with promising applications in electronics and light detection [3]. The lattice mismatch and/or misalignment between different layers naturally leads to a competition between periodicities. Therefore, in vdW structures ARPES cannot be interpreted as a direct probe to the electronic band structure. I present a general theory [4], based on tight-binding Hamiltonians, to model ARPES in both commensurate and incommensurate vdW heterostructures with arbitrary lattice mismatch/misalignment. As an example, I apply the general method to the case of twisted bilayer graphene, obtaining the ARPES bands and ARPES constant energy maps. The present theory should be useful in correctly interpreting experimental ARPES results of vdW structures and other system displaying competition between different periodicities, such as density wave phases.

References

[1] E. L. Shirley et al., PRB 51 (1995) 13614

[2] J. Voit et al., Science 290 (2000) 501

[3] K. S. Novoselov and A. H. Castro Neto, Phys. Scr. 2012 (2012) 014006

[4] B. Amorim, arXiv:1711.02499 (2017)

Figures

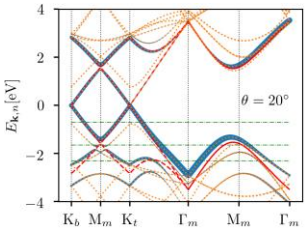

Figure 1: Computed ARPES bands (thick blue lines, the thickness is proportional to the visibility of the bands) and band structure (dotted yellow lines) for bilayer graphene with a twist angle of 20º. The ARPES bands mostly follow the bands of the decoupled layers (red dashed lines). The horizontal lines represent the energies at which the constant energy maps of Figure 2 are computed.

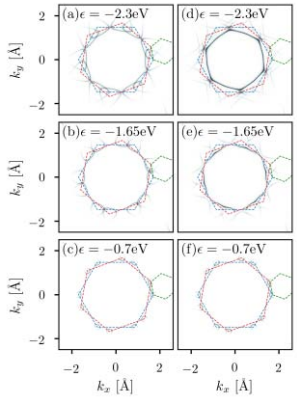

Figure 2: Computed ARPES constant energy maps for bilayer graphene with a twist angle of 20º. (a-c) ARPES maps in the absence of coupling between the layers. (d-f) Reconstructed maps due to interlayer coupling. The crescent shape of the constant energy surfaces is due to the ARPES

Isilda Amorim, Junyuan Xu, Lifeng Liu*

International Iberian Nanotechnology Laboratory (INL), Avda. Mestre José Veiga, 4715-330 Braga, Portugal

lifeng.liu@inl.int

Ternary cobalt-nickel phosphide nanowire catalysts for electrochemical oxygen and hydrogen evolution in alkaline media

Electrochemical water splitting enabled by renewable energy sources represents a promising approach to the generation of clean and high-purity hydrogen (H_2) fuels because unlike steam reforming of hydrocarbons this process does not emit any pollutants. Despite the advantages, the cost of water electrolyzers prohibits their market penetration and makes electrolysis not an economically viable approach for the production of H_2. In order to reduce the production costs and improve the overall water splitting performance it's important to develop highly efficient, low-cost and durable electrocatalysts in order to drive the hydrogen evolution (HER) and oxygen evolution reactions (OER). In this context, several new nanostructured catalysts have been recently synthetized based on the transition metal phosphides (TMPs) to expedite the OER and HER.[1,2]

In this talk, ternary Co_xNi_yP nanowires (NWs) and their catalytic performance for both OER and HER will be presented. These NWs were fabricated by a facile hydrothermal method with different Co:Ni ratios, followed by a phosphorization treatment with NaH_2PO_2 at a low temperature. The Co_xNi_yP nanowires with a Co:Ni ratio of 1:1, relative to those with Co:Ni ratios of 2:1 and 10:1 as well as binary CoP and NiP, show the best electrocatalytic performance for OER in 1.0M KOH: a benchmark anodic current density of 10 mA cm^{-2} can be achieved at a small overpotential of 301 mV, with a moderate Tafel slope of 54 mV dec^{-1}. Furthermore, all the catalysts show long-term durability. When tested under HER conditions in the same alkaline electrolyte, the catalysts also exhibit reasonably good activity with best performance achieved by CoNiP NWs with the Co:Ni ratio of 1:1.

References

[1] X. Wang, W. Li, D. Xiong, L. Liu, *J. Mater. Chem. A.*, *4* (2016) 5639.

[2] X. Wang, W. Li, D. Xiong, D. Y. Petrovykh, L. Liu, *Adv. Funct. Mater. 26* (2016) 4067.

Figures

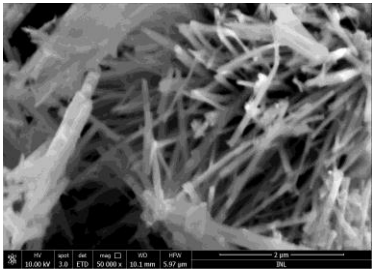

Figure 1: SEM image at high magnification of the as-fabricated CoNiP (10:1) powders.

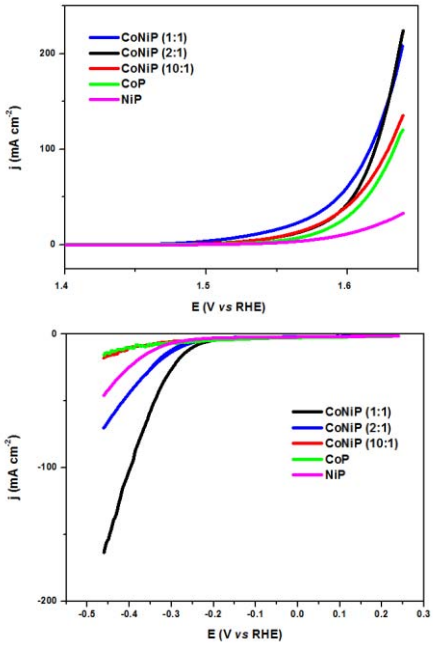

Figure 2: iR-corrected polarization curves of CoNiP with different ratios of Co:Ni on glassy carbon electrode for (top) OER and (bottom) HER in 1.0 M KOH.

Nitin M. Batra, Pedro M. F. J. Costa

King Abdullah University of Science and Technology, Physical Sciences and Engineering Division, Thuwal 23955-6900, Saudi Arabia.

Nitinkumar.batra@kaust.edu.sa

Current-induced structural changes in stressed silver nanowires

Silver (Ag) nanowires (NWs) are a potential replacement of indium tin oxide films as conductive transparent electrodes in touch screens and solar cells. Ag NWs have excellent electrical (e.g. high resistance to electromigration) and optical properties, are easy to process and would enable bendable devices. To understand their response to extreme current densities and improve the overall stability of devices, the failure mechanism of Ag NWs has been studied under different conditions in this work.[1-3] When subjected to a high current density, a straight Ag NW breaks down following a common needle-type failure (**Fig. 1**). While literature extrapolates this for devices, in reality, when NWs are processed to form layered electrodes, a number of them will be bent. Expectedly, a finite amount of internal stress is generated in the NW depending on the degree of bending. Therefore, it is important to investigate the stability and failure mechanisms of bent NWs under the influence of current. Here, we employed transmission electron microscopy (TEM) to study the vibration, self-oscillation, electromigration and stress relaxation (through elastic and plastic deformation) of Ag NWs under the influence of both current and mechanical stresses (**Fig. 2**). The response of the bent NWs is significantly different from the straight ones both in failure mechanisms and restructuring capability.

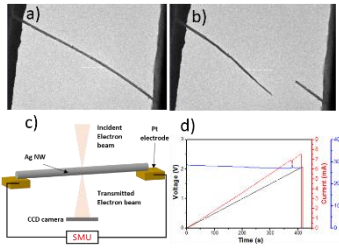

Figure 1: (a)-(b) TEM images of a Ag NW before and after failure due to Joule heating, (c) Schematic of the setup for in-situ TEM electrical characterization, (d) Voltage (current, resistance) vs. time curve.

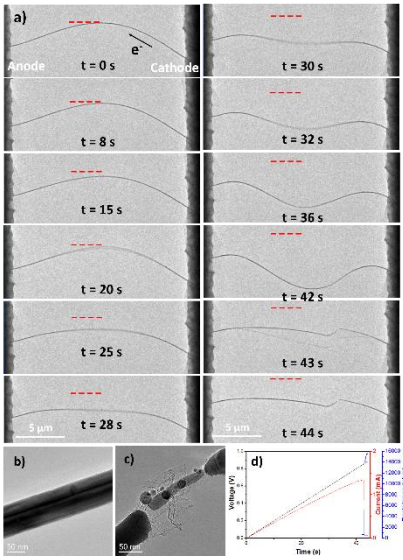

Figure 2: (a) Time-series of TEM images for the current-induced restructuring of a bent Ag NW (estimated bending strain of 0.21% and bending stress of 165 MPa) - the red dotted lines acts as a visual guide; (b)-(c) high magnification TEM images of the Ag NW in (a) before and after failure, respectively; (d) Voltage (current, resistance) vs. time curve.

References

D. Kim, S. H. Kim, J. H. Kim, J. C. Lee, J. P. Ahn and S. W. Kim, Scientific Reports 7 (2017)

B. Hwang, T. Kim and S. M. Han, Extreme Mechanics Letters 8 (2016) 266-272.

J.-Y. Lee, S. T. Connor, Y. Cui and P. Peumans, Nano Letters 8 (2008) 689-672.

David Botequim[1,2], Duarte M. F. Prazeres[2], Sílvia M. B. Costa[1], and Pedro M. R. Paulo[1]

[1]Centro de Química Estrutural, Instituto Superior Técnico, Universidade de Lisboa, Av. Rovisco Pais 1, 1049-001 Lisboa, Portugal
[2]iBB - Institute for Bioengineering and Biosciences, Department of Bioengineering, Instituto Superior Técnico, Universidade de Lisboa, Av. Rovisco Pais, 1049-001 Lisboa, Portugal

davidbotequim@tecnico.ulisboa.pt

Fluorescence Enhancement of Labeled Oligonucleotides Using Plasmonic Gold Nanorods Toward Biosensing Applications

Biosensor devices have potential application in clinical diagnosis, because some diseases may be detected from the presence of biomarkers in urine, body tissues or blood [1]. One strategy for the development of these devices is to use colloidal metal nanostructures, mostly because they strongly absorb and scatter light at characteristic wavelengths due to the localized surface plasmon resonance (LSPR) [2]. Furthermore, these plasmonic sensors can be used as optical nanoantennas to couple light more efficiently in excitation and emission from fluorescent dyes [3]. In addition, the response of the sensor is concentrated at regions of large plasmon-enhanced near field, or hot-spots, which in gold nanorods are located at their tips (Fig. 1). These hot-spots can be exploited in plasmonic sensors to probe molecular binding events. In this sense, the site-selective functionalization of plasmon hot-spots with bioreceptors is fundamental to create plasmonic sensors with improved response by capturing the target species at the most sensitive regions of the nanoparticle [4]. Here, we report the enhancement of fluorescence of oligonucleotides labeled with ATTO647N dye (Fig. 2) by using gold nanorods as plasmonic antennas. We observe strong fluorescence bursts that are attributed to the dye-labeled oligonucleotide exploring the hot-spot regions at the tip of the gold nanorods.

Acknowledgements: Authors gratefully acknowledge financial support from Fundação para a Ciência e a Tecnologia, FCT (Pest-OE/QUI/UI0100/2013/2014, PTDC/CTM-NAN/2700/2012 and SFRH/BPD/111906/2015). David Botequim thanks the BIOTECnico PhD Program and FCT for PD/BD/113630/2015 grant.

References

[1] K. M. Mayer et al., Chem. Rev., 2011, 111, 3828.
[2] El-Sayed and Eustis, Chem. Soc. Rev., 2006, 35, 209-217.
[3] S. Khatua et al., ACS Nano 2014, 8, 4440-4449
[4] P. M. R. Paulo et al., Langmuir 2017, 33, 6503-6510.

Figures

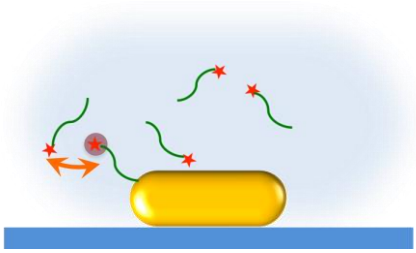

Figure 1: Scheme showing the fluorescence enhancement experiment that depicts oligonucleotides (green line) labeled with Atto-647N dye (red star) in solution diffusing around a gold nanorod and eventually exploring the hot-spot regions (tips).

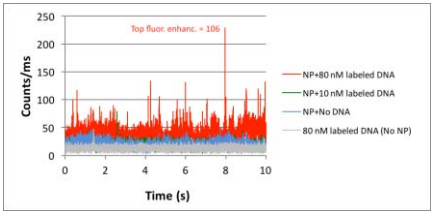

Figure 2: Emission intensity time trace measured from an individual gold nanoparticle: in the absence of Atto-647N dye labeled oligonucleotides in solution (blue curve); in the presence of oligonucleotide labeled with Atto-647N dye in solution: 10 nM (green curve) and 80 nM (red curve); emission time trace from a region of the surface without any particle, but in the presence of 80 nM oligonucleotide labeled with Atto-647N dye (grey curve).

João E. H. Braz[1], B. Amorim[1], Eduardo V. Castro[1,2]

[1]CeFEMA, Instituto Superior Técnico, Universidade de Lisboa, Av. Rovisco Pais 1, Lisbon, Portugal
[2]Beijing Computational Science Research Center, Beijing 100084, China

joao.braz@tecnico.ulisboa.pt

Valley polarized magnetic state in hole-doped monolayers of transition metal dichalcogenides

Spontaneous valley polarization was predicted and experimentally confirmed over thirty years ago for Si inversion layers [1,2]. The isolation of real 2D materials with hexagonal lattice like graphene has put valley physics in the spotlight again; yet, the manipulation of the two valleys of graphene is not easy to achieve [3]. Such manipulation has been demonstrated for the class of 2D materials known as semiconducting transition metal dichalcogenides (TMDs) [4]. In this work, we predict that hole doped TMDs, in particular those with large spin-splitting of the valence band like WS_2, display a valley polarized ferromagnetic (VPF) phase. A typical phase diagram is shown in Figs. 1(a) and (b), in the plane of intra-orbital U Coulomb interaction and hole density n_{hole}, and in the plane of U and inter-orbital U′ interaction, respectively. The valence band in the normal and VPF phases are respectively plotted in Figs. 1(c) and (e), showing how the sizable spin-splitting couples the valley and spin degrees of freedom. The VPF phase lifts the degeneracy of the inequivalent valleys, polarizing the material in the two degrees of freedom. This degeneracy lifting allows for anomalous Hall (AH) responses [5], in virtue of the Berry curvature of these bands [6]. We predict an AH response that is proportional to the Berry curvature at the K points and to the total magnetization density of the system. This response is simultaneously valley- and spin-polarized, thus providing a measurable signature of the VPF phase. This work is currently in pre-print [7].

References

[1] W. L. Bloss, L. J. Sham, and V. Vinter, Phys. Rev. Lett. 43, 1529 (1979)
[2] T. Cole, B. McCombe, J. Quinn, and R. Kalia, Phys. Rev. Lett. 46, 1096 (1981)
[3] A. H. Castro Neto, F. Guinea, N. M. R. Peres, K. S. Novoselov, and A. K. Geim, Rev. Mod. Phys. 81, 109 (2009)
[4] X. Xu, W. Yao, D. Xiao, and T. F. Heinz, Nat. Phys. 10, 343 (2014)
[5] D. Xiao, M.-C. Chang, and Q. Niu, Rev. Mod. Phys. 82, 1959 (2010)
[6] D. Xiao, G.-B. Liu, W. Feng, X. Xu, and W. Yao, Phys. Rev. Lett. 108, 196802 (2012)
[7] João E. H. Braz, B. Amorim, Eduardo V. Castro, arXiv:1712.07157 [cond-mat.mes-hall] (2017)

Figures

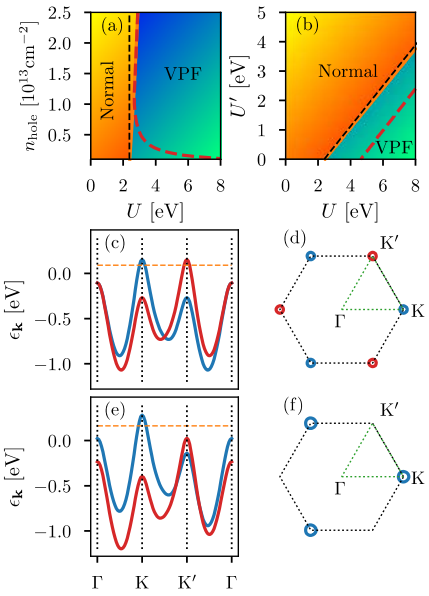

Figure 1: (a) Mean field phase diagram in the n_{hole}–U plane, indicating the normal and VPF phases, at a temperature of T=1K and U′=0 for the TMD WS_2. The dashed red line indicates the transition at T=100K. The vertical dashed line represents the estimated critical U of 2.38 eV in the limit of low T and n_{hole} obtained using a low energy model. (b) Phase diagram in the U–U′ plane at a hole density of n_{hole}=0.2×10^{13} cm^{-2} and T=1K. The dashed red line shows the transition line at the temperature of T=100K. The dashed black line indicates the critical line U=U_c+1.4U′, estimated using the low energy model. Panels (c) and (e) show the band structure for the spin up (in red) and spin down (in blue) valence bands in the normal and VPF phases, respectively. The horizontal dashed line indicates the Fermi level for a constant particle number of n_{hole}=0.2×10^{13} cm^{-2}. The Fermi surfaces for the normal and VPF phases are represented in panels (d) and (f), respectively.

V. Carnevali[1,2], G. Soldano[4], Z. Zhiyu[3,#], M. Mariscal[4], C. Africh[2], G. Comelli[1,2], M. Peressi[1,2]

[1]University of Trieste, via A. Valerio 2, Trieste, Italy
[2]CNR-IOM TASC, S. S. di Basovizza km 163,5, Trieste, Italy
[3] ICTP, viale Miramare 12, Tireste, Italy
[4] INFIQC CONICET-UNC, Córdoba, Argentina
[#] presently at Vienna University of Technology, Karlsplatz 13, Vienna, Austria

virginia.carnevali@phd.units.it

Evolution of moiré structures of graphene adlayers on Ni(100) surface

Graphene on Nickel (100) surface forms a variety of moiré superstructures, due to interfacial lattice parameter and symmetry mismatch. The moiré patterns depend on the misorientation angle and vary from stripe-like to rhombic-network morphology [1]. Physisorbed and chemisorbed regions alternate in stripe-moiré patterns, as shown by combined experimental scanning tunneling microscopy and density functional theory (DFT) simulations. Partial merging of adjacent physisorbed stripes is observed in real samples cooling down the temperature, causing local detachment of graphene from the Nickel surface. The mechanism is investigated with a Kinetic Monte Carlo approach and DFT calculations, which includes surface carbon segregation and local carbide formation.

Figures

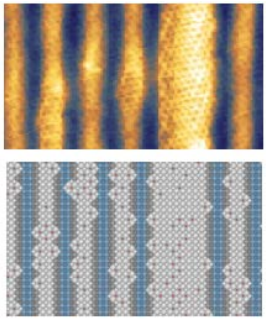

Figure 1: Comparison between STM measurement (top) and Kinetic Monte Carlo simulation (bottom) in presence of carbide segregation for the stripe-like moiré pattern.

References

[1] Zhiyu Z. et al., just accepted by Carbon

Eduardo V. Castro, Frederico Sousa e Bruno Amorim

Instituto Superior Técnico, Av. Rovisco Pais, 1049-001 Lisboa, Portugal

eduardo.castro@tecnico.ulisboa.pt

Dilute Magnetism in Graphene

Abstract

It is known that hydrogenated graphene exhibits a ferromagnetic phase when a carbon buffer layer is also present [1, 2]. The root to this magnetic ordering is the interplay between the itinerant electrons in graphene and the local magnetic moments induced by impurities. The resultant RKKY interaction is ferromagnetic for impurities on the same sub-lattice, and anti-ferromagnetic if the impurities sit on different sub-lattices. Whether the magnetic phases survive down to the lowest impurity densities, what is the effect of the disorder due to the random positions of the adatoms, and how does the critical temperature change with charge doping, are key questions that we have answered theoretically using a s-d like model [3].

For impurities on the same sub-lattice, we have obtained the phase diagram shown in Fig. 1. For low concentration of impurities, the Curie temperature decreases linearly, but this behavior changes considerably if we make the s-d interaction anisotropic. For the isotropic case, the fact that the Curie temperature is still finite for impurity densities as low as 1% is a non-trivial result. The dependence of the Curie temperature on the charge density in graphene Is shown in Fig. 2. Interestingly enough, one could switch the magnetization on and off through an electric field effect which changes the charge density.

We have applied this theory to the description of a recent experiment on graphene with sulfur impurities [4]. It provides an alternative explanation which circumvents some difficulties of the theory used in [4] to explain the experiment.

We have also simulated the case when the magnetic impurities distribute equally on both sub-lattices. We will also discuss this case.

References

[1] L. Xie et al., Applied Physics Letters, 98 (2011) 193113

[2] A. Giesbers et al., Phys. Rev. Lett., 111 (2013) 166101

[3] F. Sousa, B. Amorim, and E. V. Castro, submitted

[4] C. Hwang at al., Sci Re., 6 (2016) 21460

Figures

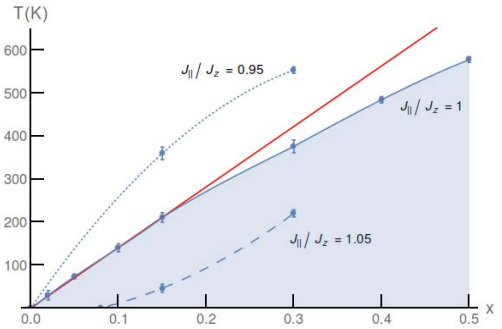

Figure 1: Critical temperature for one-lattice ferromagnetism at half-filling.

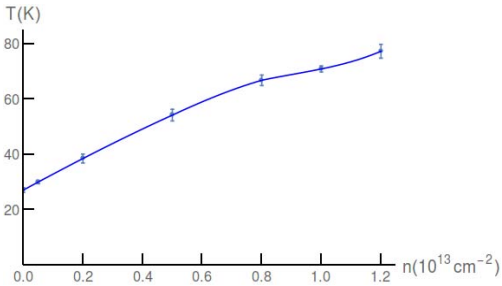

Figure 2: Critical temperature for one-lattice ferromagnetism as a function of electronic doping.

Jérôme CAYSSOL, Jonathan Atteia, Jens Bardarson

Université de Bordeaux, LOMA, 341 Cours de la Libération, 33405 Talence, France

Jerome.cayssol@u-bordeaux.fr

Ballistic transport in irradiated graphene

In this talk, i will present our results on the bulk conductance of ballistic graphene transistors driven by a circularly polarized electromagnetic wave (typically in the THz range). The differential conductance is calculated as a function of the carrier density (of the non irradiated graphene) and driving strength.

We focus on the doped regime where strong suppressions of the bulk conductance are obtained for several broad ranges of doping. These conductance dips are related to emergent gaps in the Floquet quasi-energy spectrum, leading to a transport dominated by evanescent waves in the conduction channel of the transistor. Besides, in the undoped regime, we have also studied the so-called minimum conductance of irradiated graphene-based transistor.

References

[1] J. Atteia, J.H. Bardarson, and J. Cayssol, arXiv:1709:00090

Xuecheng Chen, Ewa Mijowska

Nanomaterials Physicochemistry Department ,
West Pomeranian University of Technolgy, Piastow 45,
Szczecin, Poland

xchen@zut.edu.pl

Synthesis of Nanoporous carbon from waste Polymer and Potential Application in Electrochemical Energy Storage

Abstract

Mesoporous graphene flakes and three-dimensional hollow carbon spheres/graphene flakes were selectively prepared from decomposition of waste polymer using MgO flakes and iron oxide as the templates. Through controlling the weight ratio of MgO to polymer, different graphene flakes and three-dimensional hollow carbon spheres/graphene flakes were obtained. The electrochemical properties of obtained graphene flakes and three-dimensional hollow carbon spheres/graphene flakes were investigated in detail. As electrode materials of supercapacitor and lithium ion battery, the prepared mesoporous flakes and three-dimensional hollow carbon spheres/graphene flakes showed improved electrochemical performance. The present method paved the way for the treatment of waste polymer in the future.

References

[1] Yanliang Wen, Jie Liu, Jiangfeng Song, Jiang Gong, Hao Chen, Tao Tang, RSC Adv., 5 (2015) 105047

[2] Qianqian Li , Kun Yao , Guangchun Zhang , Jiang Gong , Ewa Mijowska , Krzysztof Kierzek , Xuecheng Chen, Xi Zhao , and Tao Tang, Part. Part. Syst. Charact. 32 (2015), 874–879.

Figures

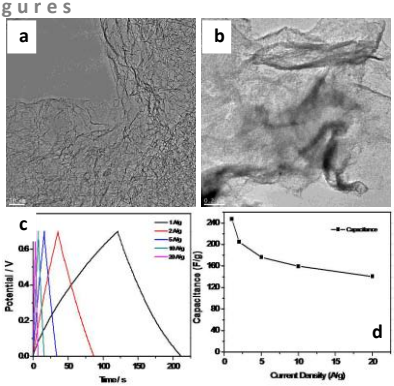

Figure 1: TEM images of graphene flakes from waste polymer (a) and (b) MnO_2 nanorods supported on graphene flakes. (c) Galvanostatic charge/discharge curves of GF/MnO_2 composites collected at different current densities. (d) Specific capacities with different current densities. (5 M KCl as the electrolyte).

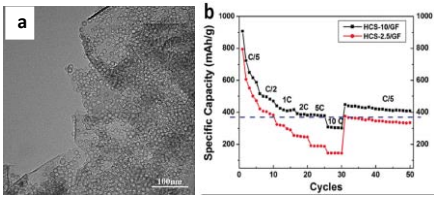

Figure 2: (a) TEM image of hollow carbon spheres/graphene flakes (b) Rate performance of hollow carbon spheres/graphene flakes used as anode materials of lithium ion battery.

Pedro M. F. J. Costa, A. Alazmi, O. El Tall, M. N. Hedhili

King Abdullah University of Science and Technology, Thuwal 23955-6900, Saudi Arabia

pedro.dacosta@kaust.edu.sa

Rational design of graphene-based adsorbents for CO_2 uptake

In the last three decades, carbon materials have been under the spotlight. The report of structures with nanoscaled dimensions such as fullerene molecules, carbon nanotubes and graphene has spurred an interest in applying these for technological applications as diverse as energy storage systems or environmental remediation.

The large-scale capture and storage of carbon dioxide is expected to mitigate climate change worldwide. One of the primary emitters of CO_2 are fossil-fueled power plants. To address these emissions, gas capture technology that can be retrofitted to existing facilities is required. In this respect, the CO_2 capture by physical adsorption in porous materials is considered to be the most feasible approach. Microporous carbons are one such material that can be easily tailored for this purpose. Interestingly, and while other options have been extensively studied (activated carbon, graphene, carbon nanotubes, etc.), the use of graphite/graphene oxide (GO) remains rather unexplored.

In this communication, we will illustrate how the synthesis conditions of graphene oxide flakes (Hummer's, HGO, and Improved Hummer's, IGO) [1] may influence its uptake capacity of carbon dioxide [2, 3]. To validate these results two benchmark materials, namely zeolite 13X and certified carbon nanotubes, were also studied under similar conditions to the GOs. As we changed the synthesis approach of GO, so was its surface area (Fig. 1a), porosity profile and CO_2 adsorption capacity modified significantly. In some instances, this resulted in doubling of gas uptake (Fig. 1b).

References

[1] Alazmi, A.; Rasul, S.; Patole, S. P.; Costa, P. M. F. J., Polyhedron 116 (2016), 153-161.

[2] A. Alazmi, O. El-Tall, M. N. Hedhili, P. M. F. J. Costa, submitted (2017).

[3] A. Alazmi, P. M. F. J. Costa, "Graphene materials and improved methods of making, drying and applications", Patent PCT/IB2017/054680.

Figures

a)

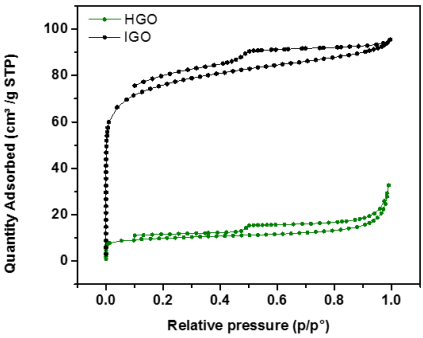

b)

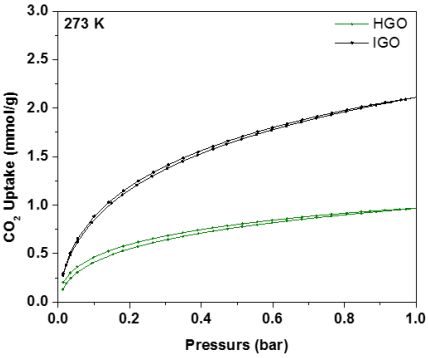

Figure 1: (a) N_2 adsorption–desorption isotherms of HGO and IGO, at 77 K; (b) Pure component CO_2 adsorption isotherms for the HGO and IGO materials.

Soraia P. S. Fernandes[a], Sara R. Pinela[a,b], Abdelkarim Mellah[a,c], Begoña Espiña[a], Laura M. Salonen[a]

[a] International Iberian Nanotechnology Laboratory, Av. Mestre José Veiga, 4715-330 Braga, Portugal
[b] CEB – Centre of Biological Engineering, University of Minho, 4710-057 Braga, Portugal
[c] Centre de Recherche Scientifique et Technique sur les Régions Arides (CRSTRA), Biskra, Algeria

soraia.fernandes@inl.int

Covalent Organic Frameworks as a New Tool for the Capture of Hazardous Compounds from Water

Hazardous compounds are found in water with increasing frequency raising concerns about their negative effects on aquatic ecosystems and human health [1]. The production of biotoxins by marine microalgae, such as okadaic acid (OA), during harmful algal blooms (HABs) and the presence of pharmaceutical contaminants, such as ibuprofen, in water resources endanger the public health and pose a worldwide environmental problem [2]. Thus, the development of more efficient sensing, monitoring, and capturing methodologies for water treatment is urgently necessary [3]. Adsorption is an attractive tecnhique for water monitoring and purification due to its simplicity and efficacy [1]. The development of novel adsorbents can provide a more effective and selective detection and capture of contaminants. Thus, the development of new and improved adsorbents is urgently needed.

Two-dimensional (2D) covalent organic frameworks (COFs) are crystalline nanoporous materials formed by the self-assembly of purely organic building blocks into sheets, which undergo stacking interactions in the third dimension. They possess high thermal stability and structural diversity [4], and show promise as adsorbents since they can meet the requirements [5] for an efficient adsorbent of water-stability and high surface area.

We found [6] the literature-known water-stable COF derivative TpBD-Me_2 [7] to adsorb OA from water over 30 times more efficiently than the most commonly used polystyrene resin HP-20 [8]. TpBD-Me_2 can be reused for at least three adsorption/desorption cycles without a significant loss in efficiency [7]. The adsorption capacity of pharmaceutical contaminants from water was also evaluated using different COF derivatives, showing good efficiency of capture. These promising results highlight the potential of these materials for water monitoring applications and demonstrate their capacity to adsorb hazardous compounds from water.

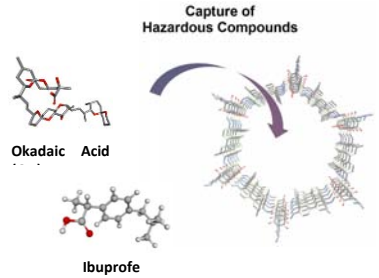

References

[1] M. M. Khin, A. S. Nair, V. J. Babu, R. Murugan, S. Ramakrishna, Energy Environ. Sci., 5 (2012) 8075–8109

[2] L. Kantiani, M. Llorca, J. Sanchís, M. Farré, D. Barceló, Anal. Bioanal. Chem., 398 (2010) 2413–2427

[3] C. Zhang, J. Zhang, Environ. Anal. Chem., 2 (2015) 1–12

[4] S. Y. Ding, W. Wang, Chem. Soc. Rev., 42 (2013) 548–568

[5] Z. P. Qi, J. M. Yang, Y. S. Kang, F. Guo, W. Y. Sun, Dalt. Trans., 45 (2016) 8753–8759

[6] L. M. Salonen, S. R. Pinela, S. P. S. Fernandes, J. Louçano, E. Carbó-Argibay, M. P. Sarría, C. Rodríguez-Abreu, B. Espiña, J. Chromatogr. A, 1525 (2017) 17–22

[7] S. Chandra, S. Kandambeth, B. P. Biswal, B. Lukose, S. M. Kunjir, M. Chaudhary, R. Babarao, T. Heine, R. Banerjee, J. Am. Chem. Soc., 135 (2013) 17853–17861

[8] A. Li, F. Ma, X. Song, R. Yu, J. Chromatogr. A., 1218 (2011) 1437–1442.

Josep Ferré-Borrull, Elisabet Xifré-Pérez, Chris Eckstein, Josep Pallarès and Lluis F. Marsal
Universitat Rovira i Virgili, Av. Paisos Catalans 26, 43007 , Tarragona, Spain
lluis.marsal@urv.cat

Optical monitoring of surface modifications in nanoporous materials

Nanoporous materials such as porous silicon (pSi) and nanoporous anodic alumina (NAA) are increasing their interest as enabling platforms for biotechnology (Figure 1). Such materials are obtained from the electrochemical etching in acidic electrolytes of bulk silicon or aluminum, respectively. Preparation methods are at present well-known, cost-effective and easily scalable[1]. In the application of such materials to biotechnologies, one crucial step is functionalization: modification of the pore surface properties in order to provide the appropriate functions. Such surface modification is achieved by the attachment of different molecules such as silane self-assembled monolayers (SAM), proteins or aptamers and has enabled applications in fields such as sensing, drug delivery or tissue engineering[2,3].

In this work we study different surface modification paths for pSi and NAA with different methods. Besides the usual SEM characterization, nanometric pores require other strategies to evaluate the amount of attached species on their walls. We apply optical methods for such evaluation: the reflection intereference spefctroscopy (RIfS)[4] and the fluid imbibition-coupled laser interferometry (FICLI)[5]. In RIfS, the reflectance spectra of thin films of porous materials are measured before and after the surface modification (Figure 2) and the change in effective optical thickness (EOT) of the thin film can be related to the change in surface structure. On the other hand, in FICLI, the infiltration of a liquid in a porous material is monitored in real time and the filling dynamics are related to the structure and surface properties (Figure 3). The work will report the latest results obtained with these two methods on both kinds of material and for different attached SAMs and proteins.

References

[1] Ferré-Borrull, J. et al., Materials, 7 (2014) 5225
[2] Baranowska, M. et al., Colloids and Surfaces B: Biointerfaces, 122 (2014) 375
[3] Baranowska M. et al., Journal of Colloid and Interface Science, 452 (2015) 180.
[4] Macias, G. et al., Analyst, 140 (2015) 4848.
[5] Eckstein, C. et al., Langmuir, 32 (2016), 10467.

Acknowledgements

This work was supported by the Spanish MINECO (TEC2015-71324-R), the Catalan authority AGAUR (2014SGR1344), and ICREA under the ICREA Academia Award.

Figures

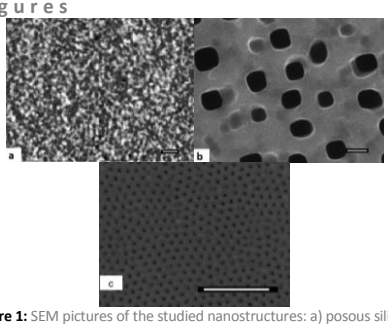

Figure 1: SEM pictures of the studied nanostructures: a) posous silicon, b) macroporous silicon and c) nanoporous anodic alumina. The bars are 1 micron.

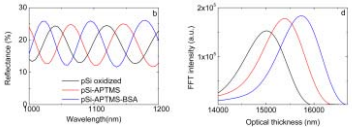

Figure 2: RIfS spectra of Psi After different surface modifications (left) and corresponding Fourier transform where the maximum corresponds to the EOT (right).

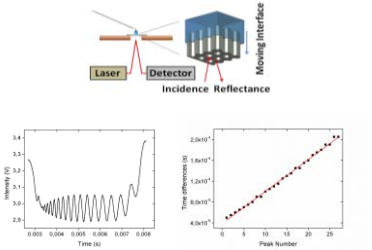

Figure 3: (Top) schematic drawing of the FICLI method to determine pore geometry and surface properties. (Bottom left) example of tiume-resolve interferogram obtained by the method and (bottom right)analysis of the interferogram.

Ana G. Silva[1,†], Dylan Marques[1,2], Adelaide Miranda[2], Peter R. T. Munro[3], Pieter A. A. De Beule[2,‡]

[1] Departamento de Física, Faculdade de Ciências e Tecnologia, Universidade Nova de Lisboa, Campus de Caparica, Caparica, P-2829-516, Portugal

[2] Applied Nano-Optics Group, Department of Life Sciences, International Iberian Nanotechnology Laboratory, Braga 4715-330, Portugal

[3] Department of Medical Physics and Biomedical Engineering, University College London, Malet Place, Gower Street, London, WC1E 6BT, United Kingdom

†acs@fct.unl.pt; ‡Pieter.de-beule@inl.int

Bioimaging of exo - or endocytosis with interference microscopic imaging

We integrate a rigorous scattering model for cellular exo- or endocytosis, taking into account lipid-induced optical anisotropy, with a rigorous model of Differential Interference Contrast (DIC) image formation (Figures 1&2). Hereby we provide a theoretical proof for the first time to a well-known experimental fact in DIC microscopy, namely, that a bias of 1/100 of the wavelength of light is optimal for the observation of intracellular components.

Some implementations of interference microscopy imaging use digital holographic measurements of complex scattered fields to reconstruct three-dimensional refractive index maps of weakly scattering, semi-transparent objects, frequently encountered in biological investigations. Reconstruction occurs through application of the object scattering potential which assumes an isotropic refractive index throughout the object. Here, we demonstrate that this assumption can in some circumstances be invalid for biological imaging due to the presence of lipid-induced optical anisotropy. We show that the nanoscale organization of lipids in the observation of cellular endocytosis with polarized light induces a significant change in far field scattering. We obtain this result by presenting a general solution to Maxwell's equations describing light scattering of core-shell particles near an isotropic substrate covered with an anisotropic thin film. By applying our solution to study light scattering by a lipid vesicle near a lipid bilayer, whereby the lipids are represented through a biaxial optical model. We conclude that effective amounts of lipid-induced optical anisotropy significantly alter far-field optical scattering in respect to an equivalent optical model that neglects the presence of optical anisotropy.

Figures

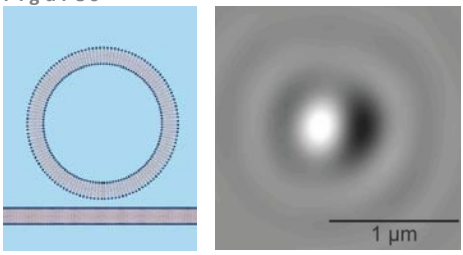

Figure 1: DIC microscopy modelling of a lipid vesicle approaching a lipid bilayer.

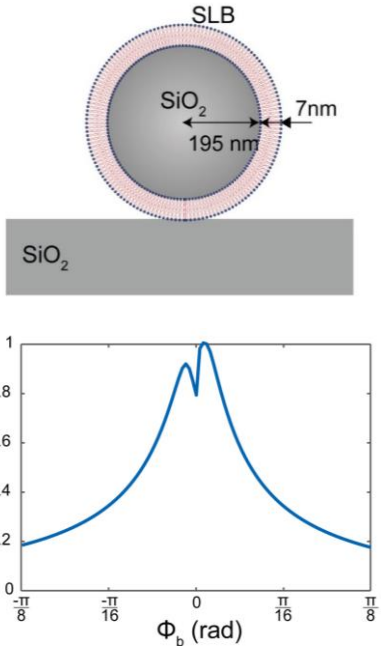

Figure 2: Influence of DIC bias on the contrast achieved for a nanoparticle surrounded by a lipid bilayer

Ana Gomez[1,2], Adelaide Miranda[1], Matej Siketanc[3], Juliane Lopes de Assis[4], Rafael RHF Valverde[4], Marcelo Einicker Lamas[4], Bruno F.B Silva[1], Pieter A. A. De Beule[1]‡ and Aline Marie Fernandes[1,4]†

[1] International Iberian Nanotechnology Laboratory, Avenida Mestre José Veiga s/n, 4715-330, Braga, Portugal
[2] Department of Applied Physics, Faculty of Optics and Optometry, s/n, Universidade de Santiago de Compostela, E-15782 Santiago de Compostela (Spain)
[3] University of Basel, Switzerland
[4] Biomembranes Laboratory, Carlos Chagas Filho Biophysics Institute, Federal University of Rio de Janeiro, Avenida Carlos Chagas Filho 373, 21941-902, Rio de Janeiro, Brasil

†aline.fernandes@inl.int; ‡Pieter.de-beule@inl.int

New lipoplex formulation to efficiently transfect human fibroblast: Fluorescence Cross Correlation Spectroscopy as tool for lipoplex characterization

We present a new formulation of DNA liposome characterized by Fluorescence Cross Correlation Spectroscopy (FCCS) to efficiently transfect human somatic cells. Liposomes have been considered as the best carrier to delivery drugs and genes to cells due to their properties[1]. It is known that the composition of the vesicle has huge impact on efficiency of transfection as well on its toxicity. For that, we tested the cytotoxicity and transfection of 28 combinations including DOPE, DOPC, DOTAP and Ceramide DiI stained lipids. As shown in figure 1, comparing to a commercial Lipofectamine® 2000, some of the liposomes presented lower toxicity and better transfection efficiency. Using a combination of previous stained plasmids (labeled with rhodamine or FITC), we used FCCS to quantitatively control the load of these genes into liposomes (figure 2). Our data shows that, not only our lipoplexes preparation had better results as delivery tool for human somatic cells but also the use of FCCS to visualize the properly formation of lipoplex[2] could be use in further applications for pharmaceuticals industry and also on nanomedicine field.

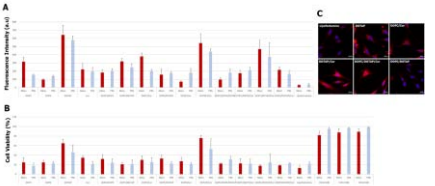

Figure 1 – Cell viability and transfection efficiency analysis: A) DiI fluorescent intensity analysis on microplate reader (549/650 nm); B) PrestoBlue assay and C) Immunofluorescence images of nucleous (DAPI, blue) and liposomes stained with DiI (red).

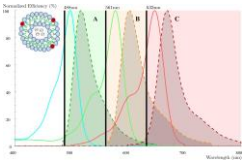

Figure 2 – Illustration showing the three colors to be analyzed at FFCS: liposome stained with DiI (561 nm), different plasmids stained with Rhodamine (633 nm) and FITC (488 nm).

References

[1] Allen,T. M. & Cullis, P.R., Adv. Drug Deliv. Rev., 65, 36-48 (2013).
[2] Ridgeway WK, Millar DP, Williamson JR. J PhysChem B.116, 6, 1908-1919 (2012).

F. Gontad, B. M. Hidalgo-Robatto, M. Doiro, S. Chiussi, J. Serra, P. González

New Materials Group, Department of Applied Physics, IISGS, University of Vigo, Campus Lagoas-Marcosende, 36310 Vigo, Spain

fgontad@uvigo.es

Development of new coatings from marine bioceramics and silver nanoparticles by pulsed laser deposition

Recent works have proposed the reutilization of marine fishing byproducts for the fabrication of ceramics with high biocompatibility [1,2]. Like other biomaterials, these new bioceramics, in addition to their use as bone fillers, can also be applied as coatings, that can be fabricated by different methods, amongst them, pulsed laser deposition [3]. It is well known that such bioceramic coatings are an excellent strategy to improve the biocompatibilty of metal implants and great advances have been achieved in this field during the last decades. However, there is still plenty of room for their improvement. Adding additional biological properties, such as bactericidal effects, increases the interest in the applicability of these materials. In this regard, it is known that silver has inhibitory and bactericidal effects and a broad spectrum of antimicrobial activities [4]. Accordingly, the use of silver (Ag) in the shape of small metallic nanoparticles on top of the bioceramic coatings, seem to be a promising approach. On the other hand, the use of Ag nanoparticles allows us to explore possible applications in the field of biosensors, based on the phenomenon known as plasmon resonance (PR), proper of noble metal nanoparticles.

Thus, this work reports on the growth of a biocompatible ceramic coating obtained from marine fishing byproducts, with silver nanoparticles on top, through a single Pulsed Laser Deposition process.

Metallic disks, simulating the implant material, were successively covered with the bioceramic film and the silver nanoparticles using a pulsed ArF excimer laser (20 ns, 193 nm). Their morphological analysis was carried out by means of Scanning Electron Microscopy (SEM) and Atomic Force Microscopy (AFM); their chemical composition was studied through X-ray Photoelectron Spectroscopy (XPS); and, finally UV-Visible spectroscopy was used for their optical characterization, taking special attention to the plasmonic character of the silver nanoparticles (Figure 1). Hence, we report the fabrication of a new coating from the combination of marine bioceramic and silver nanoparticles as promising alternatives to be used in metallic prostheses, analyzing the influence of the number of laser shots used for the deposition on their physicochemical properties and potential biological effects.

References

[1] M. López-Álvarez, E. Vigo, C. Rodríguez-Valencia, V. Outeiriño-Iglesias, P. González, J. Serra, Clin. Oral Impl. Res. 28 (2017) e91–e100

[2] M. López-Álvarez, S. Pérez-Davila, C. Rodríguez-Valencia, P. González and J. Serra, Biomed. Mater. 11 (2016) 035011

[3] B. León, Pulsed laser deposition of thin calcium phosphate coatings, in: J.A. Jansen, B. León (Eds.), Thin Calcium Phosphate Coatings for Medical Implants, Springer, New York (2009), pp. 101–156.

[4] J. H. Shepherd, D. V. Shepherd, S. M. Best, J. Mater. Sci.: Mater. Med. 23 (2012) 2335–2347

Figures

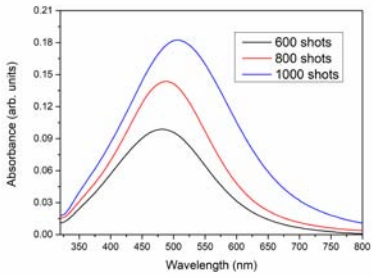

Figure 1: UV-Visible spectra of the Ag nanoparticles deposited by pulsed laser deposition with different number of laser pulses.

Nicolas F. Martinez[1], Louis Pacheco[1]

[1]Concept Scientific Instruments, 2 Rue de la Terre de Feu, 91940 Les Ulis, France
f.martinez@csinstruments.eu

Advanced nano-electrical characterization of solar cells and 2-d materials with atomic force microcopy

Over the past 30 years, Atomic Force Microscopy has evolved from a microscope to measure just the surface topography to a wide variety of measurement modes that provides a way to characterize other atomic interactions or physical properties like magnetic field, electric field, nanoscale dissipation processes, thermal conductivity, electrical conductivity, resistance, surface potential, piezoresponse, Young modulus,… Electrical nanocharacterization with AFM has emerged as a powerful tool to map electrical properties at the nanoscale, like surface potential (work function) and conductivity. However, traditional setups in AFM make difficult to obtain accurate and repeteable results over several types of samples. Specially in the solar cells field, where both in-plane and cross-section electrical characterization need to be performed.

In this contribution we will show the capabilities new developed AFM modes: High Definition Kelvin Force Microscopy (HD-KFM), ResiScope, Soft-Resiscope and Scaning Microwave that overcome the intrinsic difficulties of electrical nanocharacterization with AFM. This techniques have been applied on a variety of solar cells samples providing high stability, sensitivity and lateral resolution.

References

[1].G. Binnig, C.F. Quate, Ch. Gerber, Phys. Rev. Lett. 56, 930 (1986).
[2].Houzé F, Meyer R, Schneegans O, Boyer L.. Appl Phys Lett. 1996;69:1975.
[3].D.W. Abraham, et al, J. Vac. Sci. Technol. B 9,703 (1991)
[4].T.R. Albrecht, P. Grütter, D. Horne, D. Rugar, J. Appl. Phys. 69, 668 (1991).
[5].T.R.Rodriguez and R.Garcia App. Phys. Lett. 84(3):449-451
[6]. J. Colchero, A. Gil, A.M. Baró, Phys. Rev. B 64, 245403 (2001)

Figures

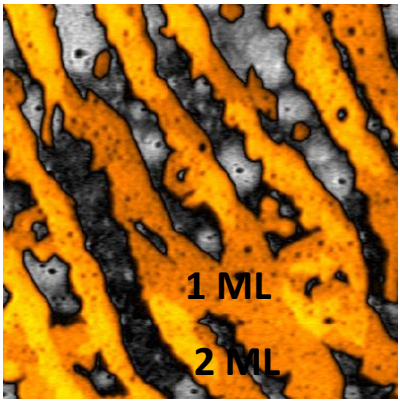

Figure 1: HD-KFM image on Graphene

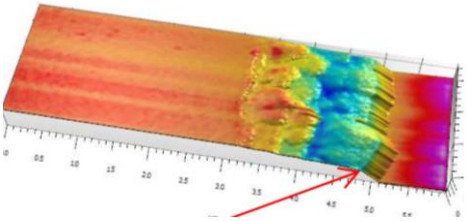

Figure 2: HD-KFM image of a cleaved perovskite solar cell

Javier Martinez[1], J. P. González[2], D. Sanz González[2], J. Morales Merino[2], S. Fernández[2], J. Cárabe[2], A. Molinero[2], J.M. Barcala[2], M.B. Gómez-Mancebo[2], R. Fernández[2], I. Rucandio[2], A. Boscá[1], J. Pedrós[1], A. Ladrón de Guevara[1],F. Calle[1]

[1]ISOM, Universidad Politécnica de Madrid, Ciudad Universitaria, Madrid, Spain.
[2]CIEMAT, Avda. Complutense 40, Madrid, Spain

javier.martinez@upm.es

Graphene Silicon-Heterojunction Solar Cells

Abstract

ONE Silicon-heterojunction cells represent one of the most promising approaches in photovoltaics, with record efficiencies above 26% [1]. These cells have very thin and relatively resistive front emitters, so they need transparent front electrodes to extract current. State-of-the-art contacts for this application are transparent conductive oxides (TCOs) having a rather limited sheet resistance, of the order of 120 Ω/□. A significant reduction of this parameter would help reduce cell series resistance and hence improve performance. The present work is aimed at developing graphene-based transparent electrodes having sheet resistances about one half of that of TCOs or less.

Graphene samples respectively having one, two and three atomic layers have been optically and electrically characterized. White-light transmission maps have been used to correlate transparency and number of layers. Transmission-line measurements (TLM) using different metal contacts have allowed to assess sheet resistances and contact resistances, leading to the choice of Ti+Ag as a good reference metal contact.

The results obtained so far have yielded graphene sheet resistances which, connected in parallel with present TCOs could well allow to attain 50 to 60 Ω/□ with an excellent optical transmission. The full compatibility between graphene transfer methods and cell materials and surfaces is being tested. Low [2]- and high-temperature transfer procedures are being compared.

The work undergone so far clearly suggests the possibility to noticeably improve transparent electrodes with this approach and therefore to further enhance silicon-heterojunction cell performance.

References

[1] M. Green et al., Prog. in Photovolt, Res. Appl, 25 (2017) 3

[2] A. Bosca et al, Scientific Reports, 6 (2016) 21676

Figures

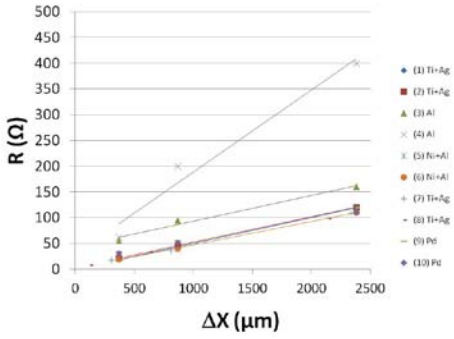

Figure 1: TLM measurement results

Acknowledgement

Work supported by MINECO project GRAFAGEN (ENE2013-47904-C3).

I.Montoya[1], L.E. Fernandez-Outon[2,3], C. Redondo[1], W. A. A. Macedo[3], R. Morales[4,5]

[1] Chemical Physics Department, Universidad del País Vasco UPV/EHU, 48940 Leioa, Spain.
[2]Departamento de Física, Universidade Federal de Minas Gerais, 31270-901, Belo Horizonte, MG, Brazil
[3]Centro de Desenvolvimento da Tecnologia Nuclear, CDTN , 30123-970 Belo Horizonte, MG, Brazil
[4] Chemical Physics Dept & BCMaterials, Universidad del País Vasco UPV/EHU, 48940 Leioa, Spain.
[5]IKERBASQUE, Basque Foundation for Science, 48011 Bilbao, Spain.

isaac.montoya@ehu.eus

Temperature evolution of antiferromagnetic domains in patterned exchange bias systems

Exchange Bias (EB) phenomenon manifests as an induced magnetic anisotropy in coupled ferromagnetic/ antiferromagnetic (FM/AFM) materials. It can be understood as an alignment and pinning of AFM spins at the FM/AFM interface parallel to FM spins upon cooling below the AFM Néel temperature. The introduction of competing anisotropies, e.g. via lateral patterning of FM/AFM thin films, can give rise to new magnetic properties. For technological reasons, this EB size dependence is of particular interest for the miniaturization of spintronic devices.

Our work investigates the thermal stability of patterned polycrystalline IrMn/FeCo (AFM/FM) bilayers. IrMn/FeCo lines were fabricated by physical etching of continuous bilayers. EB was induced by thermal annealing under external magnetic fields. Two annealing conditions were considered; external field applied either parallel or perpendicular to the line axis. The magnetic effect of imprinted AFM domains was studied at room temperature and low temperature after a field-cooling procedure.

Despite the direction of the annealing field with respect to the lines, the system always shows the same unidirectional anisotropy (EB) axis at room temperature, which is along the line axis. This unexpected behavior is observed even when high magnetic fields are applied during the annealing procedure. This is in contrast to previously reported results.[1]

After annealing, a field-cooling procedure was performed in order to study the stability of AFM domains. The magnitude of the exchange bias field increases at lower temperatures. However, positive cooling fields induce negative EB, while negative cooling fields yield positive EB, even though when the hysteresis loop was negatively shifted at room temperature. Meaning that, the unidirectional anisotropy is set by AFM domains rotating towards the cooling field direction.

This work was supported by grants: EU FP7-MCA-318901, EU H2020-MSCA-734801, Basque PRE-2015-1-0385, Spanish AEI-MINECO FIS2013-45469 and FIS2016-76058, and CNEN, Fapemig, Capes, CNPq.

Figures

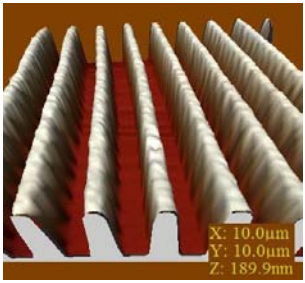

Figure 1: Atomic force microscopy image of patterned IrMn/FeCo bilayer.

References

[1] A. Hoffmann, M. Grimsditch, J.E. Pearson, J. Nogues,W.W.A. Macedo, I.K. Schuller, Phys. Rev. B 67 (2003) 220406.

Rute Nunes[1,2,3*], Francisca Araújo[1,2,3], Inês Bártolo[4], Nuno Taveira[4], José das Neves[1,2,5], Bruno Sarmento[1,2,5]

[1]i3S, Instituto de Investigação e Inovação em Saúde, Porto, 4200-135, Portugal; [2]INEB, Instituto de Engenharia Biomédica, Biocarrier Group, Porto, 4200-135, Portugal; [3]ICBAS, Instituto Ciências Biomédicas Abel Salazar, University of Porto, Porto, 4050-313, Portugal; [4] Unidade dos Retrovírus e Infecções Associadas, Centro de Patogénese Molecular e Instituto de Investigação do Medicamento (iMed.ULisboa), [5]CESPU, Instituto de Investigação e Formação Avançada em Ciências e Tecnologias da Saúde, Gandra, 4585-116, Portugal

*rute.nunes@ineb.up.pt

Efavirenz-loaded poly (ethylene oxide)-modified nanoparticles as potential rectal anti-HIV microbicides

Objective

Mucus penetrating nanoparticles (NPs) obtained by dense poly (ethylene oxide) (PEO)-coating are promising platforms for the delivery of drugs to mucosal surfaces. We developed efavirenz (EFV)-loaded poly (lactic-*co*-glycolic acid) (PLGA) NPs modified at the surface with PEO and tested their potential to be used as rectal microbicides in preventing sexual HIV transmission.

Methods

EFV-loaded PLGA NPs produced by nanoprecipitation and modified by surface adsorption of Poloxamer 407 (a surfactant containing PEO) were characterized regarding their technological and *in vitro* biological properties. Further, NPs were evaluated regarding their colorectal distribution and retention, as well as safety after 14 days of once daily rectal administration to mice.

Results

Dense surface modification of PEO-PLGA NPs (200nm) with PEO was confirmed by ^{1}HNMR analysis. Drug association with NPs did not substantially affect the antiretroviral activity of EFV and improved the cytotoxicity profile of the drug. NPs modified or not with PEO were mainly distributed throughout the last two thirds of the colon of mice. However, PEO-PLGA NPs showed significantly improved retention in colonic tissues over non-modified particles 15 min and 2 h after administration (**Figure 1**). EFV-loaded PEO-PLGA NPs were found safe after 14-day rectal administration, as assessed by histological observation and analysis of IL-1b, IL-6, IFN-γ and TNFα levels in rectal lavages.

Conclusions

EFV-loaded PEO-PLGA NPs appear to be safe and able to distribute and retain in the colorectum, potentially contributing to sustained local drug levels that could be useful in preventing rectal HIV transmission.

Figures

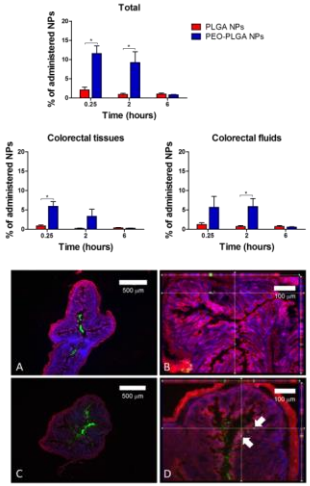

Figure 1: Graphs: Recovery of fluorescent NPs from colorectal tissues at 15 min, 2 and 6h post-administration. Results are expressed as the percentage of the initial amount of NPs. Columns represent mean values and bars the SEM (n=3). (*) denotes a significant difference (p<0.05) when comparing PLGA NPs and PEO-PLGA NPs. Images: Fluorescent microscopy images of Middle colon at 15 min (A,C) and Distal colon at 2 hours (B,D) after rectal administration of PLGA NPs (A,B) and PEO-PLGA NPs (C,D).

Shrabani Panigrahi[1]*, Santanu Jana[2], Tomás Calmeiro[1], Daniela Nunes[1], Rodrigo Martins[1], Elvira Fortunato[1]*

[1]CENIMAT/i3N, Departamento de Ciência dos Materiais, Faculdade de Ciências e Tecnologia–Universidade Nova de Lisboa and CEMOP/Uninova, Campus de Caparica, 2829-516 Caparica, Portugal.

[2] Laboratoire de Physique des Solides, CNRS, Université Paris-Sud, Université Paris-Saclay, 91405 Orsay Cedex, France

spqdot@gmail.com, s.panigrahi@campus.fct.unl.pt

Imaging the Charge Carrier Distribution inside Solar Cell Using Kelvin Probe Force Microscopy

Abstract

The internal potential of the solar cell devices depends on the basic mechanism of photovoltaic effect, such as charge carrier generation, separation, transport, recombination etc. Here we report the direct observation of the surface potential depth profile across the cross-section of the solar cell at different wavelengths of light using Kelvin probe force microscopy (KPFM). However, KPFM, a modified version of Atomic Force Microscopy (AFM), is a non-contact surface technique used to measure the local contact potential difference (CPD) between a conducting AFM tip and the sample.[1,2] We have plotted the CPD profiles across the cross-section of the device and correlated the measured potentials with the material interface positions in the device. The topography and phase images across the cross-section of the solar cell were also observed, where the interfaces of the different layers in the device were well defined in nanoscale range. The influence of the different spectra of light on the generation and transport processes of the charge carriers inside the solar cell have been investigated here. Under steady state solar illumination, a sharp difference in electrical potential is observed across the active layers of the solar cell.[3,4] The results on the distribution of the charge carriers inside the solar cells under different illuminations help to understand the basic charge transport mechanism across the interfaces which open the possibility to design the high performance solar cells in future.

References

[1] W. Melitz, J. Shen, A. C. Kummel, S. Lee, Surf. Sci. Rep 66 (2011) 1-27.

[2] J. B. Li, V. Chawla, B. M.Clemens, Adv. Mater. 24 (2012) 720-723.

[3] S. Panigrahi, T. Calmeiro, R. Martins, D. Nunes, E. Fortunato, ACS Nano 10 (2016) 6139−6146.

[4] S. Panigrahi, S. Jana, T. Calmeiro, D. Nunes, R. Martins, E. Fortunato, ACS Nano, 11 (2017) 10214 -10221.

Figure

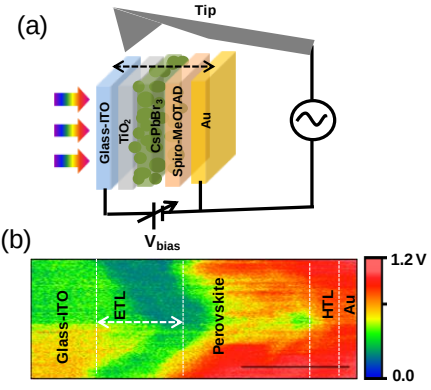

Figure 1: (a) Schematic diagram of the cross-sectional KPFM measurement system. (b) Surface potential image across the layers of the solar cell under solar illumination.

P. Parreira[1,2], C. Monteiro[1,2], V. Graça[2], IC Gonçalves [1,2,3], P. Gomes[4] and MCL Martins[1,2,5]

[1]i3S, Instituto de Investigação e Inovação em Saúde, Universidade do Porto, Porto, Portugal
[2]INEB, Instituto de Engenharia Biomédica, Universidade do Porto, Porto, Portugal
[3]FEUP, Faculdade de Engenharia, Universidade do Porto, Porto, Portugal
[4]UCIBIO-REQUIMTE, Departamento de Química e Bioquímica, Faculdade de Ciências, Universidade do Porto, Porto, Portugal
[5]Instituto de Ciências Biomédicas Abel Salazar, Universidade do Porto, Porto, Portugal

parreira@i3s.up.pt

Bactericidal nanostructured surfaces with high impact against *Helicobacter pylori*

Helicobacter pylori chronic infection leads to several gastric disorders, such as gastric cancer [1]. Success rate of available therapy, based on antibiotics, has dramatically decreased due to bacterial resistance [2]. Antimicrobial peptides (AMPs) are low molecular weight peptides that target bacterial cell membranes and cause disintegration of the lipid bilayer structure, having low propensity to induce resistance [3]. The AMP MSI-78A (GIGKFLKKAKKFAKAFVKILKK), also known as PexigananA, was effective against *H. pylori in vivo* but in dosages close to toxic level [4], which is related to AMPs loss of activity due to susceptibility to extreme pH and proteases [5]. AMP immobilization may allow overcoming these drawbacks and boosting its activity [5].

MSI-78A synthesized with an extra cysteine (C-MSI-78A) was immobilized onto biotinylated model surfaces (self-assembled monolayers; SAMs), using neutravidin as a protein bridge and a biotin-polyethylene glycol $(PEG)_n$-maleimide spacer. Spacers with different PEG_n arm length (n=2; n=11) were tested. Immobilization was characterized with Quartz Crystal Microbalance with Dissipation and best results were obtained with the spacer with PEG11 arm, allowing higher AMP surface coverage. Functionalized surfaces were tested against a human highly pathogenic *H. pylori* strain (*H. pylori* J99). *H. pylori* J99 viability was reduced in 75% for surface adherent bacterial cells and, more outstandingly, viability of planktonic bacteria was reduced in 99% after 2h of exposure to these surfaces. Also, no bacterial recovery occurred when transferred to optimal growth conditions, stressing the bactericidal effect. These results highlight the potential of AMP surface immobilization for development of non-antibiotic therapies against the gastric pathogen while demonstrating, for the first time, the activity of an immobilized AMP against planktonic *H. pylori.*

References

[1] Correa P, Houghton J, Gastroenterology, 133 (2007) 659–72.
[2] Malfertheiner P *et al*, Gut, 61 (2012) 646–64.
[3] Bahar AA, Ren D, Pharmaceuticals, 6 (2013) 1543–75.
[4] Zhang XL, *et al*, Molecules, 20 (2015) 3972–85.
[5] Costa F, *et al*, Acta Biomaterialia, 7 (2011) 1431–40.

Laura Pol, Elisabet Xifre-Perez, Josep Ferre-Borrull, and Lluis F. Marsal

Departament d'Enginyeria Electrònica, Elèctrica i Automàtica, Universitat Rovira i Virgili, Avinguda Països Catalans 26, 43007 Tarragona, Spain

lluis.marsal@urv.cat

Engineered Nanoporous Anodic Alumina Micro and Nanoparticles for Biomedical Applications

Nanometric and micrometric particles have attracted great interest in recent years due to their interesting features for the development of biomedical applications with great social impact [1,2]. Particles that respond to variables in specific tissues in the human body are a novel and promising strategy in health care and quality of life. Recent studies have presented excellent results using particles in the micrometric and nanometric size range in vitro and in vivo [3].

Nanoporous anodic alumina (NAA) is a nanostructured material, excellent for the formation of these particles. NAA consists of hexagonally-ordered straight nanometric pores arranged in an alumina matrix. Its geometric characteristics (pore size, interpore distance, porosity, and thickness) can be molded by the anodization conditions (voltage and time of anodization, temperature, and acid used as electrolyte), with a cost-effective and precise control fabrication [4,5]. Its high effective surface area (hundreds of m^2/cm^3) can be chemically modified with organic compounds [3]. The physical, chemical and optical properties of NAA together with its nontoxicity and its highly stable morphology in buffer solutions makes of NAA an interesting material for the development of particles for biological applications [6]. Another singular characteristic that distinguishes NAA particles from particles made of other materials is their inherent photoluminescence in the visible spectrum range (Figure 1). Besides, its compatibility with biological tissues has been demonstrated with its use in orthopedic prosthetics, dental and coronary stents, cell culture scaffolds, and immunoisolation devices [7].

In this work, we present different NAA particles with a micrometric and nanometric size and we study and evaluate their physical, chemical and optical properties for a wide range of applications in the biomedical and biotechnological fields.

Acknowledgements: This work was supported in part by the Spanish Ministry of Economy and Competitiveness TEC2015-71324-R (MINECO/FEDER), the Catalan authority AGAUR 2017SGR1527, and ICREA under the ICREA Academia Award.

References

[1] E. Xifre-Perez, J. Ferre-Borull, J. Pallares, L.F. Marsal, Mesoporous Biomater., 2 (2015).

[2] M. Alba, B. Delalat, P. Formentín, M.-L. Rogers, L.F. Marsal, N.H. Voelcker, Small, 11 (2015), 4626.

[3] E. Xifre-Perez, S. Guaita-Esteruelas, M. Baranowska, J. Pallares, L. Masana, L.F. Marsal, ACS Appl. Mater. Interfaces, 7 (2015) 18600.

[4] A. Santos, P. Formentín, J. Ferré-Borrull, J. Pallarès, L.F. Marsal, Mater. Lett. 67 (2012) 296-299

[5] L.F. Marsal, L. Vojkuvka, P. Formentin, J. Pallarés, J. Ferré-Borrull, Opt. Mater. 31 (2009) 860.

[6] A. Santos, M. Alba, M.M. Rahman, P. Formentin, J. Ferre-Borrull, J. Pallares, L.F. Marsal, Nanoscale Res. Lett. 7 (2012) 228.

[7] E. Gultepe, D. Nagesha, S. Sridhar, M. Amiji, Adv. Drug Deliv. Rev. 62 (2010) 305.

Figures

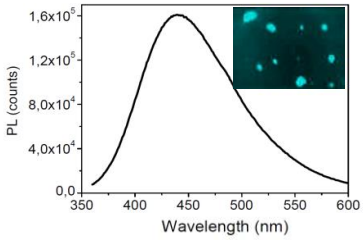

Figure 1: Photoluminescence of NAA particles (excitation wavelength 340 nm). Inset: Blue fluorescence field image of NAA particles.

Osiris Redondo Herrero, Claudio Sbarufatti, Silvia Gonzáles Prolongo, Mónica Campo Gómez

Unversidad Rey Juan Carlos, Calle tulipan sn, Móstoles, Spain.
Politecnico de Milano, Campus Bovisa Sud-Via La Masa 1 Milano, Italia

Osiris.redondo. herrero@urjc.es

ANTI-ICING AND DE-ICING GRAPHENE NAOPARTICLES REINFORCED EPOXY COATINGS

The use of renewable energy sources increases every year, replacing other more pollutants power sources. Wind turbines are frequently located in high altitude location and the snow and ice reduce their productivity due to the freezing of their components.
This research consists on inducing self-healing of nanoreinforced coatings based on Joule effect. A preliminary thermoelectrical evaluation at low temperatures is presented, using the electrical heating properties of graphene nanoparticles (GNPs) reinforced epoxy matrix to anti icing and de-icing applications. Different GNPs/epoxy nanocoatings with different nanofiller percentages and thickness of 200 um, were manufactured in a three-roll-mill machine controlling the gaps and the rollers speed. Anti-icing and de-icing tests were performed into a climatic chamber in the temperature range of -10 to -30 ºC in order to observe coating properties and functionality. The self-heating was promoted by Joule effect, applying low power in DC.

References

[1] S. K. Thomas, R. P. Cassoni, and C. D. Mac Arthur, "Aircraft Anti-Icing and De-Icing Techniques and Modeling," vol. 33, no. 5, 1996.

[2] E. Enríquez, J. F. Fernández, J. De Frutos, and M. A. De la Rubia, "Tailoring of the electrical properties of carbon black–silica coatings for de-icing applications," Ceram. Int., vol. 41, no. 2, Part B, pp. 2735–2743, 2015.

[3] R. Moriche, S. G. Prolongo, M. Sánchez, A. Jiménez-Suárez, M. J. Sayagués, and A. Ureña, "Morphological changes on graphene nanoplatelets induced during dispersion into an epoxy resin by different methods," Compos. Part B Eng., vol. 72, pp. 199–205, 2015.

Figures

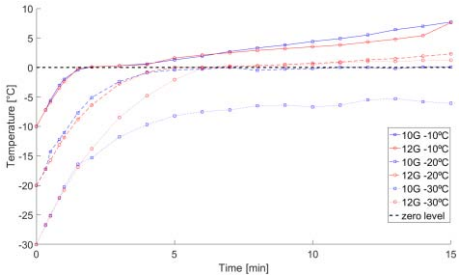

Figure 1: De-icing tests in climatic chamber at different ambient temperatures (-10ºC, -20ºC, -30 ºC) for 10 – 12% weight reinforced samples.

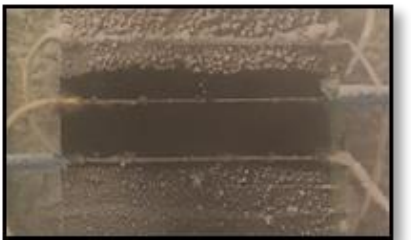

Figure 2: Anti-icing test result for 12% weight reinforced specimen.

G. Rubio-Bollinger, D. Maeso, J. Quereda, A. Castellanos-Gomez, N. Agraït.

Departamento de Física de la Materia Condensada and Condensed Matter Physics Center (IFIMAC), Universidad Autónoma de Madrid, Madrid, E-28049, Spain.

gabino.rubio@uam.es

Electronic transport and photoresponse of single- and few-layer MoS_2 vertical devices

We control electronic transport of vertical metal-atomically thin MoS_2-metal structures generating mechanical strain with the tip of a conductive atomic force microscope [1].
The structures show rectifying current-voltage (I-V) characteristics, with rectification ratios strongly dependent on the applied load. To understand these results, we compare the experimental I-Vs with a double Schottky barrier model, which is in good agreement with our experimental results and allows us to extract quantitative information about the electronic properties of the tip/MoS_2/metal structures and their dependence on the applied load. Finally, we test the stability of the studied structures using them as mechanically tunable current rectifiers.

Additionally, we study the photoresponse of vertical MoS_2 devices [2] using monochromatic illumination in the visible and near infrared range (Figure 2). We observe enhanced responsivity at the energies of the A and B excitons of MoS_2, while the responsivity drops sharply below de energy of the optical gap (1.8 eV).
By using a pulsed light source (pulse duration 1 ns) we observe photocurrent switching times in the range of one microsecond as well as high external quantum efficiency.

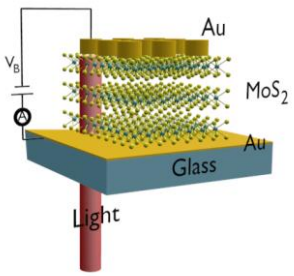

Figure 1: Schematic of vertical metal-2D semiconductor-metal devices obtained by sandwiching a few layer MoS_2 crystal between metallic electrodes.

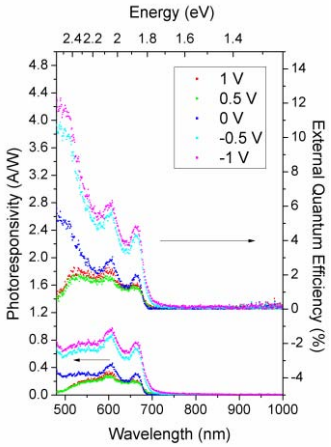

Figure 2: Wavelength dependent photoresponse and external quantum efficiency of the metal-MoS_2-metal devices for different biasing voltages.

References

[1] J. Quereda *et al. 2D Materials* **4**, 021006 (2017).
[2] D. Maeso *et al. To be submitted* (2017).

Miguel V. Vitorino, Arthur Vieria, Carolina A. Marques and Mário S. Rodrigues

Biosystems and Integrative Sciences
Institute/Departamento de Física da Faculdade de Ciências da Universidade de Lisboa,
Campus Faculdade de Ciências da Universidade de Lisboa,
Campo Grande 1749-016, Lisboa, Portugal

mvvitorino@fc.ul.pt

Direct measurement of the nucleation time of a water nanobridge

Water nanocapillary bridges are predominant in nature, have a significant impact in many physico-chemical properties of surfaces and can have a severe influence on the design of nanoelectromechanical devices[1]. They have been extensively studied using nanoscale experimental tools such as the Atomic Force Microscope (AFM). However, basic characteristics such as their nucleation time are still debated. Using AFM, different approaches were followed to measure the meniscus nucleation time, but such approaches suffer from poorly defined local geometry[2] or poor time resolution[3], producing order-of-magnitude contradicting results, that raise questions on the influence of local geometry and surface roughness on the nucleation of the bridges

In this presentation we will introduce a methodology to measure both the nucleation time and the critical nucleation distance for a simplified sphere-plane geometry. This approach is based on a custom-made Force Feedback Microscope (FFM)[4] that circumvents some of the disadvantages of conventional AFM, allowing it to measure the nucleation of a nanocapillary that forms between a carbon sphere and a flat piece of muscovite mica. We will present results demonstrating that the nucleation of these bridges happens within times on the order of a few milliseconds.

References

[1] E. Charlaix and M. Ciccoti, Handbook of Nanophysics, 1 (2010)
[2] R. Szoszkiewicz and E. Riedo, Physical Review Letters, 95 (2005) 135502
[3] B. Sung et al., Applied Physics Letters, 103 (2013) 213107
[4] Rodrigues et al., Applied Physics Letters, 101 (2012) 203105

Marcus A. Worsley

Lawrence Livermore National Laboratory, Livermore, CA, USA

Worsley1@llnl.gov

3D-Printed Graphene-Based Aerogel Electrodes for Energy-Related Applications

Aerogels are monolithic high surface area structures with great potential as electrodes for a number of energy-related applications like energy storage (e.g. supercapacitors, redox flow batteries, Li-ion batteries, etc.), and energy conversion (e.g. hydrogen evolution, oxygen reduction, etc.). However, the random, uncontrolled nature of their porous networks can hinder mass transport and negatively impact device performance. 3D printing provides a means to synthesize aerogels in a manner that can mitigate the mass transport issues by intelligently incorporating macroporous channels into the native nanoporous aerogel structure. This advance in electrode fabrication has the potential to provide an even greater level performance for these hierarchical functional materials. Here we present our recent efforts to 3D print aerogel materials. The 3D printed aerogels exhibit many of the same properties as bulk aerogels, but with some enhancements in mass transport as well as mechanical properties. Energy storage devices based on 3D printed electrodes, which exhibit great rate capability, synergistic capacity, and cycling stability, will be presented.

This work was performed under the auspices of the U.S. Department of Energy by Lawrence Livermore National Laboratory under Contract DE-AC52-07NA27344.

References

[1] P.G. Campbell, M.D. Merrill, B.C. Wood, E. Montalvo, M.A. Worsley, T.F. Baumann, J. Biener, *J. Mater. Chem. A*, 2 (2014) 17764.

[2] C. Zhu, T.Y.-J. Han, E.B Duoss, A. Golobic, J.D. Kuntz, C.M. Spadaccini, M.A. Worsley, *Nature Commun.*, 6 (2015) 6962.

[3] C. Zhu, T. Liu, F. Qian, W. Chen, S Chandrasekaran, B. Yao, Y. Song, E.B. Duoss, J.D. Kuntz, C.M. Spadaccini, M.A. Worsley, Y. Li, *Nano Today*, 15 (2017) 107.

Figures

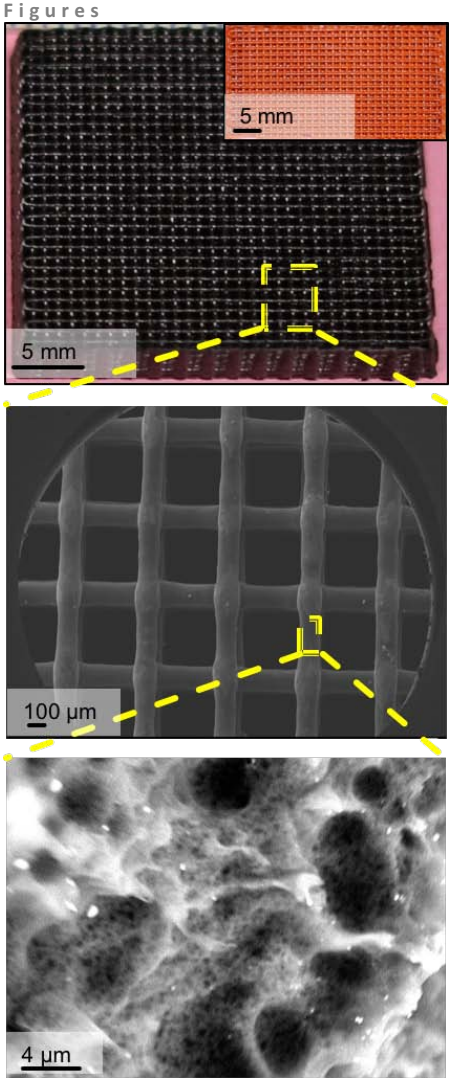

Figure 1: Photograph (top), low magnification (middle), and high magnification (bottom) SEM of 3D-printed carbon aerogel. Inset shows 3D-printed aerogel before carbonization.

Fatema Mohamed[1,2],
Manuel Corva[1,3], Zhijing Feng[1,3], Nicola Seriani[2],
Maria Peressi[1,3,4], Erik Vesselli[1,3]

[1]University of Trieste, via A. Valerio 2, Trieste, Italy
[2]ICTP, Str. Costiera 11, Trieste, Italy
[3]IOM-CNR, S. S. di Basovizza km 163,5, Trieste, Italy
[4]INSTM, Unità di ricerca di Trieste, Italy

fatema.mohamed@phd.units.it

Self-assembled monolayer films of Iron phthalocyanines on thin alumina films: characterization and properties

Electronic and reactivity properties of Iron phthalocyanines have been investigated using Density Functional Theory and scanning tunneling microscopy. Phthalocyanines (Pcs) are organic molecules possessing a central cavity which can accommodate a single metal atom (M). Metal phthalocyanines (MPcs) are able to adsorb on a variety of supports, with ordered structures determined by molecule-molecule and molecule-substrate interactions. Employing metal phthalocyanine self-assembling properties, it is possible to obtain model systems for biomimetic 1-D active centers, where unexpected properties may stem from the utmost low dimensionality. In our work we focus on Iron phthalocyanines deposited on ultrathin alumina films. These molecules self-assemble in highly ordered structures, stable enough to provide optimal candidates for model single atom catalysis. We found that it is possible to control the FePc's self-assembly decorating the alumina layer with Cu nanoclusters, switching between adsorbed structures governed by or molecule-molecule or molecule-substrate interaction.

Figures

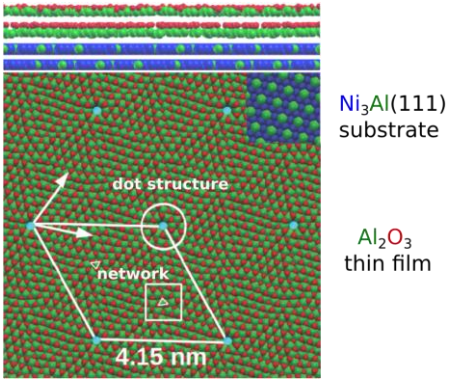

Figure 1: (Structural model of $Al_2O_3/Ni_3Al(111)$)

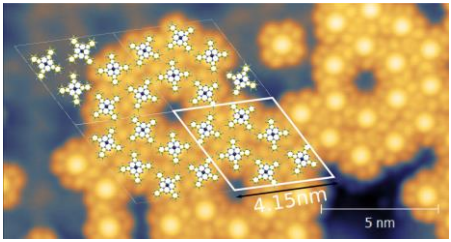

Figure 2: (STM image of FePcs on $Al_2O_3/Ni_3Al(111)$, together with DFT model)

Posters

Encapsulation of *Asparagus* extracts into polymeric nanoparticles for therapeutic purposes

Khaoula Adouni[1], Olfa Zouaoui[1], Hassiba Chahdoura[1], Pedro Fonte[2,3], Patrícia Rijo[2,4,*], Lotfi Achour[1]

[1]Laboratoire de Recherche "Bioressources: Biologie Intégrative & Valorisation, Université de Monastir, Tunisie; [2]CBIOS, ULHT, Campo Grande 376, 1749 – 024, Lisboa, Portugal; [3]UCIBIO, REQUIMTE, Department of Chemical Sciences – Applied Chemistry Lab, Faculty of Pharmacy, University of Porto, Porto, Portugal; [4]iMed.ULisboa, Faculdade de Farmácia, Universidade de Lisboa, 1649-003 Lisboa, Portugal

*patrícia.rijo@ulusofona.pt

Introduction

Plant extracts presents important medicinal properties such as antioxidant and anti-genotoxic, however, its direct application has been limited mostly due to instability during storage (temperature, light, pH, oxygen). Furthermore, to obtain plant extracts, organic solvents are often used, making it undesirable for administration. Considering this, the encapsulation of plant extracts into polymer nanoparticles is a good approach to avoid such problems due to their biocompatibility, biodegradability and controlled release properties [1]. Thus, the aim of this study is to encapsulate an *Asparagus* aqueous extracts into poly lactic-co-glycolic acid (PLGA) nanoparticles for exploitation of its therapeutic properties.

Material and Methods

Plant material and preparation of extracts: Roots and spears of *Asparagus* were dried and grounded. Then, 1 g of the powder was added to distilled water and boiled. After decoction, the extracts from the roots (DR) and the spears (DSP) were freeze-dried. The total phenolic content and antioxidant activity of DR and DSP were investigated using a described methodology [2].

Nanoparticle productions and characterization

The DR and DSP extracts were separately encapsulated into PLGA nanoparticles using a solvent-evaporation double emulsion method previously described [3]. The particle size, polydispersity index (PDI) and zeta potential of nanoparticles were evaluated. The antioxidant activity was measured by the DPPH method, and the encapsulation efficiency (EE) for each extract was determined by the quantification of the total phenolic content (TPC).

Results

As shown in **Table 1**, a variation in the TPC content and antioxidant capacity results was observed between the extracts. The higher antioxidant activity was related with higher TPC values. The nanoparticles characteristics are shown in **Table 2**. A small size particle and PDI values close to 0.1 were find in both formulations. A PDI values around 0.1 indicates a homogenous and mono-dispersity and hence a better particle size distribution [4]. The values of zeta potential were -37 and -41 for DR and DSP respectively, demonstrating a good colloidal stability [5]. Both extracts presented an EE superior of 50%, which is a good achievement for aqueous plant extracts.

Conclusion

The results showed that *Asparagus* is a source of antioxidant compounds. It is foreseen that its encapsulation into polymeric nanoparticles can potentiate the therapeutic benefits of *Asparagus* extracts for multiple health conditions and for administration by different administration routes

References

[1] Armendáriz-Barragán,B., Zafar, N., Badri, W., Galindo-Rodríguez, S.A., Kabbaj, D., Fessi, H. & Elaissari, A. Expert Opinion on Drug Delivery, 8 (2016) 1165–1175.

[2] Jelled A., Ben Hassine, R., Thouri A., Flamini, G. Chahdoura, H. El Arem, A. Ben Lamine, J. kacem, A. Haouas, Z. Ben Cheikh H. and Achour, L. Ind Crops Prod, 95 (2016) 434-443.

[3] Fonte, P., Soares, S., Costa, A., Andrade, J.C., Seabra, V., Reis, S., Sarmento, B. Biomatter, B, 2:4 (2012) 329-339.

[4]Zigoneanu, I.G., Astete, C.E. and Sabliov, C.M. Nanotechnology 19 (2008).

[5] Qi, L., Xu, Z., Jiang, X., Hu, C. and Zou, X. Carbohydrate Research, 339 (2004) 2693-2700.

Tables

Table 1: Total phenolic contents (mg GAE/g) and antioxidant activity (TEAC, µmol TE/g) of *Asparagus* extracts.

	DR	DSP
TPC	81.19±3.33	31.93±0.41
DPPH	207.8±1.2	93.23±1.51

Table 2: Particle size, polydispersity index, zeta potential, and entrapment efficiency (EE) of *Asparagus* nanoparticles

	Size (nm)	PDI	Zeta Potential (mV)	EE (%)
PLGA DR	263.2±3.00	0.17±0.02	-37±4.42	74.72±2.70
PLGA DSP	225.8±13.54	0.14±0.01	-41.7±4.64	52.20±3.41

DEVELOPMENT OF NANOSTRUCTURED-LIPID CARRIERS USING BIOSURFACTANTS FOR ENCAPSULATION OF VITAMINS

Maria A. Azevedo[1,2*], Miguel A. Cerqueira[1], José A. Teixeira[2], Lorenzo Pastrana[1]

[1] INL - International Iberian Nanotechnology Laboratory, Braga, Portugal; [2] CEB – Centre of Biological Engineering, University of Minho, Braga, Portugal;

*alexandra.azevedo@inl.int

Vitamins have an important role in human diet, being essential for normal maintenance, growth and development of human organism. Moreover, their absence can lead to specific deficiency syndromes [1]. Liposoluble vitamins exhibit poor solubility in aqueous mediums and are very sensitive and unstable when exposed to inadequate conditions (e.g. temperature and pH). With that in mind, it is important to preserve the properties of these molecules and to improve their biological efficiency. Nanoencapsulation can be an alternative and lipid-based nanosystems are presented to be a good alternative for vitamins encapsulation due to their unique features (e.g. easy scalability, presence of digestible lipids, possible absence of solvents and the use of food-grade materials during production) [2]. The main ingredients (i.e. lipids and surfactants) are important in their production and focusing in the food sector it is important to find new bio-based and biodegradable food-grade materials with new well-known properties, such as biosurfactants (produced by microorganisms) [3, 4]. The biosurfactants are already used in the food industry to improve, for example, texture, organoleptic properties and creaminess of products, this way and taking account their physico-chemical properties (low toxicity, high biodegradability, high selectivity, low micelle concentrations and effectiveness at extreme temperatures, pH's and salinities) the main objective of this work is the development and characterization of nanostructured-lipid carriers (NLC's) using biosurfactants for encapsulation of liposoluble vitamins. The NLC's were prepared by melt-emulsification, using ultra-homogenization followed by ultrasonication technique. For NLC's productions, Neobee 1053 (liquid lipid) and glycerol monosterate (solid lipid) were used as the lipid phase and rhamnolipids (biosurfactant produced by *Pseudomonas aeruginosa*) dissolved in ultra-pure water was used as the aqueous phase. A full factorial design was employed for optimization of the process, designing a set of experiments with different ratios of aqueous:lipid phases, solid:liquid lipids and concentration of rhamnolipids. Size and polydispersity (evaluated by dynamic light scattering, DLS) were used as response variables. Morphology of the NLC's system were further evaluated by transmission electron microscopy (TEM). Size (124-430 nm) was mainly dependent on the water content of the system, while the aqueous:lipid phase ratio and concentration of rhamnolipids were the main factors affecting the polydispersity, which ranged from 0.227 to 0.945. TEM observations confirmed the size determined by DLS and the spherical morphology of the NLC's. The results represent an important step for the encapsulation of vitamins and the consequent production of functional foods.

Financial Support:

Maria A. Azevedo (SFRH/BD/123364/2016) is the recipient of a fellowship from Fundação para a Ciência e Tecnologia (FCT, Portugal).

References:

[1] Combs Jr G. The Vitamins: Fundamental Aspects in Nutrition and Health. Fourth. USA: ACADEMIC PRESS LTD - ELSEVIER SCIENCE LTD; 2012. 557 p.

[2] Gonnet M, Lethuaut L, Boury F. New trends in encapsulation of liposoluble vitamins. J Control Release. 2010 Sep 15;146(3):276–90.

[3] Tamjidi F, Shahedi M, Varshosaz J, Nasirpour A. Nanostructured lipid carriers (NLC): A potential delivery system for bioactive food molecules. Innov Food Sci Emerg Technol. 2013; 19:29–43.

[4] Chassenieux C, Durand D, Jyotishkumar P, Thomas S. Biopolymers : State of the Art , New Challenges , and Opportunities. In: Thomas S, Durand D, Chassenieux C, Jyotishkumar P, editors. Handbook of Biopolymers-Based Materials: From Blends and Composites to Gels and Complex Networks. First Edit. Wiley-VCH Verlag GmbH & Co. KGaA; 2013. p. 1–6

[1]Barrios Bermúdez N, [2]Calvino Casilda V, [1]Cerpa Naranjo A, [3]Rojas Cervantes ML

[1] Escuela Arquitectura Ingeniería y Diseño, Universidad Europea de Madrid, c/ Tajo s/n, Villaviciosa de Odón 28670 (Madrid), España
[2]ETS de Ingenieros Industriales, UNED, c/ Juan del Rosal 2, Madrid 28040, España
[3]Facultad de Ciencias, UNED. Paseo Senda del Rey 9, Madrid 28040, España

niurka.barrios@universidadeuropea.es

Synthesis and physico-chemical properties of multiwall carbon nanotubes doped with transition metals.

Abstract

The carbon nanotubes are materials exhibiting interesting properties [1] could being applied in numerous fields, including catalysis [2]. However, most of the times it is necessary to increase the reactivity of the surface of these materials by functionalization with groups of acid character, which can serve as anchoring groups for metals or other functionalities. Our research group has recently prepared doped alkaline multiwall carbon nanotubes, which have resulted to be efficient catalysts in the Knoevenagel condensation [3].

In this paper we show the synthesis and characterization of multiwall carbon nanotubes (CNT) doped with different transition metals, M-CNT (with M= V, Cr, Mo, Ni). The goal is to obtain acid catalysts active for the synthesis of Fine Chemicals. Other carbonaceous materials containing those metals, in particular, carbon xerogels, were tested in the synthesis of chalcones, resulting as active catalysts [4]. The solids have been prepared by treatment of commercial multiwall carbon nanotubes with nitric acid (CNTO) and subsequent doping with the metals by ionic exchange of the corresponding salts under ultrasonic activation. The materials thus obtained were dried at 60 º C and pyrolyzed at 500 º C to decompose the salts. A reference solid without metal was also prepared (CNTOp).

The analysis by different techniques shows that the doping of the CNT with the metals has been produced. Thus, FTIR-ATR spectra show the disappearing of the bands assigned to the carboxylic groups and the appearing of new bands. The TG curves in air of the pyrolyzed samples lead to a higher residue than that for CNTOp, following the V > Cr > Ni > Mo order. The thermal stability of C=C bonds of the skeleton of nanotubes functionalized with nitric acid (CNTO) increases with respect to commercial nanotubes; however, in samples doped the temperature of decomposition of nanotubes is lowered in approximately 100ºC, with respect to that of CNTOp. This fact indicates that the metallic phases contribute to the destabilization of the nanotubes, promoting their oxidation. The exception is the Mo-CNT sample, whose TG curve is not altered with respect to that for CNTOp, the final residue being almost the same for both samples. Therefore, in the case of sample containing Mo, the doping has been produced in a less extent than for the rest of metals.

XRD patterns of samples show the formation of vanadium pentoxide in the V-CNT sample, whereas no crystalline phase is detected for the rest of samples, indicating a higher dispersion of the metals in the carbon nanotubes.

The commercial carbon nanotubes are mesoporous solids. The oxidation causes a decrease in S_{BET} and the pore volume due to the pore blockage by oxygenated functionalities, which are partially removed during pyrolysis. The value of the BET areas also decreases in nanotubes doped with the transition metals, due to the blockage of micropores and small mesopores by the metals.

References

[1] P.J.F. Harris, Carbon Nanotube Science: Synthesis, Properties and Applications, Cambridge University Press, New York 2009.

[2] P. Serp, M. Corrias, P. Kalck, Appl. Catal. A Gen. 253 (2003) 337.

[3] F.J. Delgado-Gómez, V. Calvino-Casilda, A. Cerpa-Naranjo, M .L. Rojas-Cervantes. Mol. Catal., *in press.*

[4] J. Aguado-Serrano, M.L. Rojas-Cervantes, R.M. Martín-Aranda, A.J. López-Peinado, V. Gómez-Serrano, Appl. Surf. Sci. 252 (2006) 6075.

J. Benavente[1], L. Gelde[1], A. Cuevas[2], V. Vega[3], V. Romero[1], Mª.V. Martínez de Yuso[4], A. S. González[5], V.M. Prida[5], B. Hernando[5]

[1] Dpto. Física Aplicada I, Facultad de Ciencias, Universidad de Málaga, E-29071 Málaga, Spain
[2] Laboratorio de Nanotecnología. Universidad de Málaga. 29071 Málaga. Spain.
[3] Laboratorio de Membranas Nanoporosas. S Universidad de Oviedo, E-33006 Oviedo, Spain
[4] Servicios Centrales de Investigación, Universidad de Málaga, E-29071 Málaga, Spain.
[5] Dpto. de Física, Facultad de Ciencias, Universidad de Oviedo, E-33007 Oviedo, Spain

J_Benavente@uma.es

Changes associated to ceramic oxides surface modification of a nanoporous alumina membrane by ALD technique

Atomic layer deposition (ALD) technique has demonstrated to be an adequate procedure for geometrical and surface modifications of nanoporous membranes with well-defined morphology (parallel array of straight nano-channels without practically pore radii dispersion) obtained from polymeric (polycarbonate track etched procedure) and ceramic (two-step aluminium anodization method) membranes [1-2]. Moreover, the election of the deposited material can open the common field of application of these membranes (drug delivery and microfluidics) to optical and electro-catalytic devices.

This work presents geometrical, chemical, electrochemical and optical characterizations of nanoporous structures (NPSs) obtained by deposition of different metal (Ti, Fe, Si,..) oxides by ADL technique on a nanoporous alumina membrane (NPAM) with the following geometry: average pore radii of 12 nm, porosity of 12 % and 63 μm in thickness (Fig. 1 left). NPSs have been characterized by X-ray photoelectron spectroscopy (XPS) and scanning electron microscopy (SEM) imagine analysis to establish the presence of the coating material on the alumina surfaces (external and pore walls) and its effect on NPAM morphology (Fig. 1 right). Optical characterization of both NPAM and NPSs was performed by UV-Vis-NIR spectroscopy measurements (wavelength between 200 nm and 1000 nm), which give information on samples behaviour in the visible and near-ultraviolet regions. Diffusive ionic transport was also considered by analyzing concentration potential measurements performed with NaCl solutions [3]. This set of measurements allows a rather complete picture of NPSs characteristics, which permits the election of the most adequate ceramic oxide coating material depending on NPS application.

References

[1] A. Spende, N. Sobel, M. Lukas, R. Zierold, J.C. Riedl, L. Gura, I. Schubert, J.M. Montero Moreno, K.
[2] Nielsch, B. Stühn, Ch. Hess, Ch. Trautmann, M.E. Toimil-Molares, Nanotechnology 26 (2015) 335301.
[3] V. Romero, V. Vega, J. García, R. Zierold, K. Nielsch, V. M. Prida, B. Hernando, J. Benavente; ACS Appl. Mater. Interfaces 5 (2013) 3556−3564.

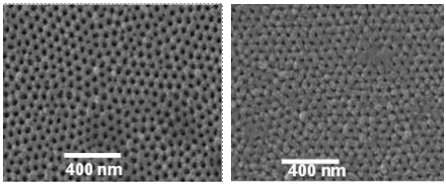

Figure 1: SEM top view images of: NPAMs (left); NPAM+SiO_2 (or NPS) (right).

A. Cuevas[1], V. Vega[2], Mª.V. Martínez de Yuso[3], A. S. González[4], V. Prida[4], B. Hernando[4], F. Martin[1], J. Benavente[5]

[1] Unidad de Nanotecnología. Universidad de Málaga. E-29071 Málaga. Spain.
[2] Laboratorio de Membranas Nanoporosas. Servicios Científico-Técnicos, Universidad de Oviedo, E-33006 Oviedo, Spain
[3] Servicios Centrales de Investigación, Universidad de Málaga, E-29071 Málaga, Spain.
[4] Dpto. de Física, Facultad de Ciencias, Universidad de Oviedo, E-33007 Oviedo, Spain
[5] Dpto. Física Aplicada I, Facultad de Ciencias, Universidad de Málaga, E-29071 Málaga, Spain

Analaura.cuevas@uma.es

Characterization of alumina-based nanoporous structures by spectroscopic ellipsometry

Nanoporous alumina membranes (NPAMs) obtained by the two-step aluminum anodization method are nowadays commonly used in nanofiltration, biosensors and drug delivery due to their well-defined nanoporous structure, but surface modification might open the areas of application [1-3]. For that reason, an optical characterization of NPAMs by spectroscopic ellipsometry technique is presented in this work.

NPAMs with similar thickness but different pore size and inter-pore distance/porosity, depending on the first step anodization conditions (electrolyte and voltage), were morphological, chemical and optically analyzed. Moreover, different alumina-based nanoporous structures (NPSs), obtained by atomic layer deposition (ALD) technique of different ceramic oxides on the NPAMs, have also been studied. Optical characterization was performed by spectroscpic ellipsometry measurements, which were carried out with a commercial apparatus (GES 5E, Semilab, energy ranging between 1.0 and 5.0 eV) at different incidence angles. Consequently, differences in basic optical parameters such as the real part of the refractive index, n, and the extinction coefficient, k, (imaginary part) depending on samples porosity and composition anisotropy could be obtained [4] and, for comparison, values at a given wavelength is also presented [5]. Transmission spectra (UV-Vis-NIR spectroscopy with wavelength ranging between 200 nm and 1000 nm)) were also recorded, and the obtained curves were compared to get information on the optical influence of ceramic oxide coverage. NPAMs and NPSs surfaces were morphological and chemically characterized by SEM images and XPS analysis, respectively, for wider and more complete characterization of the studied samples.

References

[1] X. Jiang, N. Mishra, J.N. Turner, M.G. Spencer, Nanofluids, 5 (2008) 695-701.
[2] S. M. George, Atomic Layer Deposition: An Overview, Chem. Rev., 110 (2010) 111–131
[3] V. Vega, L. Gelde, A. S. González, V.M. Prida, B. Hernando, J. Benavente; Ind. & Chem. Ingeniering Journal 52 (2017) 66-72.
[4] A.C. Gâlca, E.S. Kooij, H. Wormeester, C. Salm, V. Lecca, J.H. Rector, B. Poelsema, J. Appl. Phys. 94 (2003) 4296-4305.
[5] W. Ogielo, H. Wormeester, M. Wessling, N.E. Benes, ACS Appl. Mater. Interfaces 4 (2012) 935–943.

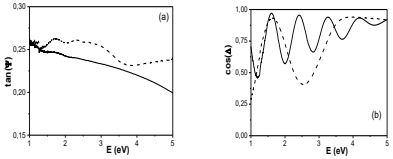

Figure 1: Changes in phase angle (a) and amplitude (b) with energy, at incident angle of 65°, for NPAMs with different average pore size: solid line, 11 nm; dashed line, 16 nm.

Esteves, H. [2], Gomes, J.[1,2], Miranda, R. [4], Albuquerque, P.[2,3]
[1]Área Departamental de Engenharia Química, ISEL – Instituto Superior de Engenharia de Lisboa – Instituto Politécnico de Lisboa, R. Conselheiro Emídio Navarro, 1959-007 Lisboa, Portugal.
[2]CERENA – Centro de Recursos Naturais e Ambiente / Instituto Superior Técnico – Universidade Técnica de Lisboa, Av. Rovisco Pais, 1049-001 Lisboa, Portugal.
[3] ESTeSL - Escola Superior de Tecnologia da Saúde de Lisboa, Instituto Politécnico de Lisboa, Av. D. João II, Lote 4.69.01, 1990-096 Lisboa, Portugal.
[4] UNIDEMI, Departamento de Engenharia Mecânica e Industrial, Faculdade de Ciências e Tecnologia, Universidade Nova de Lisboa, 2825-516 Caparica, Portugal.

Email: helder.esteves@tecnico.ulisboa.pt

Occupational exposure to nanoparticles in differentiated ceramic production processes

Abstract

Some studies on occupational exposure to particulate matter have pointed to dangerous effects for workers as regards inhalable and respirable particles. These occupational exposure scenarios are extremely complex, as they involve components inherent to individuals, working conditions and the activity developed (Sousa-Uva, 2006). In what concerns the ceramic industry, workers may be exposed to nanomaterials during the whole process of production due to its involuntary release (Hristozov and Malsch, 2009). Taking these considerations into account, measurement campaigns were carried out in Portuguese ceramic industries, producing different products, in order to characterize and evaluate the occupational exposure of workers to nanoparticles in order to be able to understand:

- the existence of different measured values in the ceramic units;
- the typology of nanoparticles emitted;
- pulmonary accumulation from different manufacturing processes.

To perform the evaluations, a Nanoparticle Surface Monitor, TSI, Model 3550 was used which measured the superficial area of nanoparticles deposited in the lung expressed as $\mu m^2/cm^3$, and also a NanoScan SMPS Nanoparticle Sizer, TSI, Model 3910 which measured the size distribution as well as its concentration in real-time workplaces.

References

[1] Hristozov, D., Malsch, I., Sustainability, 1, 1161-1194 (2009).

[2] Sousa-Uva, A. - Diagnóstico e Gestão do Risco em Saúde Ocupacional. Lisboa, Instituto para a Segurança, Higiene e Saúde no Trabalho, 2006.

Figures

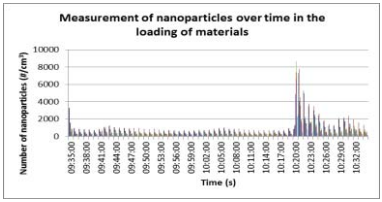

Figure 1: Measurement of nanoparticles in a refractory brick company

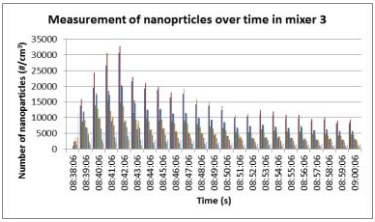

Figure 2: Measurement of nanoparticles in a sanitary ware company

Thais Paseto[1], **Patrícia Filipe[2]**, Patrícia Rijo[2], Catarina Rosado[2], Patrícia Maia Campos[1], Pedro Fonte[2,3,*]

[1]Faculty of Pharmaceutical Sciences of Ribeirão Preto, University of São Paulo, Ribeirão Preto, Brazil
[2]CBIOS-Research Center for Biosciences and Health Technologies, Lusófona University, Lisbon, Portugal
[3]UCIBIO, REQUIMTE, Department of Chemical Sciences – Applied Chemistry Lab, Faculty of Pharmacy, University of Porto, Porto, Portugal

*pedro.fonte@ulusofona.pt

A new approach for development of nanostructured lipid carriers for topical drug delivery

Nanostructured lipid carriers (NLC) are the second generation of lipid nanoparticles, that were created to overcome some problems of solid lipid nanoparticles (SLN) [1]. NLCs are composed by a mixture of solid and liquid lipid, usually in a ratio up to 70:30 [2]. The addition of a liquid lipid in the formulation promotes changes in the structure of the nanoparticle, leading to higher drug loading than SLN [3]. There are several techniques to produce NLC, but most of them use heating in the process making it undesirable to encapsulate thermolabile drugs [4]. The aim of this work was to produce NLC without heating by a modified solvent-evaporation double emulsion technique.

NLCs were produced using a modified solvent evaporation method [5], by placing the liquid lipid in the organic phase. It was performed an experimental design to evaluate the capacity of several lipids, surfactants and its combinations to obtain particles in the nanosized range with low polydispersity (PdI), good colloidal stability and high association efficiency (AE) of the drug. After production, it was evaluated the diameter, PdI, zeta potencial and association efficiency of the model drug, lidocaine hydrochloride.

The nanoparticles diameter may be affected by many factors, but the most important parameters include the amount of lipid, type of lipid and surfactant concentration [3]. The criteria used to choose the best formulation was to have the lower diameter, good zeta potencial, formulation homogeneity and higher drug association efficiency. Considering all these parameters, the best formulation was Tween 80® 2% (w/v) + Precirol® ATO 5 and Oleic Acid (Figure 1). The polidispersity index ranged between 0,18 and 0,84 and AE of the formulation was higher than 70%.

The developed protocol allowed to produce NLC with good physico-chemical properties and without the need of heating, and with high association efficiency of the drug. It is foreseen the application of this encapsulation protocol to load thermolabile drugs, such as therapeutic proteins.

Figures

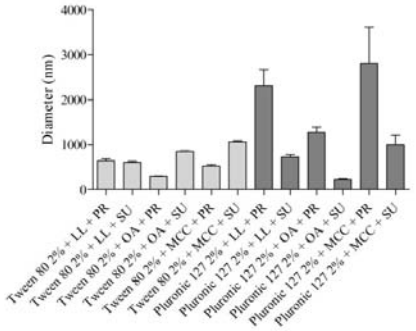

Figure 1: Particle size characterization of NLC formulations. LL: Labrafac Lipophile WL 1349; OA: Oleic Acid; MCC: Maisine CC; PR: Precirol ATO 5; SU: Suppocire DM Pallets

References

[1] Muller, R.H., M. Radtke, and S.A. Wissing, *Adv Drug Deliv Rev*, 2002. 54,131.
[2] Beloqui, A., et al., Nanomedicine, 2016, 12, 143.
[3] Pathak, K., L. Keshri, and M. Shah, Crit Rev Ther Drug Carrier Syst, 2011, 28, 357.
[4] Parhi, R. and P. Suresh, Curr Drug Discov Technol, 2012, 9, 2.
[5] Fonte, P., et al., Biomacromolecules, 2014, 15, 3753.

Catarina Garcia[1], Catarina P. Reis[2], Amilcar Roberto[1], Pedro Fonte[1,3], Eleonora Colombo[4], Gaia Fumagalli[4], Danielle Passarella[4], Patrícia Rijo[1,2*]

[1]CBIOS, ULHT, Campo Grande 376, 1749 – 024, Lisboa, Portugal; [2]iMed.UL, FFUL, Av. Prof. Gama Pinto, 1649-003 Lisboa, Portugal; [3]UCIBIO, REQUIMTE, Department of Chemical Sciences – Applied Chemistry Lab, Faculty of Pharmacy, University of Porto, Porto, Portugal; [4]Dipartimento di Chimica, Università degli Studi di Milano, Via C. Golgi 19, 20133 Milano, Italy

* patricia.rijo@ulusofona.pt

Preparation of self-assembled 6,7-dehydroroyleanone nanoparticles

6,7-dehydroroyleanone (**Figure 1**) is an abietane diterpene that can be isolated from *Plectranthus madagascariensis* Pers. Benth. var. *madagascariensis* essential oil, and has already shown significant cytotoxic activity against different tumoral cells [1].

In this work, the reactivity of the lead molecule was explored through its functionalization by the introduction of a proper linker on the C-12 hydroxyl group (12-OH) attached to a self-assembling inducer: squalene. Squalene is a natural precursor of many steroids and has shown the ability, when linked to biologically active compounds, to achieve a spontaneous formation of nanoassemblies in water [2].

As such, the introduction of a squalene-type chain using a labile linker, including a squalene conjugate with a labile disulfide bond (**Figure 2**) was performed through a Sterglich reaction.
The previously prepared monoester – obtained through the condensation and esterification of a dicarboxylic acid (ditiobutiric acid) with a squalene-type chain (1,1',2-tris-norsqualene alcohol) - was then used to be coupled with the abietane compound. 1D-NMR spectra was performed in order to confirm the structure of the obtained compound, and its results were then compared to the NMR spectra of the lead compound as well as the monoester.
Afterwards, the nanoparticles were prepared through the solvent displacement method: an organic solution was prepared by dissolving the compound in organic solvent to then be subjected to nanoprecipitation in water. After the addition of Milli-Q water, the organic solvent was removed in vacuo, thus assuring the presence of the compound in the aqueous phase.

In terms of physical characterization, the diameter (particle size) and polydispersity index (PI) of the diterpene conjugated nanoparticles were assessed by dynamic light scattering and its general toxicity assessed by the *Sacharomyces cerevisae* model.

Figures

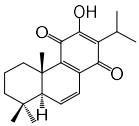

Figure 1: 6,7-dehydroroyleanone

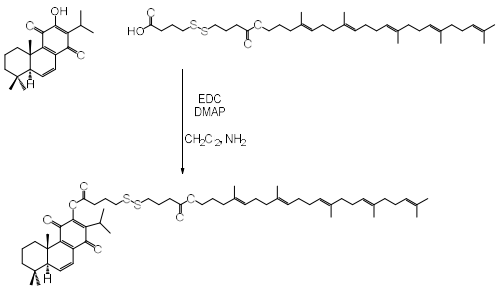

Figure 2: Conjugation of 6,7-dehydroroyleanone with squalene-type chain using a labile linker

References

[1] Catarina Garcia *et al.*, Future Medicinal Chemistry (2017), under review.

[2] Stella Borreli *et al.*, European Journal of Medicinal Chemistry, 85 (2014), 179-190

Jeonghong Ha[1], Hyun Young Jung[2], Yung Joon Jung[3], and Dongsik Kim[1]

[1]Department of Mechanical Engineering, Pohang University of Science and Technology, Pohang 790-784, Republic of Korea
[2] Department of Energy Engineering, Gyeongnam National University of Science and Technology, Jinju 660-758, Republic of Korea
[3]Department of Mechanical and Industrial Engineering, Northeastern University, Boston, Massachusetts 02115, United States

dskim87@postech.ac.kr

Femtosecond laser-induced structural modification with formation of linear carbon chains in single-walled carbon nanotube networks

There has been a growing need for technologies to modify the structure of carbon nanotubes (CNTs). Also, an effective method to generating molecular junctions between adjacent tubes is essential because the performance of a CNT network significantly deteriorates at the interface between tubes.[1] Therefore, intensive investigations were performed for transforming the CNT structures with formation of covalently bonded junctions between adjacent CNTs by electron beam irradiation[2] and Joule heating.[3]

In this work, a femtosecond laser was employed as a tool to induce structural transformations in CNTs since an ultrashort laser pulse can selectively deposit energy over a period shorter than the electron phonon relaxation time. We demonstrated that femtosecond laser irradiation can transform single-walled nanotubes (SWNTs) into multi-walled nanotubes (MWNTs) and form molecular junctions between adjacent SWNTs.[4]

Commercial SWNT (signle-walled nanotube)-DI(deionized) water solutions from Brewer Science were used in this work. Template-guided fluidic assembly was used to assemble SWNT arrays on SiO_2/Si substrates. Metal pads were patterned on the assembled SWNT sample using the conventional lift-off process. A Ti:sapphire femtosecond laser (wavelength = 800nm, full width half maximum = 50 fs, pulse energy < 3 mJ, repetition rate = 1 kHz) was employed in the experiment.

The diameter and wall number of the transformed nanocarbons increased with the laser pulse number. The transformed nanocarbon networks exhibit extraordinarily strong coalescence induced mode in Raman spectra. By controlling the number of incident laser pulses, the electrical conductivity of CNT networks was enhanced two-times. The density function theory computation and experimental results indicate that the linear carbon chains between CNT walls expanded the interlayer spacing, with the linear carbon chain being under higher strain.

This work indicates that the proposed process has strong potential in practical applications of CNTs because the transformed CNTs retained their tube structures without increasing structural defects. Furthermore, the femtosecond laser processing technique is controllable and easily extendible into multiscale (nano- to macro- scale) applications as a fast, selective, scalable and non-destructive method.

References

[1] R. Saito et al., Chem. Phys. Lett. **348**, (2001) 187.
[2] M. Terrones et al., Phys. Rev. Lett. **89**, (2002) 0755051.
[3] C. Jin et al., Nat. Nanotech. **3**, (2008) 17-21.
[4] J. Ha et al., Nanoscale **9**, (2017) 16627-16631.

Figures

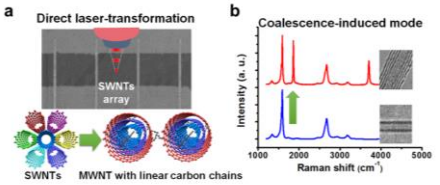

Figure 1: (a) Schematic of the laser transformation process and (b) Raman spectra and TEM images of the carbon nanotubes before and after laser irradiation.

Ana Júlio[1], Tânia Santos de Almeida[1,*], Pedro Fonte[1,2,*]

[1]CBIOS-Research Center for Biosciences and Health Technologies, Lusófona University, Campo Grande 376, 1749-024 Lisbon, Portugal
[2]UCIBIO, REQUIMTE, Department of Chemical Sciences-Applied Chemistry Lab, Faculty of Pharmacy, University of Porto, Rua de Jorge Viterbo Ferreira 228, 4050-113 Porto, Portugal
*Shared senior authorship

*tania.almeida@ulusofona.pt; pedro.fonte@ulusofona.pt

Polymeric Nanoparticles and Ionic Liquids hybrid systems for delivery of poorly soluble drugs

Introduction: Poor drug solubility and low permeation are two challenges when developing drug delivery systems. Nanotechnology may avoid these problems, by allowing a controlled or targeted delivery system [1]. Ionic liquids (ILs) are salts, liquid below 100 °C and have been used to increase drug solubility and permeation [2].
Our aim was to develop nanoparticle-IL hybrid systems to deliver a poorly soluble drug, Rutin.
Materials and Methods: Nanoparticles were produced using Poly(lactic-co-glucolic) Acid (PLGA) 50:50 or PLGA 75:25 by a modified solvent evaporation, w/o/w double emulsion technique[3]. The inner phase was an aqueous solution of 0.2 % (v/v) of IL, (2-hydroxyethyl)-trimethylammonium-L-phenylalaninate ([Cho][Phe]) or (2-hydroxyethyl)-trimethylammonium-L-glutamate ([Cho][Glu]) [2], dissolving rutin at its maximum solubility. The nanoparticles were also prepared with an inner phase at pH 6.7, the isoelectric point of rutin [4]. The association efficiency (AE) and the loading capacity (LC) were assessed by UV at 354 nm. The antioxidant activity was evaluated by DPPH assay.
Results and Discussion: The nanoparticles had a diameter in the range of 250-300 nm with a good PdI and colloidal stability (Figure 1). The AE of rutin, was around 70 % for the formulations with [Cho][Phe] and around 50 % for formulations with [Cho][Glu] (Table 1), representing a good improvement for a drug with poor solubility. There are no relevant differences between the two ratios of PLGA used. The LC of rutin showed that, for the same IL, results were similar for both ratios of PLGA (Table 1). However, when comparing both ILs, [Cho][Phe] showed a higher LC than [Cho][Glu]. The nanoparticles with the inner phase at pH 6.7, presented a significant increase in diameter (data not shown). The AE of rutin, only increased using [Cho][Glu], with an increase of about 8 % for both ratios of PLGA, while the LC presented the same tendency (data not shown).

Conclusion: This work showed the potential of nanoparticle-IL hybrid systems to deliver poorly soluble drugs, since they allow a higher loading of Rutin, compared with nanoparticles without IL. Stable and robust hybrid IL-nanosystems were obtained, regardless of the pH adjustment.
Acknowledgments: The authors would like to thank to FCT, Portugal (UID/DTP/04567/2016).

References

[1] P. Fonte et al. *Biomacromol*., 15 (2014) 3753-3765.
[2] T. Santos de Almeida et al. *Drug Dev. Ind. Pharm.* 11 (2017) 1858–1868.
[3] P. Fonte et al. *Int. J. Pharm.* 2 (2015) 850–862.
[4] X.D. Cui, Z. H. Wang, *Food Chem.* 1(2012) 60-66.

Figures

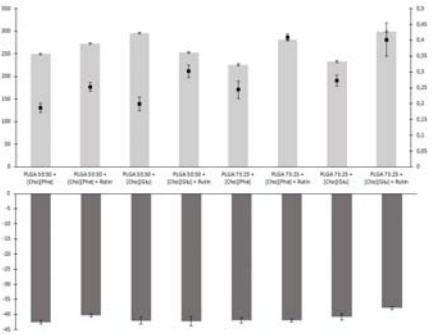

Figure 1: Diameter (nm), PdI and ZP (mV) of Rutin-loaded choline-based ILs PLGA nanoparticles hybrid systems. n=3, mean ± SD.

Table 1: AE (%) and LC (%) of Rutin-loaded ILs PLGA nanoparticles hybrid systems.n=3, mean ± SD.

Polymer	IL	AE (%)	LC (%)
PLGA 50:50	[Cho][Phe]	75.6 ± 1.0	1.0 ± 0.01
	[Cho][Glu]	53.8 ± 2.4	0.5 ± 0.04
PLGA 75:25	[Cho][Phe]	73.2 ± 0.9	1.0 ± 0.08
	[Cho][Glu]	51.3 ± 1.3	0.4 ± 0.03

David Maeso, Andrés Castellanos-Gomez, Nicolás Agraït and Gabino Rubio-Bollinger

Departamento de Física de la Materia Condensada, Universidad Autónoma de Madrid, 28049 Madrid, Spain

Email: david.maeso@uam.es

High photoresponsivity in vertically stacked MoS_2 photodevices

Semiconductor two-dimensional (2D) materials are an emerging class of materials with a wide range of electrical and optical properties. Molybdenum disulfide (MoS_2) is one of the most studied 2D materials because of its unique quantum confinement.

Vertical photodevices are prepared using a physical vapor deposition method to fabricate the gold (Au) substrate. MoS_2 nanosheets are produced by mechanical exfoliation using a polydimethylsiloxane (PDMS) viscoelastic stamps and are transferred onto the Au substrate by an all-dry deterministic method[1]. The photodevice is completed by evaporating 8 µm Au disks over the MoS_2 nanosheets as seen in Figure 1. The photodevices are illuminated using a white supercontinuum laser source and a single grating Czerny-Turner monochromator is used to select the excitation wavelengths.

I-V characteristics are measured using an asynchronous set-up and allow us to determine either dark *IV* or illuminated *IV*. Our metal-semiconductor-metal (MSM) photodevice can be modeled as two metal-semiconductor diodes connected back to back[2]. Experimental *IV* characteristics are fitted to the model demonstrating a very good agreement. Schottky barriers and ideality factors are extracted from the fitted data and are consistent with the literature[3].

Figures of merit of spectral photoresponsivity and spectral external quantum efficiency at different voltages are extracted from the *IV* characteristics as seen in Figure 2. Two peaks at 1.86 and 2.05 eV are observed and are related to the bound excitons A and B.

High photoresponsivity and external quantum efficiency are obtained in vertical photodevices opening a new path to explore this vertical photodevices.

References

[1] Castellanos-Gomez, A. et al. *2D Materials* **1**, 011002 (2014).
[2] Bao, H. et al. *Small* **4**, 1125-1129 (2008).
[3] Quereda et al. *2D Materials* **4**, 021006 (2017).

Figures

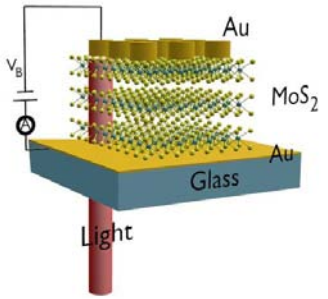

Figure 1: Schematic illustrating the experimental set-up.

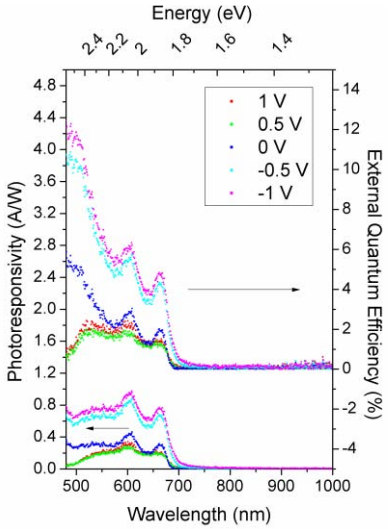

Figure 2: Photoresponsivity and External Quantum Efficiency of the vertical MoS_2 photodevices.

Javier Martinez[1], M. B. Gómez-Mancebo[2], R. Fernández-Martínez[2], N.B. Goikoetxea[2], S. F. Carretero[2], A. Boscá[1], J. Pedrós[1], F. Calle[1], S. Fernández[2], J. Cárabe[2], A. Molinero[2], J. M. Barcala[2], A. J. Quejido[2], I. Rucandio[2]

1 ISOM Universidad Politécnica de Madrid, ETSITelecomunicación Ciudad Universitaria, Madrid, Spain

2 CIEMAT, Avda. Complutense 40, Madrid 28040, Spain

javier.martinez@isom.upm.es

Thermally Reduced Graphene Oxide for Hydrogen Storage

Abstract

Graphene is one of the most promising materials due to its remarkable properties. One of the noticeable features of graphene is its high specific surface area (2630 $m^2.g^{-1}$). This property is highly desirable for hydrogen storage applications (1-2), one of which main challenges is the production of graphene materials in large quantities.

Thermal treatments of graphite oxides have been promising methods for the mass production of reduced oxide graphene (rGO) with high specific surface areas (3).

In this study, we present a simple method for thermal reduced graphene production that can be used later for hydrogen storage.

Two different temperatures were probed (250º C and 450º C) in four different instruments: a) an electrical furnace under air conditions, b) microwaves under air conditions, c) a fusion instrument under air conditions, and d) a tubular reactor inside an electrical furnace. In the last case, a 100 $mL.min^{-1}$ Ar flow was used, and the reactor characteristics allowed the control of the heating rate.

Successful reduction of thermal reduced oxide graphene (T-rGO) samples was confirmed by elemental analysis and X-ray diffraction (XRD). These materials showed high specific surface areas, of about hundreds of $m^2.g^{-1}$ in the Brunauer, Emmett Teller (BET) test. The scanning electron microscopy (SEM) showed very porous structures.

This method does not require high-cost and long processing time and could be useful to make graphene materials in large quantities for industrial applications such as hydrogen storage.

References

[1] Guo CX, Wang Y, Li CM. ACS Sustainable Chemistry and Engineering, 1 (2013) 14

[2] Kim JM, Hong WG, Lee SM, Chang SJ, Jun Y, Kim BH, et al., Int. J. Hydrog. Energy, 39 (2014) 3799

[3] Nguyen ST, Nguyen HT, Rinaldi A, Nguyen NPV, Fan Z, Duong HM, Colloids and Surfaces A, 414 (2012) 352

Acknowledgements

Supported by MINECO project GRAFAGEN (ENE2013-47904-C3)

M. P. Montero-Rama, J. G. Sánchez, C. Stenta, A. Viterisi, J. Pallarès and L. F. Marsal*

Departament d'Enginyeria Electrònica, Elèctrica i Automàtica. Universitat rovira I Virgili.
Av. Països Catalans 26, Tarragona, Spain.
lluis.marsal@urv.cat

Thin Film Metal Oxides as Electron Transport Layer for Efficient Polymer Solar Cells

Polymer solar cell (PSCs) have attracted great interest in the field of renewable energy due to their recent increase in power conversion efficiency and low manufacturing costs. [1, 2] In conventional PSCs, calcium and PEDOT:PSS films are commonly used as metal cathode and anode, respectively.[3] Nevertheless, these devices exhibit poor long-time stability and operational lifetimes under environment conditions, and thus require strict encapsulation strategies to reduce degradation under oxygen and moisture.[4] To solve these problems, PSCs with an inverted structure (iPSCs) have been developed. In iPSCs, PEDOT:PSS is replaced by MoO_3 or V_2O_5, while TiOx and ZnO films are used as electron transport layer (ETL) because of their high air-stability, non-toxicity, and high transparency.[5, 6] Our research is focused on TiOx and ZnO nanometric films used as ETL in iPSCs. Several devices were fabricated based on PTB7:PC_{70}BM and PTB7-Th:PC_{70}BM as active layer. The iPSCs based PTB7:PC_{70}BM were fabricated with TiOx as ETL, while devices based PTB7-Th:PC_{70}BM were fabricated with ZnO as ETL. All iPSCs were fabricated using a V_2O_5/Ag bilayer cathode as depicted in Figure 1 (insert). Figure 1 shows the *J-V* characteristics of the best-performing devices. To shed light on the morphological characteristics of the active layers, we recorded AFM micrographs of TiOx and ZnO films as shown in Figure 2. The topography of the TiOx and ZnO films show rather distinct features. The ZnO film exhibits a high surface roughness in comparison to TiOx film that shows a rather flat topography. We found that iPSCs based on PTB7-Th:PC_{70}BM exhibit the best performing using thin films of ZnO of about 30 nm, while the best performing of devices based on PTB7:PC_{70}BM was obtained using 15 nm of TiOx.

References

[1] V. S. Balderrama, F. Avila-Herrera, J. G. Sánchez, J. Pallarès, O. Vigil-Galán, L. F. Marsal, M. Estrada. IEEE J. Photovolt. **6,** (2016) 1–7.

[2] T. D. Nielsen, C. Cruickshank, S. Foged, J. Thorsen, F. C. Krebs. *Sol. Energy Mater. Sol. Cells* 94, (2010) 1553–1571.

[3] P. L. Han, A. Viterisi, J. Ferre-Borrull, J. Pallarès, L. F. Marsal. Org. Electron. physics, Mater. Appl. 41, (2017), 229–236.

[4] V. S. Balderrama, M. Estrada, P. L. Han, P. Granero, J. Pallarés, J. Ferré-Borrull, L.F. Marsal. Sol. Energy Mater. Sol. Cells 125, (2014) 155–163.

[5] J. G. Sánchez, V. S. Balderrama, M. Estrada, E. Osorio, J. Ferré-Borrull, L.F. Marsal, J. Pallarès. Sol. Energy 150, (2017) 147–155.

[6] M. Thambidurai, J. Y. Kim, J. Song, Y. Ko, H. Song, C. Kang, N. Muthukumarasamy, D. Velauthapillai, C. Lee. J. Mater. Chem. C 1, (2013) 8161.

Figures

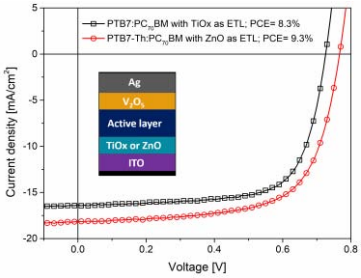

Figure 1: J-V characteristics of best-performing devices. Device structure employed in this study (insert).

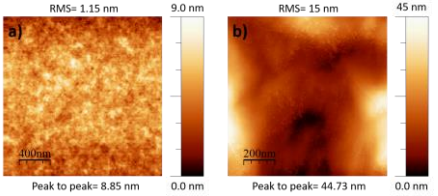

Figure 2: Topography images of a) TiOx film and b) ZnO film. Scale bar: a) 400 nm and b) 200 nm.

Acknowledgements: This work was supported in part by the Spanish Ministry of Economy and Competitiveness TEC2015-71324-R (MINECO/FEDER), the Catalan authority AGAUR 2017SGR1527, and ICREA under the ICREA Academia Award.

Simona Gabriela Muntean,[1] Maria Andreea Nistor,[1] Robert Ianos,[2] Cornelia Pacurariu[2]

[1]Institute of Chemistry Timisoara of Romanian Academy, 24 Mihai Viteazul, Timisoara, Romania
[2]Faculty of Industrial Chemistry and Environmental Engineering/ Politehnica University Timişoara, Romania

sgmuntean@acad-icht.tm.edu.ro;
sgmuntean@yahoo.com

Magnetite/silver/carbon nanocomposites: Synthesis, Characterization and Evaluation as Specific Sorbent

Fe_3O_4/Ag/C nanocomposites have attracted much interest in many applications due to their valuable properties. These nanocomposites combine the good catalytic and antibacterial activity provided by silver and high adsorption capacity supplied by carbon with the advantage of easy magnetically manipulation given by magnetite. Meanwhile, the carbon presence prevents the oxidation or erosion by acid or base and agglomeration of the composite in aqueous solution[1,2]. Generally, the methods reported for the synthesis of Fe_3O_4/Ag/C nanocomposites require multi-step routes, high temperatures or long reaction times[2]. In this work we report the synthesis of magnetite/silver/carbon nanocomposites nanocomposites (MSC) with different mass ratio by the combustion method, working in controlled atmosphere. This method is environmentally friendly and has many advantages such as simplicity, short reaction time, low energy consumption[3,4]. The presence of magnetite in the samples was certified by Mössbauer spectroscopy. The thermal behaviour and textural properties of the samples are significantly influenced by the high carbon content. The values of the saturation magnetization of the samples are in accordance with their phase composition, decreasing with the decrease of magnetite content, from 2.6 to 2.0 emu/g. The SEM images of the samples indicate the presence of small agglomerated magnetite and silver particles located on the surface of activated carbon. Combustion synthesis allows obtaining magnetite/ silver/carbon nanocomposites with large surface area and ferrimagnetic properties, which ensure good adsorbent properties, easy separation of the phases and opportunities for regeneration and reuse that recommend them as efficient adsorbents for the removal of different pollutants from wastewater. The obtained nanocomposites were tested as adsorbents for the removal of anionic and cationic dyes from single and binary systems in aqueous solution, in selected working conditions. In binary systems the removal efficiency slightly decreased due to competitive effect. Even after five adsorption-desorption cycles the magnetite/carbon nanocomposites still present a good efficiency (greater than 75%) for dyes removal from aqueous solution, indicating the possible industrial application of MSC.

References

[1] A.-H. Lu. E.L. Salabas, F. Schüth, Angew. Chem. Int. Ed., 46(8) (2007) 1222-1244
[2] H. Xia, B. Cui, J. Zhou, L. Zhang, J. Zhang, X. Guo, H. Guo, Appl. Surf. Sci., 257 (2011) 9397-9402
[3] R. Ianoş, C. Pacurariu, G. Mihoc, Ceram. Int., 40 (2014) 13649-13657
[4] R. Ianos, A. Taculescu, C. Pacurariu, I. Lazau, J. Am. Ceram. Soc., 95(7) (2012) 2236-2240

Figures

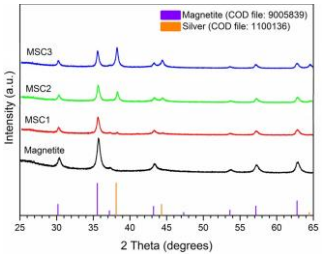

Figure 1: XRD patterns of the nanocomposites

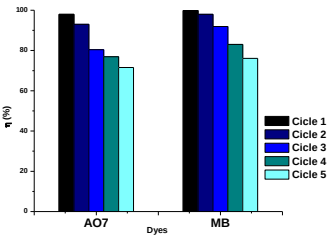

Figure 2: Removal efficiency of MSC1 in five adsorption-desorption cycles.

Lili Nadaraia[1], Nikoloz Jalabadze[1], Roin Chedia[2], Levan Khundadze[1]

[1]Georgian Technical University, Tbilisi, Georgia
[2]Iv.Javakhishvili Tbilisi State University, P. Melikishvili Institute of Physical and Organic Chemistry, Tbilisi, Georgia
nadaraia@gtu.ge

SPS sintering of graphene reinforced ceramic matrix

Graphene has recently garnered significant interest as a reinforcing phase in composite materials (mostly in Al_2O_3, Si_3N_4, TiO_2, ZrB_2….) because of its excellent electrical, thermal and mechanical properties. Mechanical mixing used to be conventional method for dispersion graphene nanoplatelets (GNP) into the ceramic matrix.

However, there are several challenges during manufacturing process of graphene-ceramic composites (GCC). One of the obstacles is associated with preparation of graphene via routes that produces good dispersion of its layers in the ceramic matrix. The quality of the graphene dispersion in a ceramic matrix significantly affects to the final properties of composite. Thus, to avoid these problems rapid sintering techniques such as spark plasma sintering (SPS) is mostly used.

Although, there is possibility to inject ceramic precursor at the initial stage of graphene reduction. Leading to the deposition of GNP at the particles of the ceramic material.

An investigation has been conducted for producing of aluminum-graphene composition and results are quite promising. First reduction of graphene oxide has been conducted due to long ultrasonic mixing in charge of potassium permanganate and sulfuric acid. Graphene reducing has been possible by hydrazine assisted hydrothermal method. Obtained GNP has been mechanically mixed with ceramic elements. At the same time, powder of ceramic-graphene composition has been obtained via modified method. Precursors of ceramic materials have been injected at an initial stage of the graphene reduction. At first oxides of graphene and aluminum was dissolved in hydrazine suspension. After drying and ultrasonic treatment obtained powder has been sintered using spark plasma sintering method. Investigation of the structure, physical-chemical and mechanical properties of the elaborated composite materials was performed. Multi-layer agglomerations of graphene have been observed in to the ceramic structure (Fig.1.). Obviously, graphene clusters prevents formation of expected positive effects on properties of composite. Beside of this, slight relevant improvement has been detected. Especially fracture toughness of sintered Al_2O_3 – GO material has been improved and Vickers test showed twice better hardness with comparison of pure Aluminum oxide (Fig. 2). Moreover, crack propagation at the edges of indentation has not been detected.

Consequently, main goal of the research was reduce number of layers in the graphene clusters and its homogeneous distribution in ceramic matrix. The results of this study provide a better understanding of the effects of GNP on sintering behavior and mechanical properties.

Acknowledgment: The part of research described in this work was made possible in scope of projects funded by Shota Rustaveli National Science Foundation.

Figures

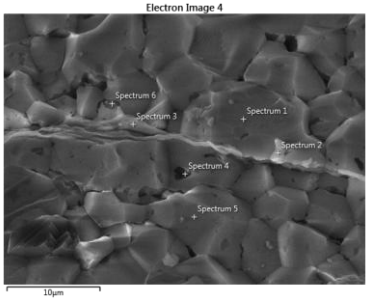

Figure 1: SEM micrographs of Al_2O_3 – GO with GO cluster (Spectrum 3)

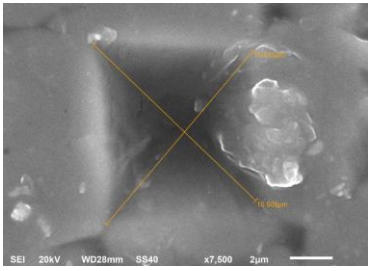

Figure 2: SEM micrograph of Vickers indentation.

Jihun Noh, Jeonghong Ha, and Dongsik Kim

Department of Mechanical Engineering, POSTECH, Pohang, 790-784, Republic of Korea
dskim87@postech.ac.kr

Femtosecond laser sintering of silver nanoparticles on a flexible substrate

The technology for sintering metal nanoparticles has recently attracted substantial attention owing to its potential in future micro/nano electronic devices including flexible devices, novel electric circuits, solar cells and mobile devices. Particularly, laser sintering or joining of nanomaterials using short pulsed lasers is emerging as a useful tool for fabricating metal patterns on flexible substrates without substrate damage. [1, 2]

This work investigates femtosecond laser sintering of silver (Ag) nanoparticles on a flexible substrate. Electrical and mechanical properties of the laser-sintered samples as well as their microstructures were examined under various conditions. Ag nanoparticles were deposited on a polyethylene terephthalate (PET) substrate using a spin coating method. A Ti:sapphire femtosecond laser with a regenerative amplification system (wavelength = 800 nm, full width at half maximum = 50 fs, pulse energy < 3.5 mJ, repetition rate = 1 kHz) was employed in the experiment.

Femtosecond laser irradiation could not fully melt the Ag nanoparticles but formed porous structures composed of Ag nanoparticles bonded by surface necking. Mechanical crack, as well as the surface necking, increased with the laser fluence. The laser sintering process decreased the sheet resistance of the sintered Ag film (1.7 Ω/sq) because of formation of the electrical pathway. Furthermore, adhesion strength of the film was substantially enhanced by the process (5B according to ASTM-3359 standard). The laser-sintered film was not separated from the PET substrate in the tape test. Notable was that the femtosecond laser-sintered Ag film attained high flexibility. Compared with the spin coated Ag nanoparticle layer, the sintered film had substantially increased crack resistance. Accordingly, the femtosecond laser-sintered film maintained its high electrical conductivity even after severe bending, for example, after repeated cycles with a radius of curvature as small as 1 mm.

This work suggests that ultrafast laser sintering of metal nanoparticles can be a powerful tool in manufacturing of flexible devices.

Figures

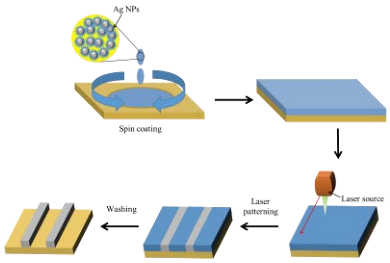

Figure 1: Schematic of laser sintering steps

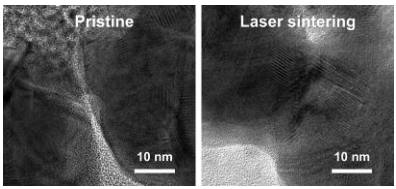

Figure 2: TEM images of before and after laser sintering

References

[1] J. Ha. et al., RSC Advances, 6 (2016), 86232-86239.
[2] Y. Son, et al., Advanced Materials, 23 (2011), 3176.

Jungju Oh[1], Gyeungyun Kim[1], Jaewon Lee[1], Kuen-Yong Lee[1], Taiyoun Rhim[1], Ji Hoon Jeong[2], and Minhyung Lee[1*]

[1]Department of Bioengineering, College of Engineering, Hanyang University, 222 Wangsimni-ro, Seongdong-gu, Seoul 04763, Korea
[2]School of Pharmacy, Sungkyunkwan University, Suwon 16419, Korea

*minhyung@hanyang.ac.kr

Nanoparticle-based delivery system of therapeutic nucleic acids and peptides for the treatment of ischemic stroke

Abstract

Receptor for advanced glycation end products (RAGE) is a multi-ligand receptor that is involved in ischemia/reperfusion (I/R) injury. In this study, RAGE binding peptide (RBP) was produced by recombinant DNA technology for blocking the RAGE signaling. RBP was originated from the RAGE binding domain of high mobility group box-1. Cytokine assays and immunohistochemistry results showed that RBP was an effective antagonist of RAGE, reducing inflammatory cytokines and RAGE. Along with RBP, the heme oxygenase-1 gene (pHO-1) was used as a therapeutic gene for protection of brain cells in ischemic stroke animal models. For combination delivery of RBP and pHO-1, deoxycholic acid-conjugated low molecular weight polyethylenimine (DA-PEI) was synthesized and used as a gene delivery carrier. A ternary-complex was prepared with pHO-1, DA-PEI and RBP by charge interaction. The size of the ternary-complex was approximately 130 nm. In vitro transfection assay to hypoxic neuron cells showed that the ternary-complex had higher gene delivery efficiency than pDNA/DA-PEI, pDNA/PEI, pDNA/lipofectamine binary-complexes. Furthermore, the toxicity of the ternary-complex was lower than those of the binary-complexes. In addition, the cyto-protective effect of the ternary-complex was confirmed by Annexin V and TUNEL assay. The animal models of ischemic stroke were produced by middle cerebral artery occlusion (MCAO) and reperfusion. The ternary-complex was injected into the animal model by stereotaxic injection. The results showed that the ternary-complex reduced the infarct volume effectively in the stroke animal models. The results suggest that the pHO-1/DA-PEI/RBP ternary-complex has anti-inflammatory and cyto-protective effects in the cells under hypoxia. Therefore, the ternary-complex, composed of pHO-1, DA-PEI, and RBP may be useful for the treatment of ischemic stroke.

Figures

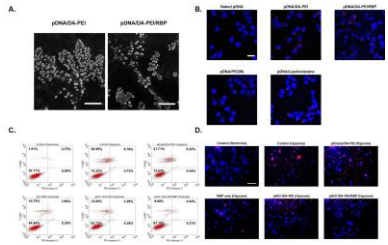

Figure 1: Characterization of ternary-complex and cyto-protective effect under hypoxia. (A) Morphology of ternary-complex measured by SEM (scale bar = 1 μm). (B) Cellular uptake of ternary-complex using Cy5 labeled-DNA in Neuro2a cell (scale bar = 20 μm). (C) and (D) Cyto-protective effect of ternary-complex under hypoxia. (C) Annexin V assay. (D) TUNEL staining (scale bar = 100 μm).

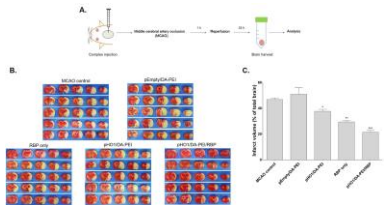

Figure 2: Reduction of infarct volume by ternary-complex in MCAO. (A) Scheme of *in vivo* experimental procedure. (B) TTC staining. (C) Quantification of infarct volume. *p<0.05 compared with MCAO control and pEmpty/DA-PEI. **p<0.05 compared with MCAO control, pEmpty/DA-PEI, and pHO1/DA-PEI. ***<0.05 compared with other groups.

References

[1] S.Y. Chae, H.J. Kim, M.S. Lee, Y.L. Jang, Y.H. Lee, S.H. Lee, K.L. Lee, S.H. Kim, H.T. Kim, S.C. Chi, T.G. Park, J.H. Jeong, *Marcromol. Biosci*. 11 (2011) 1169

[2] Muhammad, S., W. Barakat, S. Stoyanov, S. Murikinati, H. Yang,K.J. Tracey, M. Bendszus, G. Rossetti, P.P. Nawroth, A.Bierhaus, and M. Schwaninger. *Journal of Neuroscience* 28 (2008) 12023-12031.

P. Pereira [a,b], L. Roque[a,c], M. Nicolai[a], P. Rijo[a,d] P. Fonte[a,e], M. Gabriela Gil[b], Catarina P. Reis[d,f], M. J. Cebola[a,f]

[a]Center for Research in Biosciences & Health Technologies (CBIOS), Lusófona University, Lisbon; [b] CERENA - Centre for Natural Resources and the Environment, Lisbon; [c] Faculty of Pharmacy, Alcalá de Henares, Spain; [d] Instituto c Investigação do Medicamento (iMed.ULisboa), Lisbon; [e]UCIBIO- Faculty of Pharmacy, University of Porto, Portugal; [f]IBEB/FCUL, Lisbon [g]Escola Superior Náutica Infante D. Henrique (ENIDH), Paço de Arcos, Portugal.

E-mail.: p1204@ulusofona.pt

Anti-aging nanoformulation with extract of *Myrtus communis L.*

Abstract

Myrtle (*Myrtus communis* L.) is an evergreen shrub belonging to the family of Mirtaceae that grows spontaneously throughout the Mediterranean area. This plant is widely used because its medicinal properties such as anti-inflammatory and immune-stimulatory properties [1].

In this study, supercritical fluid extraction (SFE) extracts were obtained at 23 MPa, 45◦C and a CO_2 flow of 0.3 kg h^{-1}using ethanol as co-solvent with a flow rate of 0.09 kg h^{-1}[2]. Their *in vitro* antioxidant capacity was determined using DPPH method. Then, the extract was encapsulated into nanocarriers. The last aim was to improve the skin permeation of the loaded extract to prevent or treat skin problems.

Methods:

PLGA nanoparticles (NPs) were prepared by emulsification/solvent diffusion method and their mean particle size/polydispersity index (PI) were measured by dynamic light scattering. Encapsulation efficiency was also determined [3].

Results:

Concerning antioxidant activity of the extract, this study showed that the extract had 93% of activity.

Results of nanoparticle characterization are displayed in Table 1. Particles were very small and monodisperse. The particle size is crucial for skin permeation through the hair follicles. This fact is reported in several papers. As example, Otberg et al. [4] applied caffeine in a mixed solution of ethanol:polylene glycol to volunteers before and after blocking all hair follicles with a varnish solution. In this study, caffeine was observed in blood 20 min after application on the hair follicle-blocked skin, but 5 min after topical application to normal skin. A possible reason for the more rapid appearance of drug in blood is the rapid absorption of the substance penetrating through hair follicles to blood capillaries. We expect that our polymeric nanoparticles will permeate hair follicles.

Table 1: Characterization of the loaded NPs

	Size (nm)	PI	Zeta Potential (mV)
Mean	219.67	0.11	*-20.32*
SD	9.86	0.05	1.27

Our future studies will include permeation studies using in vitro models simulating the skin permeation.

References

[1] V. Aleksic, P. Knezevic, Antimicrobial and antioxidative capacity of extractsand essential oils of Myrtus communis L., Microbiol. Res. 169 (2014) 240–254.

[2] Paula Pereira, M. Gabriela Bernardo-Gil, M. João Cebola, Elisabete Mauricio, Anabela Romano, Supercritical Fluid Extracts with Antioxidant and Antimicrobial Activities from myrtle (Myrtus communis L.) leaves. Response Surface Optimisation, J. of Supercritical Fluids, 83 (2013) 57– 64.

[3] Luís V. Roque, Ines S. Dias, Nuno Cruz, Ana Rebelo, Amílcar Roberto, Patrícia Rijo, Catarina P. Reis, Design of Finasteride-Loaded Nanoparticles for Potential Treatment of Alopicia. Skin Pharmacology and Physiology, 30 (2017) 197-204.

[4] Otberg, N.; Patzelt, A.; Rasulev, U.; Hagemeister, T.; Linscheid, M.; Sinkgraven, R.; Sterry, W.; Lademann, J. The role of hair follicles in the percutaneous absorption of caffeine. Br. J. Clin. Pharmacol. 65 (2008) 488–492.

Thais P. Pivetta [1], Tânia Carvalho [2], Sandra I. D. Simões [3], Priscyla D. Marcato [1]

1 Nanobiolab, School of Pharmaceutical Sciences of Ribeirão Preto, University of São Paulo, Ribeirão Preto, Brazil
2 Instituto de Medicina Molecular, Faculdade de Medicina, Universidade de Lisboa, Lisboa, Portugal
3 Nanostructured Systems for Overcoming Biological Barriers group of iMed.ULisboa, Faculdade de Farmácia, Universidade de Lisboa, Lisboa, Portugal

thaisppivetta@gmail.com

Investigation of the anti-inflammatory potential of thymol encapsulated in lipid nanoparticles

Inflammation can be generated due to many causes including microbial infection, immune reactions and physical damage. To treat these disorders it is common the use of anti-inflammatory agents such as steroidal and non-steroidal medicines but some of these drugs are related with undesirable side effects [1]. Thus, there is a search for alternative therapeutics that are less toxic. Thymol is a phenolic monoterpene that exhibits antimicrobial, antioxidant, anesthetic and anti-inflammatory effects. Therefore, thymol could be a promising compound for the treatment of inflammatory processes and wound healing [2]. However, constituents of essential oil such as thymol can easily decompose. Nanostructured lipid carriers (NLCs) are able to provide chemical protection and sustained release. Also, NLCs enable the inclusion of natural lipids with biological properties and suitable for topical application [3].

The aim of this study was to evaluate the anti-inflammatory potential of thymol encapsulated in NLCs aiming its topical application. The nanoparticles were produced by hot emulsion and sonication method and characterized regarding to size, zeta potential and entrapment efficiency. Nanoparticles were incorporated in carbopol gel and used to study the anti-inflammatory activity in an anthralin ear swelling mouse model. The anti-inflammatory potential was determined through the measure of mice's ears thickness and histopathological analysis.

The average particle size was 108 nm (polydispersity index of 0.220), zeta potential of -12mV and 89% of the drug encapsulation efficiency. The ears treated with the betamethasone commercial ointment (positive control) exhibited total inhibition of ear edema. Thymol-NLCs inhibited 68% and the other samples presented lower inhibition (20% for empty-NLCs-gel and 37% for thymol-gel). The animals treated with thymol-NLCs showed histopathological scores similar to betamethasone (positive control) and the other samples exhibited higher scores of inflammation (Figure 1). Therefore, the encapsulation of thymol in NLCs appears as a promising manner for its topical administration in inflammatory skin diseases.

References

[1] R. Gautam, S.M. Jachak, Med. Res. Rev. 29 (2009) 767–820.
[2] K.R. Riella, R.R. Marinho, J.S. Santos, R.N. Pereira-Filho, J.C. Cardoso, R.L.C. Albuquerque-Júnior, S.M. Thomazzi, J. Ethnopharmacol. 143 (2012) 656–663.
[3] E.S. Averina, R.H. Müller, D. V. Popov, L.D. Radnaeva, Pharmazie. 66 (2011) 348–356.

Figures

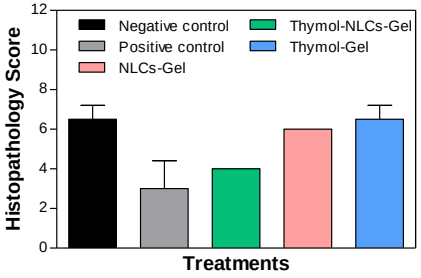

Figure 1: Histopathological score of mice ears treated with positive control (betamethasone), thymol-NLC-gel, empty-NLC-gel and thymol-gel after challenge with anthralin (negative control).

F. M. Quintana, J. Pizarro, M.P. Guerrero-Lebrero, G. Bárcena-González, D. Nimo, J. C. de la Torre, P.L. Galindo
Sistemas Inteligentes de Computación. University of Cádiz, Spain

fernando.quintana@uca.es

Parallel software for the simulation of high angle annular dark field images at low magnifications

This work presents a novel parallel low resolution High Angle Annular Dark Field Scanning Transmission Electron Microscopy (HAADF-STEM) software based on the multislice algorithm[1][2]. HAADF-STEM images, also known as Z-contrast, are obtained by scanning an electron probe of atomic dimensions across the specimen and collecting electrons scattered at high angles.

In the low resolution simulation approach[3] the specimen is represented by an arrangement of 3D cubes, where each cube is composed of some atoms and described by a set of parameters, such as its chemical composition, atomic density and atomic number.

The probe is set to an specified position (x,y,z) and illuminates the surface of the specimen.

The whole process consists on a sequence of transmission-propagation of the wavefunction across all the slices. The intensity diffused at slice z is calculated as the weighted sum of all the n elementary cubes bombarded by electronic probe. This process is repeated slice by slice and the total intensity is computed by summing up contributions from all slices which determine the pixel intensity at each position in the image.

This simulation process has a high computational cost and therefore its use is limited to computer centers with large supercomputing systems. However, with the advent of GPUs, some tasks may be implemented in parallel and run in usual PCs. In this paper, we have analyzed three parallel alternatives to the usual sequential programming implementation.

For the first approach, all calculations are splitted into different threads and each one is run in a different core of the CPU. The second option is to call high-level programming specialized functions for GPUs. For the last approach, we do not divide the problem in blocks, but we make use of the philosophy of massive parallel processing present in the GPUs architecture.

To test the algorithm, we calculated the computational time of simulating several images at different resolutions of bulk boron-doped carbon (Figures 1 and 2). We can observe in figure 3 that the computation time is reduced exponentially using the GPU, and specially using the CUDA approach toolkit making possible the simulation of an image in a reasonable time in a personal computer without great economic effort.

Acknowledgments

This work was supported by the Junta de Andalucía (project P12-TEP-3055 and University of Cádiz "Intelligent Systems" research group)

References

[1] Ishizuka K. MacHREM/WinHREM package. http://www.hremresearch.com/, HREM Research Inc. (2018).
[2] Ishizuka K. Ultramicroscopy 90 (2002) 71
[3] J. Pizarro et Al., Appl. Phys. Lett. 93 (2008) 153107

Figures

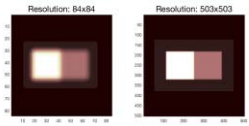

Figure 1: Bulk boron-doped carbon low resolution HAADF simulated electron microscopy images with a resolution of 84x84 pixels and 503x503 pixels

Figure 2: Simulation of a low resolution (100px) image projections from different angles (0°, 45° and 90°)

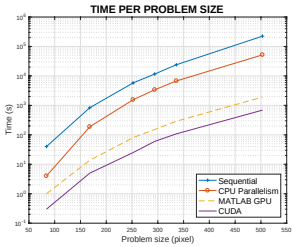

Figure 3: Time in seconds for each image resolution on an Intel Xeon CPU E5-2620 v2 with 12 cores and a NVidia Tesla K20c

A. Rebelo[1], L. Fonseca[1], P. Fonte[1,2], A. S. Viana[3], M. Nicolai[1], M. Figueira[4], J. Molpeceres[5], P. Rijo[1,6] and C. Reis[4,7*]

[1]CBIOS, Lusófona University, Campo Grande 376, 1749 – 024, Lisboa, Portugal;
[2]UCIBIO, REQUIMTE, Faculty of Pharmacy, University of Porto, R. Jorge Viterbo Ferreira 228, 4050-313, Porto, Portugal;
[3]CQB, FCUL, Campo Grande 1749-016, Lisboa, Portugal;
[4]FFUL, Av. Prof. Gama Pinto 1649-003, Lisboa, Portugal;
[5]Department of Biomedical Sciences, Faculty of Pharmacy, UAH, Ctra.A2km 33,600 Campus Universitario, 28871 Alcalá de Henares, Spain;
[6]iMed.UL, FFUL, Av. Prof. Gama Pinto, 1649-003 Lisboa, Portugal;
[7]IBEB, FCUL, Campo Grande 1749-016, Lisboa, Portugal;

*e-mail: catarinareis@ff.ulisboa.pt

BSA Nanoparticles with Parvifloron D for Pancreatic Cancer Treatment

Introduction: Pancreatic cancer is the thirteenth most common cancer and the eighth leading cause of cancer death worldwide. An improvement in the outcome of patients with pancreatic cancer is strongly dependent on the development of more effective therapies [1]. Nanotechnology can play a crucial role by targeting the drugs to the malignant cells [2]. In another hand, medicinal plants, as an example, *Plectranthus* species, have exhibited cytotoxic and antiproliferative activities against human tumor cells, like the present abietane diterpenoid, Parvifloron D [3]. The aims of this work were to isolate Parvifloron D from *P. ecklonii* and to prepare and characterize albumin nanoparticles using different processes. **Material & Methods:** Parvifloron D was obtained by extraction through an acetone ultrasound-assisted method and isolated by a chromatography column over silica gel using mixtures of increasing polarity eluents. Albumin nanoparticles were produced through desolvation method [4]. The formulation was optimized using different cross-linking processes (glutaraldehyde, glucose, glucose with UV light and UV light), albumin concentrations (30, 50 and 150mg), cross-linking times (30min and 24h) and organic solvents (DMSO, acetone, ethanol and hexane). Resultant particles were then characterized in terms of stability, particle size by photon correlation spectroscopy, zeta potential by laser Doppler anemometry, cross-linking efficacy by Bradford method and shape and size by atomic force microscopy (AFM). Parvifloron D was encapsulated in the optimized formulation and then characterized by using the same techniques. Encapsulation efficacy (%) was determined by measuring the non-encapsulated drug lost in the supernatant (i.e., indirect quantification) by HPLC analysis. **Results & Discussion:** Extraction was carried out as previously described [5]. A yield of 28.54 g was obtained and subjected to successive chromatographic processes and 0.882 g of Parvifloron D was isolated (0.45% (w/w) of the dry plant). The particle size range obtained was between 90 and 520nm. Some agglomerates were visible in some of the methods. All nanoparticles showed a negative zeta potential, independently of the different production conditions. In terms of morphology, nanoparticles were spherical and AFM confirmed the particle size. Different cross-linking efficacies in the methods were observed and ranged between 43.8% and 99.6%. Then, Parvifloron D was encapsulated in the chosen formulation. Particle size was around 95nm and nanoparticles maintained a negative zeta potential. The cross-linking efficacy was up to 85% and the encapsulation efficacy was 91.2%. **Conclusions:** This study confirms the feasibility of producing uniform and well-defined albumin nanoparticles, encapsulating Parvifloron D. Further ligand-attachment onto the nanoparticle surface and efficacy studies against tumor cells will be performed.

References

[1] N. Silvestris, et al., Curr. Med. Chem., 21 (2014) 948– 965
[2] C. Silva, et al., Int. J. Pharm., 493 (2015) 1-2
[3] H. Niknejad, et al., Iran J. Pharm. Res., 14 (2015) 385-394
[4] W. Qi, et al., Mol. Pharm., 12 (2015) 675-683
[5] M. Simões, et al., Phytochem. Lett., 3 (2010) 234–237

L. Roque[1,2], P. Castro[3], P. Fonte[1,4], E. Hagesaether[5], J. Molpeceres[2], P. Rijo[1], I. Tho[5] and C. Reis[6,7*]

[1]CBiOS - ULHT, Lisbon, Portugal
[2]Faculty of Pharmacy, Alcalá de Henares, Spain
[3]CBQF - Universidade Católica Portuguesa, Porto, Portugal
[4]UCIBIO- Faculty of Pharmacy, University of Porto, Portugal
[5]School of Pharmacy, University of Oslo, Oslo, Norway
[6]iMed.ULisboa/Faculty of Pharmacy, University of Lisbon, Portugal
[7]IBEB/FCUL, University of Lisbon, Portugal

*catarinareis@ff.ulisboa.pt

Mucoadhesive assessment of different antifungal nanoformulations

Introduction:
Oral candidiasis is an important opportunistic fungal infection, and polyenes and azoles are still the most used antifungal agents. However, most of those treatments present a poor oral absorption. Therefore, the major challenge is the improvement of the absorption of the antifungal agents in oral mucosa, and the encapsulation technology may be considered as a possible strategy to achieve this objective. Three types of mucoadhesive nanoparticles (NPs) will be prepared using nystatin (Nys) as model antifungal drug, and then drug-loaded NPs will be included in toothpaste (TP), oral gel (OG) and film patches or oral films (OF).

Materials and Methods:
For the development of NPs, alginate from brown algae, acquired from Sigma-Aldrich (St. Louis, USA), PLGA and PLA both obtained from Purac (Gorinchem, Netherlands), were applied as encapsulant material. The mean particle size, polydispersity index (PI) and zeta potential of the NPs were measured. The interaction between mucin and NPs was determined using a TA-XT2i Texture Analyser [1]. The in vitro muchoadhesion was assessed using mucus producing HT29-MTX cells as mucosal surface in a biorelevant oral cavity model [2].

Results and Discussion:
The nanoparticles had a size of about 300-400 nm and a surface charge between -26.03 and -43.52 mV. Regarding the association efficiency, it showed that these NPs systems are very successful drug carriers since they present values of 95 ± 0.41%, 71 ± 9.60% and 72 ± 15.65% for PLA, PLGA and alginate NPs, respectively. The interaction between mucin and the formulation was more evident in the mucoadhesive formulations loaded with NPs, where the peak force was around 4.90, 3.43 and 2.94 Newtons for OF, OG and TP, respectively, in comparison to the values of the formulations without NPs (Figure 1). The mucin interaction with Nys-loaded NPs was supported by *in vitro* tests using HT29-MTX cells. Nys solution showed an interaction with the mucosal surface around 3.94 ± 2.96% after 2 hours under HBSS buffer flow (1.6 mL/min). For drug-loaded formulations, this percentage increased up by a ten-fold factor.

Conclusions:
Based on analysis of all samples, we observed that the best formulation in terms of mucoadhesion was the oral film loaded with PLGA NPs. This fact was also confirmed by *in vitro* tests using HT29-MTX cell as an oral cavity cell model. Further studies will focus on *in vivo* experiments.

References

[1] E. Hagesaether, M. Hiorth, S. A. Sande, EJPB, 71 (2009) 325–331
[2] K. D. Madsena, C. Sandera, S. Baldursdottira, A. M. L. Pedersenb, J. Jacobsen, IJP, 448 (2013) 373-381.

Figures

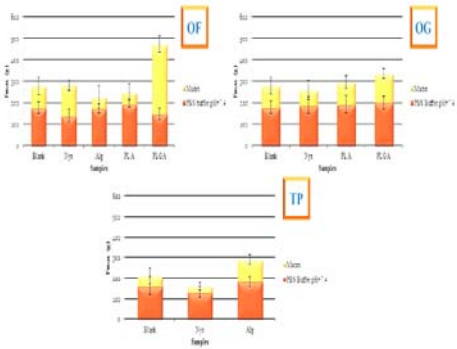

Figure 1: *In vitro* detachment test of the formulations *versus* buffer (unspecific adhesion-the orange columns) and mucin dispersion (the estimated mucin interaction-yellow columns (n= 10).

Teddy TITE[1], Stefan SLAVE[1], Luisa PILAN[1],
George Mihail VLĂSCEANU[1], Adi GHEBAUR[2]
Jorge S. BURNS[1], Mariana IONIŢĂ[1,2]

[1]Faculty of Medical Engineering, University Politehnica of Bucharest, Gh Polizu 1-7, 011061, Bucharest, Romania
[2]Advanced Polymer Materials Group, University Politehnica of Bucharest, Gh Polizu 1-7, 011061, Bucharest, Romania
Organization, Address, City, Country

titedfr@yahoo.fr

GRAPHENE-BASED ELECTROCHEMICAL BIOSENSORS FOR DNA DETECTION IN HEALTHCARE DIAGNOSIS

Quantification of biological events are of great importance for biomedical applications. Electrochemical biosensors based on graphene materials are modern and future approaches to healthcare diagnosis [1]. In this work, we propose to develop electrochemical graphene biosensors using conventional glassy carbon electrode (GCE) and industrial screen-printed electrode (SPE) (figure 1) for DNA detection, molecules which play key roles in the regulation of gene expression. Cyclic voltammetry and electrochemical impedance spectroscopy (EIS) measurements were performed with a potentiostat/galvanostat Autolab model Pgstat 204. The structure, chemistry and morphology of graphene electrodes was investigated by optical microscopy, Raman spectroscopy (Renishaw Invia), and XPS (Thermoflex 1400). This study presents a comparison of various graphene electrodes (multilayer graphene, graphene oxide, reduced graphene oxide, functionalized graphene oxide) highlighting how their structural, morphological and chemical properties influence their ability to sense a DNA probe and DNA target molecules; a key aspect for biosensor development. After DNA immobilization (probe) and hybridization (target), we observed a sensitive decrease of the current in cyclic voltammetry and an increase in the charge transfer in the impedance spectroscopy curves (figure 2).

Figures

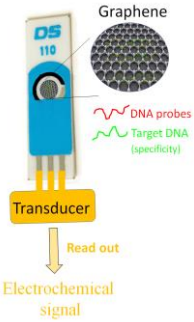

Figure 1: Graphene-based SPE biosensor

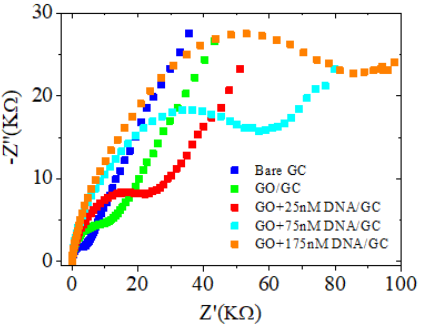

Figure 2: Nyquist plots of GO/GCE upon DNA deposition

References

[1] P. Abdul Rasheed et al., Biosensors and Bioelectronics, 97 (2017) 226

Acknowledgments : This work was supported by a grant of the Ministry of Research and Innovation, Operational Program Competitiveness Axis 1 - Section E, Program co-financed from European Regional Development Fund "Investments for your future" under the project number 154/25.11.2016, P_37_221/2015, "A novel graphene biosensor testing osteogenic potency; capturing best stem cell performance for regenerative medicine" (GRABTOP).

G. Vilão[2], C.A. Ramos[2], T.P. Iglesias[1]

1 - Dep. de Física Aplicada, Universidad de Vigo,
36210 Vigo, Spain tpigles@uvigo.es
2 - CIETI, Instituto Superior de Engenharia do Porto,
4200-072 Porto, Portugal

gmr@isep.ipp.pt

Influence of sonication time on the permittivity of a graphene nanofluid

Abstract

The preparation of nanofluids is one of the most important tasks for the stability of nanofluid, and therefore, for its electromagnetic characterization. In the present work, the preparation of the nanofluido was carried out by the two steps method, using an ultrasonic homogenizer so that the dispersion of the nanoparticles be uniform, thus avoiding the formation of aggregates. The time interval to which the ultrasound is subjected is a variable yet to be improved. There are several studies on this point, but there is still no consensus on the subject.

The influence of the sonication time on the determination of the permittivity for the nanofluid liquid paraffin with 0.75% (*V*/*V*) of graphene nanoparticles was investigated to determine the best time interval for the performance of nanofluid. The intervals that were analyzed were those of 40 min and 150 min. The choice of these two ranges is due to the previously realized UV-Vis spectra. Figure 1 shows the variation of the loss factor as a function of the angular frequency for 150 min(o) and 40 min(•) at the temperature of 293.15K, without the contribution of electrical conductivity d.c..

The characteristic parameters of the *Cole-Cole's* dielectric function[1][2][4] were determined for nanofluid with 40 min sonication and *Cole-Davidson* dielectric function for nanofluid with 150 min of sonication. [1][3][4]

Figure 2 shows the *Argand diagram*[5] for a better visualization of the difference in the response of both systems to the sonication time. It is verified that an excess of sonication time can result in the lose of the physical characteristics of the nanofluid.

T. P. I. gratefully appreciates the financial support ED431C 2016–034 provided by the *Xunta de Galicia* (Spain). G.V. and C. R. thanks FCT (Portugal) by project FCT/UID/EQU/04730/2013.

References

[1] Broadband Dielectric Spectroscopy, edited by F. Kremer and A. Schönhals (Springer-Verlag, Berlin, 2003)

[2] K.S. Cole, R.H. Cole, J. Chem. Phys., 9, (1941) 341–352

[3] D.W. Davidson, R.H. Cole, J. Chem. Phys., 19, (1951) 1484–1491

[4] T.P. Iglesias, G. Vilão, João Reis, J. Appl. Phys, 122, (2017) 074102

[5] C.J.F. Böttcher, P. Bordewijk, Theory of Electric Polarization, Vol.II., 2nd ed. (Elsevier, Amsterdam, 1978).

Figures

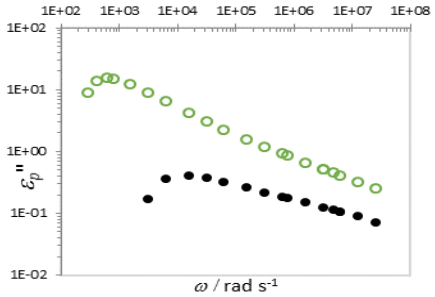

Figure 1: Variation of the loss factor as a function of the angular frequency of the nanofluid for 150 min (o) and 40 min(•).

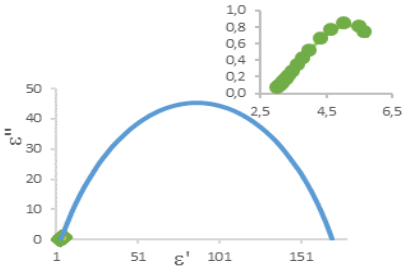

Figure 2: Argand diagram for 150 min of sonication (•) and for 40 min (--) of paraffin nanofluid with graphene.

www.nanopt.org

Edited by

Phantoms Foundation

Alfonso Gomez 17
28037 Madrid - Spain

info@phantomsnet.net
www.phantomsnet.net